Novel Skin Stretching Device

A Major Qualifying Project Report
submitted to the Faculty of
Worcester Polytechnic Institute
in partial fulfillment of the requirements for the
Degree of Bachelor of Science
by

_____

Katie Hutchinson

_____

Daniel Keenan

_____

Laura Piccione

_____

Hussein Yatim

May 2012

Approved by:

_____

Professor George Pins, Advisor

_____

Professor John Sullivan, Advisor

Amanda Clement

Dr. Michael Chin

Dr. Raymond Dunn

Dr. Ronald Ignotz

Dr. Janice Lalikos

Keywords: skin graft, *in vitro*, cyclical testing

Table of Contents

Authorship Page

All group members contributed equally to the writing, editing, and formatting of this report.

Acknowledgements

We would like to extend sincerest appreciation to Professor George Pins and Amanda Clement, our primary advisors. We would also like to thank our advisor Professor John Sullivan, whose input was essential to the success of our device. We appreciate the guidance provided by our respected advisors Doctors Michael Chin, Raymond Dunn, Ronald Ignotz, and Janice Lalikos from the UMass Medical School. Finally, we would like to acknowledge Lisa Wall and Timothy Sharood for their tremendous assistance throughout this project.

Abstract

In response to the poor mechanical stability and long growth time of tissue-engineered skin substitutes, we present a novel skin-stretching device that mechanically stimulates skin grafts during *in vitro* culture to accelerate tissue growth. Mechanical loading has been shown to accelerate epidermal proliferation, increase expression of growth factors, and improve mechanical stability. Also, changing the loading parameters can have varied effects on the growth response. Preliminary research and evaluation matrices were integral to come up with a list of objectives that the device must meet. The most important objectives included that the device be precise and accurate during testing, minimally damage the tissue sample, and be able to apply varied testing regimes. Through the iterative design process, ultimately a fabrication of a final device was created that successfully applied multiaxial stretch to skin samples during culture. Since the device is used in a biohazard environment, it was able to be sterilized and maintain a sterile culture environment while either in a fume hood or incubator setting. The mechanical portion of the device used an Arduino Uno microcontroller with a 2 ft/lb. vex motor. Testing parameters such as motor speed, displacement, start position, and wait time between stretches were able to be changed using C++ programming to fit the user's needs by varying numerical inputs. ANSYS modeling was used to simulate a 15 mm diameter epidermal tissue sample being stretched mulitaxially at six discrete locations. This model was used to calculate a value of 0.2N for the maximum allowable force, along with a maximum stress and strain of 0.04 MPa and 10% respectively, to ensure minimal damage to the sample.

Table of Figures

Chapter 1: Introduction

Annually, 6.5 million people in the United States suffer from non-healing wounds that have estimated treatment costs of more than $25 billion (Mathieu, Linke and Wattel 2006; Menke, et al. 2007; Sen et al., 2009). Additionally, 450,000 burn injuries receive medical treatment each year (American Burn Association, 2011). Skin grafts are used in a variety of applications, many of which involve the treatment of skin wounds and conditions. Each year, over 163,000 split or full thickness grafting procedures are performed on Medicare recipients alone (Wysocki & Dorsett-Martin, 2008). Grafts are also commonly used in the treatment of diabetic ulcers, which are a risk for approximately 15% of the 20 million individuals with diabetes (Blotzik & Scherer, 2008). Diabetic ulcers will not heal with conventional treatment and can lead to hospitalization or amputation (Blotzik & Scherer, 2008). Overall, skin serves as the body's first layer of defense, providing invaluable protection for the vulnerable systems within the body (Padbury, 2008). The skin barrier must be in tact to prevent adverse events such as infection and dehydration (Bouzari, Kim, & Kirsner, 2009).

Biological grafts such as autografts, allografts, and xenografts are either taken from the patient, a donor, or another species, respectively. Autografts, which necessitate a second surgical procedure and wound site on the patient, can cause pain, infection, and scarring. Allografts and xenografts introduce a substantial risk of infection, rejection, and disease transmission (Shevchenko, James, & James, 2010). The limitations of biological grafts have led to the exploration of tissue-engineered skin grafts.

The field of tissue engineering has made significant advances in wound healing, introducing engineered skin substitutes that diminish risks and drawbacks associated with biological donor tissue. There are a number of commercially available skin substitutes on the market, such as Apligraf, Integra, and cultured epithelial autografts. The main limitations of current skin substitutes are their lengthy culture time and mechanical instability (Boyce, 1996). Mechanical strength and elasticity of tissue-engineered skin are less than 10% of those of native skin (Blackstone & Powell, 2012; Boyce, 1996). The substitutes today cannot fully replace

biological grafts because of an inability to withstand necessary shear forces, or offer adequate durability for long-term wound healing.

Improving health care treatment of non-healing wounds, diabetic ulcers, and burn trauma is critically important. The current limitations associated with skin grafting technologies highlight the need for a method of generating durable, viable, mechanically stable skin substitutes. One promising solution is the use of mechanical stimulation to accelerate tissue growth. Skin, in its native environment, is in constant tension; research has indicated that tension has a large role in the development and functionality of skin. (Zöllner, Buganza Tepole, & Kuhl, On the biomechanics and mechanobiology of growing skin, 2012). The body has the ability to use mechanical stimuli to trigger chemical responses, a phenomenon known as mechanotransduction; when skin is stretched beyond its physiological limit, the tension triggers an increase in mitotic activity and collagen synthesis, ultimately leading to a net gain in surface area (Zöllner, Buganza Tepole, & Kuhl, On the biomechanics and mechanobiology of growing skin, 2012). Studies have shown that cyclical stretch leads to a significantly greater expression in epidermal growth factor (EGF), transforming growth factor beta1 (TGF-β1), and nerve growth factor (NGF) when compared to static stretch (Chin, 2010). The DermiGen D70-1, a bioreactor currently on the market, stretches skin uniaxially at the air-liquid interface (DermiGen, 2012). However, it is hypothesized that stretching skin multiaxially will better mimic *in vivo* conditions and elicit a stronger growth response.

The goal of this project was to apply the benefits of mechanical loading to a multiaxial system in which engineered skin grafts could be stretched at a cyclical, programmable waveform during culture. The engineering design process was used to maintain thorough detail and organization throughout the project. The team established goals and constraints, generated viable and effective solutions, and engineered a device to address the limitations of current technology. It was established that the device should stretch a skin sample at the air-liquid interface, and that testing should be reproducible, multiaxial, and waveform-specific. The team designed and manufactured a controlled servo-motor stretching device that works in an

incubator and mechanically stimulates a 15 mm diameter skin graft while maintaining sterility and only minimally damaging the sample.

Recommendations for future research include the analysis of mechanical signaling pathways to gain further insight in order to improve tissue-engineered skin. Future modifications might include adding components that could identify an optimized applied stress, test duration, and loading waveform.

Chapter 2: Literature Review

2.1 Clinical Significance

Ranging from wounds to diseases, there is a constant need for substantial medical treatment regarding skin. Annually in the United States, 6.5 million people suffer from wounds that will not heal without medical intervention, accounting for $25 billion in excess healthcare costs (Sen, et al., 2009). Approximately 450,000 people per year require medical treatment for burns alone, and certain skin conditions, surgeries, and large wounds necessitate treatment before further compilations arise (American Burn Association, 2011). Diabetic ulcers account for 15% of the medical visits of 20 million diabetes patients and commonly lead to hospitalization and amputation (Blotzik & Scherer, 2008). Diabetes continues to increase in prevalence year after year (Gale, 2002). With countless diseases, burns, and non-healing wounds that require the restoration and reconstruction of skin, the interest in skin substitutes is clear.

2.1 A The Importance of Skin

Skin: The First Layer of Defense

Skin is the outermost layer of an intricate and largely vulnerable biological system, the body. Skin is the largest organ of the body and is critical for protection serving as the first layer of defense against injury, dehydration, infection, and pathogens. In addition, skin helps to regulate electrolytes and body temperature (Padbury, 2008; Bouzari, 2009).

The Anatomy of Skin

Skin is composed of three major components: the epidermis, dermis, and subcutaneous layer, as seen in Figure 1. The epidermis is the outermost layer that serves as a protective layer and waterproof barrier. It is comprised of multiple layers: the stratum corneum, stratum lucidum, stratum granulosum, stratum spinosum, and stratum basale. *In vivo* keratinocyte proliferation takes place primarily in the stratum basale, the innermost layer of the epidermis. Cells from each newly formed epidermal layer in the stratum basale slowly move upwards to the stratum corneum replacing older dead cells.

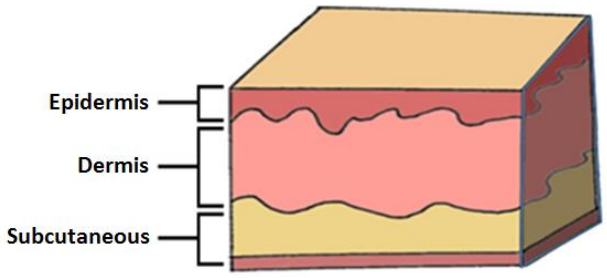

Figure 1: A cross-sectional image of the skin's anatomy.

As dead cells are shed, the cells beneath are revealed, continuing the cycle of skin barrier formation and function (Powell J. , Skin physiology, 2006). Underneath the epidermis is the dermis, a layer of dense irregular connective tissue. Within it are all the accessory constituents of skin including blood vessels, hair follicles, nerve receptors, and glands. The dermis provides structural support for the epidermis from (Powell J. , Skin physiology, 2006). The subcutaneous tissue is located beneath the dermis. A transitional layer comprised of connective and fatty adipose tissues connects the dermis to the muscles beneath (Scanlon & Sanders, 2011).

2.1 B The Need for Skin Substitutes

As stated previously, the epidermis can regenerate by recruiting cells from the stratum basale. These cells differentiate and ultimately keratinize to repair damage (Powell J. , Skin physiology, 2006). The dermis can be restored as well, if minimally damaged, although it cannot regenerate as easily or as quickly as the epidermis. When damage is extensive or a wound penetrates all the way through the dermis, there is limited regenerative capacity. After withstanding such trauma, the dermis will repair itself in a process that leads to the formation of scar tissue instead of complete regeneration of the damaged tissue. Non-healing wounds can arise in the event of a large wound site, chronic infection, and compromised wound healing (Scanlon & Sanders, 2011). Moreover, without the solid foundation of the dermis, epidermal regeneration is hindered. Non-healing wounds create weak points in the body's defenses and negate the protection that skin provides (O'Dell, 1998). A medical solution to this problem will improve skin barrier function.

2.2 Current Skin Grafts

The vast diversity of skin grafts and application techniques has increased exponentially in accordance with the growing field of tissue engineering. Many scientists in the field have attempted to pioneer skin grafts mimetic of native tissue. A feasible skin substitute would have similar mechanical properties to native skin, while stimulating tissue regeneration. Skin grafting dates back to 1869 when Jacques-Louis Reverdin performed the first autograft procedure (Kishi & Shimizu, 2012). In 1929, it was established that graft thickness is very important. The two types of grafts are full-thickness and split-thickness grafts. Full thickness grafts are comprised of the epidermis as well as the whole thickness of the dermis (Shevchenko, James, & James, 2010). The sample of the patient's skin is cut into the correct size and shape to fit the wound. In comparison with full-thickness grafts, split-thickness grafts contain the entire epidermis and only require portions of the dermis. The amount of dermis in a split-thickness graft is dependent upon how much of the dermis is needed for the specific application. Split-thickness grafts exhibit better results than full-thickness grafts. The use of skin grafts is an essential component in the fields of plastic surgery and dermatology today (Kishi & Shimizu, 2012).

Applications for the clinical use of skin grafts include but are not limited to the repair of traumatic wounds (large punctures and lacerations), defects after oncologic resection (superficial tumors), burn reconstruction (usually for third degree burns), scar contracture release, and congenital skin defects (large areas or sensitive location) (Kishi & Shimizu, 2012). Skin grafts have been implemented, with positive results, to wounds that do not heal because of infection, large wound size, poor nutrition, malnutrition, and other factors (Fox, 2011).

The practice of skin grafting is evolving and advancing, providing current medical professionals with several skin graft types to choose from for patient procedures. Skin grafts are classified as either biological or tissue-engineered. Medical professionals need to account for patient, wound, and financial-specific situations. Multiple options at the doctor's disposal allows for doctor's preference toward the procedure, and thus the best solution and treatment for the patient. Each graft has limitations in mechanical properties, cost, treatment time, and effectiveness.

2.2 A Biological Tissues

The three main types of biological grafts are autografts, allografts, and xenografts. Autografts are a portion of skin taken from a local donor site on the patient. Autografts can be performed as full-thickness or split-thickness grafts depending upon the severity and depth of damaged skin. A full-thickness graft may be placed as a sheet graft or a meshed skin graft. Sheet grafts are undamaged portions of skin that are harvested from a donor site and placed on the wound site without any other treatment (Kishi & Shimizu, 2012). These grafts shrink after being removed from the donor site as a consequence of the elastic properties of skin (Shevchenko, James, & James, 2010). Sheet grafts limit the total coverage to areas smaller than the donor site. In contrast, meshed skin grafts are modified after being harvested to cover a larger area than the donor site. The graft is run through a machine called a mesher, which makes small slits in the skin increasing the graft size. This is commonly done when the burn is extensive leaving a small amount of viable tissue for grafting, or to allow fluid to drain from the wound. These types of grafts are used to cover a large skin injury that may not have enough blood vessels left intact (Kishi & Shimizu, 2012). If the wound is on the face, neck, or hands, a split thickness graft is applied as a sheet graft rather than meshed grafts due to aesthetic concerns. While autografts are highly effective, the donor site from which they are taken can experience complications in healing known as donor site morbidity. Additionally, a patient's skin damage may affect a large enough portion of his body that a graft cannot be taken, especially in the case of burns (Bar-Meir, Mendes, & Winkler, 2006).

Allografts are used when there is an insufficient amount of viable tissue to be used as donor tissue. An allograft is donor tissue that is taken from one person, living or cadaveric, and used on a different person. Allografts will work, like autografts, to close a wound and reestablish the protective barrier while promoting healing of underlying tissues. Allografts can be used as a treatment to the aforementioned skin conditions and wounds until an autograft can be used to permanently close the wound (University of Michigan, 2012). A disadvantage of allografts is that they have an increased risk of rejection and disease transmission.

Xenografts can also be used when there is a limited donor site, and are generally comprised of porcine or bovine tissues. Xenografts are useful because they are ubiquitous and readily available; however, they run the risk of disease transmission and rejection (Manning, 1973).

Surgery is conducted similarly for all biological skin grafts. For autografts, skin is harvested from the donor site and placed onto the wound bed (Shevchenko, James, & James, 2010). The graft is harvested from the donor site using an oscillating surgical blade called a dermatome to remove the skin. Attachment of the graft to the wound site can be achieved through the use of sutures, staples, or skin glue. The donor site must be closed, and then the graft is attached to the wound site. Dressings are then applied around the wound site and graft in the form of bandages, films, or foam containing substances that promote wound healing. The healing process of the graft occurs through intake of the local blood supply of the wound site and of the resulting angiogenesis (Shevchenko, James, & James, 2010).

2.2 B Engineered Tissues

Engineered skin substitutes present a solution to skin wounds that does not entail a second surgery and the associated risk of donor site morbidity; skin substitutes can improve the recovery of function and appearance (Bar-Meir, Mendes, & Winkler, 2006). Over the past few decades the field of tissue engineering has made large strides in an effort to address limitations such as poor graft adhesion to the wound site, time-consuming preparation, high production cost, and initiation of a foreign body response.

One of the options for engineered tissues is a Cultured Epithelial Autograft, or CEA, which functions similarly to a biological skin graft. In the generation of this type of cellular-engineered graft, a small skin biopsy is isolated from the patient; keratinocytes are cultured into sheets in an aseptic lab setting and then seeded onto tissue taken from the patient (Gutierrez, 2006). The cultured skin is then transplanted back into the patient. Smaller grafts are sewn on while larger grafts are glued on and held into place by a dressing. There are advantages and disadvantages in using this type of graft. CEA's are useful because within four weeks a 2cm x 2cm biopsy can expand 5,000x the original size. This decreases the size of the

minimum skin surface area required for grafting. A disadvantage is that this graft is fragile. Complications in the initial application of the graft or failures of the graft because of mechanical instability require restarting the process. These setbacks cause breakdowns and delays in the healing process (Shores, Gabriel, & Gupta, 2007). The mechanical instability of this graft can reduce the treatment's effectiveness.

A more commonly used skin substitute, Integra, is one of the most widely accepted synthetic grafts for burn treatment (Bar-Meir, Mendes, & Winkler, 2006). This artificial scaffold has a bilayer structure comprised of a porous silicone membrane and a cross-linked collagen layer (Dantzer & Braye, 2001). The bovine collagen layer acts as a matrix for the recruitment of fibroblasts and endothelial cells. Vascularization occurs about 3 to 6 weeks post-operation, at which point the silicone layer is removed and a thin split-thickness autograft is applied (Bar-Meir, Mendes, & Winkler, 2006). A limitation of Integra is the inadequate mechanical strength due to its layered structure (Ghattaura & Potokar, 2009). Furthermore, Integra can be expensive relative to cadaveric allografts (Bar-Meir, Mendes, & Winkler, 2006).

Dermagraft is another tissue-engineered skin substitute that is widely used for wound coverage (Bar-Meir, Mendes, & Winkler, 2006). The mechanical properties of the classical degradable polyesters used in Dermagraft are not always ideal for tissue engineering due to their relative inflexibility and tendency to crumble upon degradation (Griffith, 2002). This can lead to mechanical instability of new tissue being formed.

Apligraf® is an FDA-approved living skin substitute for chronic venous leg ulcers and diabetic foot ulcers (Shores, Gabriel, & Gupta, 2007; Balasubramani & Ravi Kumar, 2001). The bi-layered graft consists of a deep layer of a type I bovine collagen gel combined with living neonatal fibroblasts as well as a superficial layer of neonatal keratinocytes (DeCarbo, 2009). Similar to Integra, its bilayer construction entails a decrease in mechanical integrity. In clinical studies, this graft has been applied more than once, though limited to a maximum of five applications in accordance with FDA approved labeling (UK Medicines Information, 2001); this makes Apligraf an expensive treatment option, as one application can cost over $1,100 (Bar-Meir, Mendes, & Winkler, 2006).

2.2 C Limitations

To reiterate the limitations of biological grafts, autografts require a second surgery, can lead to donor site morbidity, and are not always available. Allografts and xenografts carry the potential for disease transmission and rejection.

While skin substitutes address the limitations of biological grafts, they entail considerable drawbacks of their own: synthetic tissues require a long amount of time to grow a small sample. Growth rates of cultured keratinocytes and fibroblasts have been quantified at approximately one population doubling per day with a keratinocyte colony-forming efficiency of 1-10%. These values indicate the limit in population expansion, with cell number increasing by a factor of ~$1X10^3$ in 10 days and ~$1X10^6$ in 20 days (Boyce, 1996). Additionally, engineered grafts can be expensive (Boyce, 1996; Bar-Meir, Mendes, & Winkler, 2006). Another main issue with engineered skin is mechanical instability; current generations of skin substitutes have poor mechanical integrity, with less than 10% the strength of native skin (Boyce, 1996). Instability makes handling and application difficult and can lead to high failure rates, evident from the steep learning curve associated with Integra, one of the most commonly used skin substitutes (Bar-Meir, Mendes, & Winkler, 2006). Additionally, weak grafts are prone to mechanical damage during fabrication and application, and demonstrate less elasticity and strength once applied (Blackstone & Powell, 2012).

If these drawbacks were addressed, a new gold standard could be established for skin grafting. The mechanical instability of engineered grafts can be partly attributed to the absence of a supporting dermis; thicker grafts, such as full thickness grafts, are recommended to reduce the chances of skin graft failure (Ghattaura & Potokar, 2009). Furthermore, research indicates that the poor mechanical stability can be a product of the *in vitro* culture environment. The next successful skin substitute would eliminate the need for a second wound site or donor tissue, the potential for disease transmission, and inadequate properties such as mechanical instability, culture time, cost, cell recruitment and proliferation, and scar formation.

2.3 Improving the Current Gold Standard

A major factor in tissue engineering is the mechanical compatibility of engineered tissues; it is desirable (Leventon, 2002) and often essential that engineered tissue closely mimics the natural tissue that it serves to replace, support, or enhance (Place, George, Williams, & Stephens, 2009). The mechanics of biological tissues are complex and difficult to achieve in synthetic tissues. Current engineered skin is orders of magnitude weaker than naturally occurring skin, and engineered skin grafts have failed during short- and long-term mechanical testing (Bannasch, et al., 2003). This instability can lead to complications in application, damage during fabrication, or reduced graft elasticity and strength after the graft is applied (Blackstone & Powell, 2012). Wolff's Law theorizes that form follows function; it is only logical to question how the function of constantly withstanding tension drives the form of skin (Ruff, Holt, & Trinkaus, 2006).

2.3 A The influence of Mechanical Stress

Previous studies have proved that one way to improve the mechanical properties of a material is often by *in vitro* preconditioning. When the mechanical cues shown to increase tensile strength, epidermal proliferation, and cell cohesion in natural tissues can be recreated, cells can be guided to respond functionally (Place, George, Williams, & Stephens, 2009), and mechanical stretch has shown to increase epidermal proliferation (Reichelt, 2007). Mechanical stretching has been shown to cause upregulation of cells with BrdU, a nucleoside used to observe cell division (Hsieh & Lin, 1999), to 200%–220% making for a thicker, more cellular, denser graft (Yano, Komine, Fujimoto, Okochi, & Tamaki, 2004). It has been hypothesized that imparting tension on engineered skin grafts can improve their mechanical stability, driving tissue to adapt to an environment more similar to the natural one (Blackstone & Powell, 2012).

An incidence of skin responding to mechanical stress can be seen in tissue expanders, which use a combination of strain and biological creep. Tissue expanders consist of a silicone balloon expander that is inserted under the skin near the area to be repaired and then gradually filled with saline over time, causing the skin to stretch and grow. Creep is a viscoelastic phenomenon in which the skin will continue to expand when a constant stress is

applied to the tissue for an extended period of time. Biological stretch involves a response to applied force in which the tissue will enlarge without altering the original quality (Zöllner, Buganza Tepole, Gosain, & Kuhl, 2012). Tissue expanders utilize these responses to stretch the skin, generally for plastic surgery, with either a subcutaneous expander or an external device such as a vacuum (Denkler, 2008).

There has also been development of devices that mechanically stretch skin in bioreactors. With respect to variations in the application of stress, an *in vivo* experiment on dorsal murine skin indicated that mechanical loading led to significantly increased epidermal proliferation (Chin, 2010). This experiment included variations on loading cycles, including static and cyclical loading at either 1 hour or 4 hour durations. The 1 hour testing period showed that cyclical stretch incited a stronger response, while the 4 hour testing period showed that static stretch incited a stronger response. These results indicate that experimentation with varied cycle parameters is necessary to define the relationship between mechanical loading and the associated growth response. Additionally, real-time RT-PCR of epidermal growth factor (EGF), tissue growth factor beta1 (TGF-β1), and nerve growth factor (NGF) showed greater expression in cyclically stretched skin when compared to static stretch, (Chin, 2010).

To summarize, stress applied to skin with a cyclic waveform showed significantly increased epidermal proliferation, cutaneous perfusion, angiogenesis, and growth factor expression with respect to statically stretched samples (Chin, 2010). These effects have also been studied with respect to tissue-engineered skin grafts; it has been established that stretching of engineered skin grafts can lead to increased cell proliferation and expression of growth factors in an *in vitro* environment.

DermiGen has created two bioreactors, D70-1 and D70-4, which stretch engineered tissue samples statically and cyclically at the air-liquid media interface for applications regarding growth stimulation (Bolland, Fisher, Ingham, Kearney, & Korossis, 2005).

2.3 B The Limitations of Current Technology

While tissue expanders highlight the concept of stretch-induced proliferation, they are not easily applicable to the field of grafts. Such devices could largely decrease the amount of

skin that could be taken for an autograft, but a secondary wound site is still created to harvest that tissue. Novel devices have been made to stretch skin grafts *in vitro*, such as the D70-1 and D70-4 bioreactors from DermiGen, but they provide only uniaxial stretch. There is a need for a device that can culture tissue at the air-liquid interface while applying a uniform, multiaxial stretch with controllable strain rates.

2.3 C Moving From an *in vivo* to an *in vitro* Model

Mechanical stimuli can largely influence physiological tissue growth and development. According to research endothelial cell stretching *in vitro* has led to an increase in proliferation and vascularization (Erba & Meile, 2011). Mechanical stretch has been shown to induce vascular remodeling and increase vessel density. Furthermore, research has shown that multiaxial loading can have varied results from uniaxial stretch (Powell, Smiley, Mills, & Vandenburgh, 2002) . It has been shown that most cells react to mechanical stimuli (Reichelt, 2007), and that mechanical stimulation increases cellular proliferation (Powell, Smiley, Mills, & Vandenburgh, 2002). Experimental studies regarding the mechanical stretch of tissue confirm a net gain in skin area, and that this is a result of the generation of new tissue, not the recruiting of tissue from neighboring regions (DeFilippo & Atala, 2002), implicating that skin is able to increase its area upon mechanical overstretch (Zöllner, Buganza Tepole, & Kuhl, On the biomechanics and mechanobiology of growing skin, 2012).

2.3 D Proposed Contribution to the Field

The team asserts that more closely mimicking the natural environment of skin will improve the mechanical properties of traditionally cultured skin substitutes. The application of multiaxial stretch will produce more robust results, showing a more clear relationship between stress, strain, and strain rate and the mechanical properties and epidermal proliferation of skin. Furthermore, a system that provides a large range of possible waveforms and cycle durations will allow investigation into the relationship between the loading cycle parameters and the incited growth response. These improvements to the field will ultimately help patients in need of skin grafts by producing grafts with mechanical properties more consistent with native skin.

Studies have indicated that large enough stress and strain values can cause damage to tissue; therefore, it is important to remain well below these values. It is also important to find the appropriate time during the culturing process to apply the stress and strains.

Studies have indicated that large enough stress and strain values can cause damage to tissue; therefore, it is important to remain well below these values. It is also important to find the appropriate time during the culturing process to apply the stress and strains.

2.4 Relevant Mathematical Models

In order for testing of the skin samples to be accurate, the models with which the team characterizes skin must be accurate. *In vitro and in vivo* skin research models are expensive, therefore several methods have been established that predict the skin's response to mechanical loading. These models rely on complex equations and computer computation to represent the stress strain gradients across the skin as accurately as possible.

With a device that mechanically loads skin, a complex tissue, there are many details that must be considered. The grafts must remain mechanically stable and physiologically sound throughout testing, as the goal of this device is to improve current engineered grafts. Excessive stress, strain, or cycle durations have the potential to damage the tissue. Beyond the extreme of loading the skin to fracture, smaller stresses well within the yield stress can cause damage to the constituents of the tissue, and can change the overall properties. Because biological tissues are viscoelastic, loading and unloading cycles exhibit hysteresis, a phenomenon in which the loading cycle and the unloading cycle follow different paths, representing a loss in energy. An example of hysteresis can be seen in Figure 2, in which the circles represent the loading cycle, and the triangles represent unloading. In this situation, force is applied and then removed, but the viscoelastic material has a delayed response in recovering deformation.

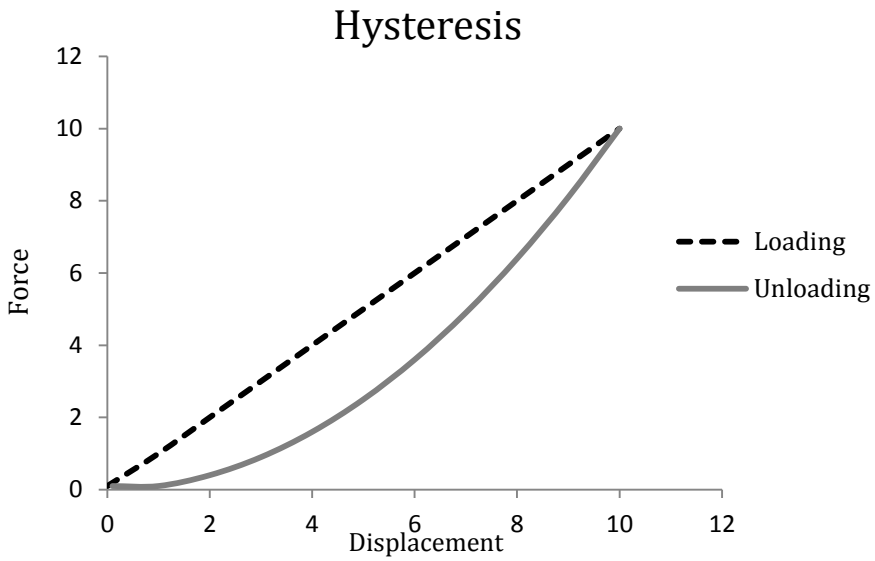

Figure 2: An example of hysteresis.

Additionally, the rate at which strain occurs correlates to the effective stiffness and, ultimately, to the stress experienced. As the strain rate increases, the stiffness of skin increases as well.

Modeling the mechanical responses of skin and predicting the skin's stress strain response is very complex. It is important that we use a mathematical model that allows the user to vary stresses on the skin and obtain feedback. Most models use assumptions that skin is a linear, elastic, and isotropic material. Unfortunately, this assertion is only true for small stresses and strains (Zöllner, Buganza Tepole, & Kuhl, On the biomechanics and mechanobiology of growing skin, 2012). Generally, skin has been found to be anisotropic, non-linear elastic, and non-homogeneous (Ní Annaidh, Bruyère, Destrade, Gilchrist, & Otténio, 2012). With respect to this project, the stress applied was less than 0.2 N due to the results of the finite element analysis, presented in (sec 0). This approximated skin as a linear, elastic, and isotropic material. Unfortunately skin is actually a hyperelastic, non-linear elastic, and anisotropic material. Any solution obtained from an approximation method had to be validated by comparison to an exact solution gathered from collected data or calculated by an ideal equation. The similarity of the two solutions determined the reliability of the estimation method.

One method of modeling skin is a continuum mechanics model. Continuum mechanics assumes that the material is linear, elastic, homogeneous, and isotropic, obeys Hooke's law, is a smooth flat surface, and is infinite in extent. Skin is not an ideal medium and does not behave like one, but for very small deformations, within 1 to 2% strain, this approximation is appropriate. This model also assumes that a complex stimulus can be determined evaluating it on a more basic level, breaking it down into more simple subunits, and then combining the effect of each into one net stimulus (Philips & Johnson, 1981). This will allow for decomposition of the multiaxial stress concentrations into a specified polar or Cartesian range and approximation of their values through superposition.

Models have been determined that approximate the elastic behavior as well as the failure behavior of skin, with focus on equations that have been applied to blood vessels and skin (Federico, Grillo, Giaquinta, & Herzog, 2008). These Fung-type equations (Fung, 1993) approximate soft tissues under loading in the elastic region, and can also characterize skin as it enters the hyperelastic region.

Fung based his models off of the Green-Lagrange strain equations. Green-Lagrange strain defines the values in terms of ε(x), ε(y), and ɤ. Each term of Green-Lagrange strain contains a linear part and a quadratic part. These two sets allow the Fung-type equation above to model both elastic and non-elastic behavior. For small values of strain, the second portion of the equation has little effect on the curve, and for large values of strain, the first portion of the equation has little effect on the curve. These equations display error when fitting data sets other than the original one the equations were derived from. One way proposed to fix this stated in the literature was to ensure the equation modeled a convex curve (Federico, Grillo, Giaquinta, & Herzog, 2008). The study concluded that keeping the quadratic form Q (E) in the equation above positive ensured convexity. By doing this, some of the error associated with this type of modeling can be ruled out, and the equation can be considered a better approximation for global data.

Finite element analysis can be applied to skin approximation as well. This type of analysis can better approximate a material with mixed characteristics such as skin with

viscoelastic behavior and partial incompressibility (Weiss, Maker, & Govindjee, 1996). Depending on the element chosen for approximation, finite element modeling could approximate skin as an ideal solid or a hyperelastic material. Custom elements can be created in the software that are based off the shaping function (N(x)) defined by the user. The shaping function can then be differentiated to obtain the geometric matrix (B(x)) and finally derive the stiffness matrix (K). A unique stiffness matrix for a material can be very useful when trying to do multiple calculations and obtain unique solutions for the material.

Unique elements can be used to approximate skin as an anisotropic material. Analysis could then be done on the element to determine when the material would exit the elastic region. Then base values could be set for the estimation of stresses and strains that cause damage. Elastic solids defined by a finite element model can be used to approximate the stress concentrations. By applying a force or pressure along one side of the solid and a displacement boundary condition along another side, different force patterns can be simulated. Finite element modeling does a good job of displaying the results and allowing for easy manipulation of the variables.

These methods can all be applied with varying amounts of success to determine values relevant to *in vitro* testing. Values able to be calculated include reaction forces at grips, stress gradients across the sample, ultimate tensile stress, and limitations based on the project set up. By weighing the pros and cons of each system, the appropriate methods for different applications were determined.

Chapter 3: Project Strategy

The need associated with our client statement was too broad to begin the design process; narrowing the scope of the project was necessary in establishing a clear track for progress. Four processes were completed including revising the client statement, listing final objectives, providing metrics for those objectives, and listing the final constraints. The team brainstormed and asked many questions about the initial client statement. The final objectives were determined using background research, interviews, pairwise comparison charts, and an objective tree. Lastly, the project approach was described in accordance with the objectives and constraints.

The designer's first task was to clarify what the client wants. Once determined, the wants can be translated in objectives and constraints. This section will present an overview of the design process and the methods used to generate and rank design goals.

The three stakeholders of the project consist of the user, designer, and the client. It is the responsibility of the designer to create a device that meets the needs of both the client and user. The designers of this project are the Major Qualifying Project (MQP) team: Daniel Keenan, Laura Piccione, Hussein Yatim, and Katie Hutchinson. The clients are Professor George Pins, Professor John Sullivan, Doctor Michael Chin, Doctor Raymond Dunn, Doctor Janice Lalikos, and Doctor Ronald Ignotz. Professor Pins provided the original client statement, project description, and expectation of deliverables. The user, Amanda Clement, is a Worcester Polytechnic Institute graduate student, who works full-time culturing bioengineered skin substitutes. Throughout the design process, the design team was constantly meeting with the clients and user to gain valuable feedback when deciding on the final objectives for the device.

3.1 Initial Client Statement

Design a device that can perform uniform multiaxial stretch of tissue-engineered skin grafts during culture to accelerate *in vitro* growth.

3.2 Objectives

This section will present the key objectives of the design and how the team generated and evaluated them. The design team participated in a series of interviews with the clients and users to gather information on what they needed and wanted to see in the device, how the device would be executed, and current limitations of skin grafting. The team also corresponded with Dr. Chin to gain insight on the advantages and disadvantages of his *in vivo* skin stretching device. Finally, the team toured Professor Pins's lab to understand the process of culturing keratinocytes into tissue-engineered skin grafts.

Next the team was able to come up with a list of objectives, functions, and constraints. Objectives describe desired performance characteristics, functions describe what the device must do, and constraints describe what the limiting factors of the design are. The objectives were organized in an objective tree, shown in Appendix B, to compile similar objectives and arrange them in a hierarchical structure with the main and sub objectives. There were nine level one objectives including cost efficiency, accuracy, precision, varied testing regimes, durability, minimally damaging tissue, efficiency, visually appealing, and user friendliness.

A goal of our device is that the design must be **inexpensive**, both in its construction and also in its use. The materials used in construction of the device should be easy to find, easy to replace, and relatively inexpensive. Similarly, the parts should be sterilizable or incorporate disposable parts. Next, the device should be **accurate** and **precise**. The team will aim for accuracy with the device's performance and the testing regimes. Precision will increase the reliability and reproducibility of the device. All stress values should be within 10% of the ideal stress as calculated using the applied force and cross sectional area of the skin. To validate reproducibility and accuracy, the force pattern and the method of gripping the sample must be optimized, so the results will reflect the same stretch on each similar sample, and there will be little to no slippage of the sample from the grips.

The device must be capable of a **controllable varied testing regime**, including:

-Static or cyclical stretch

-Stretch magnitude variability

-Strain rate variability

This includes the dimensional factor of stretch, e.g. uniaxial, biaxial, and multiaxial, as well as a controllable waveform, e.g. static or cyclic. It would be beneficial to be able to study the samples under a multiaxial stretch with both static and cyclic waveforms, as well as a variable strain rate and stretch magnitude.

This device must also be **durable**. The device and all working components must last at least one year or 20 complete testing regimes. A durable product will allow for more consistent results because all parts will remain constant throughout the testing.

Another objective would be that the device is **minimally harmful to tissue**. This is a complex problem including three main facets: fixturing, stretching, and nourishing the samples. First, in gripping the tissue, the device can easily damage the tissue graft. It would be best to minimize or limit the amount of damaged tissue. Next, exceeding the tissue's maximum strain rate or stretch magnitude could damage the tissue, so the team intends to avoid any damage by applying a stretch well below the maximum values. Finally, the tissue must be nourished in a bioreactor in order to stay alive and maintain the characteristics of skin, so we intend to fully soak the samples in media. Also the device must prevent contamination of the sample and sample loss. The grafts need the proper orientation when cultured at the air/liquid interface. The final design should compensate for these issues and provide a procedure for operation that minimizes these outcomes.

The team aims to make an **efficient** device, in the hopes that the cost of production can be balanced with a high rate of testing. The goal is to be able to stretch and test as many samples simultaneously as possible without compromising the environment or testing of any of the samples.

A final objective is that the device be **visually appealing**; aesthetically pleasing products have shown to do better in the market and have better user feedback. Also our device should be something that fits well in a sophisticated laboratory setting.

In the best case scenario, the device will meet or exceed every single objective. In some cases it may turn out that the initial objective was set too high and cannot be achieved in the time frame or for the budget. A tool used for ranking these objectives is the Pairwise Comparison Chart seen in Appendix A.2, a chart that allows the team, client, and user to weigh each objective against the others, deciding, for example, whether "inexpensive" is more important than "visually appealing." Each objective is judged equally against the others, with the more important objective receiving a score of 1, while the less important receives a score of 0. In cases where the objectives had equal importance, a ½ was given. The Pairwise Comparison Charts were each received a 1/3 weight (for each of the 3 stakeholders). The results can be seen in Appendix A.2.

3.3 Constraints

This project is constrained in several ways that limit the design space. The team met with the advisor and the clients at UMass Medical School to develop an approach that will meet the objectives while still conforming to the constraints.

The device must cost less than the budgeted amount. This device had a budget of only $608. Culturing and testing skin grafts through assays and experiments is prohibitively expensive. In order to stay within the budget, grafts and skin samples were acquired through the advisor, Professor Pins, and UMass. The client agreed to supply the initial tissue for validation of the device and the skin graft for characterizing the tissue mechanical properties. Excised human skin was used to test the mechanical device. Human skin was the best choice because this device will stretch cultured human tissue if applied in practice. The properties of the cultured skin will closely match the properties of excised human skin. Synthetic grafts that could be acquired for this project contained a synthetic dermis scaffold and a keratinocyte cultured epidermis using previously published methods (Shores, Gabriel, & Gupta, 2007). Eventual testing will use tissue-engineered skin grafts from Professor Pins's lab.

The device must be completed within the allotted time. Every objective was held by the 28-week constraint. Each objective contained a time frame to complete and had to be completed before the final paper was due. Because the project involved cell culture and sample

loading cycles, a single phase of the project took up to three weeks solely in preparation time. Because each stage of the project required adequate time, the 28-week limitation was a very important consideration with respect to the constraints of the project.

The device could not be cytotoxic; therefore, bioinert, biocompatible materials were the apparent class of materials to choose from. If the materials used to create the device are cytotoxic, it would defeat the purpose of the stretching device. Cell death caused by cytotoxicity was considered unacceptable. Several other tissue culture applications have used polycarbonate as a good biocompatible interface (Gebelein, 1986). One portion of the device that had to be bioinert was the chamber in which the sample was held, whether that would be a well plate or a full bioreactor. Polycarbonate was a great option for this application because is very machinable and autoclavable. This material was very useful because the bioreactor was custom built. The second component that contacted the skin was the clamps. Metals would potentially be best for this application; though many metals are biocompatible, some have deleterious effects. The clamps were machined out of 316 L stainless steel. This stainless steel alloy is low carbon and the most corrosion resistant. 316 L stainless steel is listed as medical grade stainless and worked well in this setting as well.

The applied stresses and strains as well as the attachment of the skin to the device could not compromise the mechanical stability of the tissue. The stresses and strains were the most important component. Strain rate as a subset of stain became vitally important because of the viscoelastic properties of skin. The mechanical stimuli needed to increase cell growth. Applying too much stress would result in cell death. Additionally, straining the skin at a high strain rate and increasing the stiffness of the skin would cause higher and potentially harmful stresses at normally safe strains. Actual human tissue and cultured human tissue will have different damage thresholds; however, the device was limited so as not to be able to exceed the ultimate tensile strength (UTS) or the max strain of skin, 22.67 MPa and 0.63 respectively. This device was limited to 40KPa and 10% strain to avoid even minimally damaging the tissue (Pedersen & Jemec, 2006). The attachment of skin was a difficult component. In order to apply multiaxial stresses and strains, the device needed to attach at several locations. Some cell damage from

attachment was acceptable as long as it did not compromise the structural and mechanical stability of the tissue sample. This made determination of where the sample experienced stress concentrations and where the most cell proliferation occurred critically important. If approximations are made with the assumption that stress is uniform across the sample then calculating stress concentrations will not be necessary. Beyond the benefit of simplifying calculations, a uniform stress will ensure that effects increasing proliferation and stability are relatively equal across the entire sample. Several options for attachment are clamps, cryogenic grips or cryogrips, hooks, and adhesives.

3.4 Revised Client Statement

The original client statement was:

"Design a device that can perform uniform multiaxial stretch of tissue-engineered skin grafts during culture to accelerate *in vitro* growth."

In order to narrow the scope of the project, the team conducted background research, interviewed UMASS Medical doctors, and determined a ranked objectives list. Based on qualitative and quantitative data, the team came up with the following revised client statement:

"Design a novel skin stretching device within a bioreactor that can perform uniform multiaxial stretch of tissue-engineered skin grafts during culture to accelerate *in vitro* growth. The device must reproducibly apply controllable stresses and strain rates with a maximum stress and strain of 40 KPa and 0.1 (Pedersen & Jemec, 2006), respectively, without compromising the mechanical integrity of the sample.

The device must be easy to use, assemble, and sterilize. It must be safe for the user, and all components that contact the sample must be fully biocompatible and bioinert. The measure of accelerated growth and of the results' reproducibility must be statistically significant ($p \leq 0.05$).

The design process must be completed in less than 28 weeks with a budget of $608 to yield a device that is marketable, useful, and visually appealing."

3.5 Project Approach

An overall layout of the project was set up to determine what needed to be done to complete the project by the required deadline. The distribution of labor for the project was divided specific to skills, knowledge, and experience of each member. The tasks and tentative deadlines associated with the project were collected and organized into a Gantt chart. All tasks were listed and assigned a time length. The Gantt chart, seen in Appendix A.1, organizes the design process so that the team can visualize the scope of the project and break a large, long-term assignment into smaller, more manageable tasks. The Gantt chart is useful because it keeps the team on track, bringing into consideration the time that can be allotted for each task and the net time the project will take, barring unexpected delays.

The initial phase of the project focused on problem definition and background research. First, the client statement was analyzed so that the group could gather what the clients actually wanted from this project. These wants were then shaped into clear objectives. The team also formally defined the design space. The outermost boundaries of this imaginary space were the constraints. Defining constraints oriented the project in the proper direction and focused the creativity of the team toward one ultimate and achievable goal. Research was undertaken to better understand the project topic as well as gain insight into solutions to the problem the project sought to solve or similar problems with different applications. The research focused on the objectives, functions, and constraints. Extensive preliminary topics included the background information, current solutions, limitations to products on the market, and gaps in technology on the market. The understanding gained from thoroughly researching problems in this scientific field helped the team to establish a need for the proposed project and a clear path to engineer a viable solution.

The next stage was the design phase. The team had gained enough knowledge on the state of the art and potential for improvement to begin brainstorming. The team established methods of satisfying each function, also known as means. Then the means were ranked based

on performance and viability, and were used to generate a number of design alternatives. The design alternatives were evaluated in the same manner and then a final design was chosen.

Once the design was chosen, the realization phase began. This included researching potential materials to form the design, identifying solutions to design problems, and machining the actual parts. The design space was taken into consideration with each decision made about the final design.

After the design was fully realized, testing proceeded. Testing included acquiring materials to conduct each test as well as tuning the device so that it works properly and reproducibly under test conditions.

The final phase of the project was data collection and analysis. With all the previous steps completed, the team advanced toward implementing the device in its intended use, acquiring data that demonstrated the effectiveness of the device and analyzing those results to deduce the far-reaching implications.

Chapter 4: The Design Process

4.1 Introduction

Once the necessary objectives for the final device were established, the focus changed from what the device needed to be to what the device needed to do. The functions, specifications, and the different means of accomplishing them needed to be determined. The team conducted brainstorming sessions, read literature reviews, and participated in interviews with the advising team to create a set of promising alternative designs. The final design was chosen after a thorough ranking against each objective, function, and constraint. The choice was primarily justified by its performance in initial conceptual testing.

The objectives were ranked using a pairwise comparison chart, a tool for comparing objectives against each other in order to establish importance. Objectives were scored with either a 1, indicating that the objective takes precedence over the objective with which it is compared, or a 0, indicating that the objective does not take precedence. The pairwise comparison charts of each client, the team, and the user were evaluated equally and averaged. These objectives ranked in the top three ordered from first to third: the device is accurate, is precise, and minimally damages the tissue.

The functions were determined by brainstorming sessions oriented toward the use of the device. The device needed to stretch skin. All sub functions were branches off of the overall function. Specifications were determined after researching for textbook values that could be reasonably compared to this project. Techniques such as reverse engineering, in which devices with similar functions are theoretically dissected and analyzed, were employed. Ideas gained from this tool increased the variety of ideas that were considered and added to the creativity of the device. A comprehensive functions-means tree was also used to inspire creative ideas by imagining all possible ways to address a need. Specifications for each function were determined by previous literature, with special attention to the results of Dr. Chin's experiment. Specifications were vital in determining the design's functional performance and capabilities.

Similar to previous parameters design alternatives were determined by brainstorming sessions in which the team combined different means into a viable complete conceptual idea. The top four design alternatives, which will be outlined in detail shortly, were the column design, the ring design, the custom fit design, and the piston design. The final two designs, the custom fit design and ring design, were ranked extremely closely in the evaluation matrices completed by the team. The ring design was chosen as the final design based on feedback from advisors and taking into consideration the composite score of 93% it received from the evaluation matrix. Evaluation matrices can be viewed in their entirety in Appendix A.4 and sketches of designs can be viewed in Appendix A.5.

4.2 Needs Analysis

In order to address the process of successfully making a mechanical device to stretch tissue-engineered skin grafts, the team needed to construct a pairwise comparison chart (PCC) with the potential objectives. The objectives list that was formed contained items such as minimally damages tissue, safe for the user, easy to use, precise, accurate, can apply various testing regimes, durable, visually appealing, efficient, and inexpensive. The team, the users, and the clients each filled out the pairwise comparison chart. The clients for this project were Dr. Raymond Dunn, Dr. Michael Chin, Dr. Ronald Ignotz, and Dr. Janice Lalikos from UMass Medical, and, Professor George Pins and Professor John Sullivan from Worcester Polytechnic Institute. The effective user was our graduate student advisor, Amanda Clement. The design team took each client's response, the user's response, and the team's response and averaged them. The results of the averaged rankings are shown in Figure 3, including the percent breakdown of how important, comparatively, each objective was decided to be. A more comprehensive set of tables, including the completed charts of each advisor, the user, and the team, can be found in Appendix A.2.

Rank	Objective	% Score
1st	Precise	15.7 %
2nd	Minimally damages tissue	13.7 %
3rd	Accurate	13.1 %
4th	Safe for user	12.8 %
4th	Can apply varied testing regimes	12 %
6th	Durable	7.8 %
7th	Efficient (max data per test)	7.4 %
8th	Inexpensive	7.4 %
9th	Easy to use	6.3 %
10th	Visually appealing	3.7 %

Figure 3: Ranking of objectives

Precision and **accuracy** were seen as two of the most important objectives because stretching the sample needed to be reproducible every time the device was used and accurate to whatever stress or strain was desired. **Minimally damaging the tissue** was ranked second because the device was designed to improve engineered tissue grafts through mechanical loading, and substantial damage would render the tissue useless and defeat the purpose of the device. Conjointly, being able to **apply varied testing regimes** based on the user's needs was another top objective. The properties of skin can vary greatly. One example is strain rate dependence. If this device is intended to quantify how strain rate affects tissue growth it then becomes very important to be able to change the loading cycle parameters. Because of this importance, this objective was ranked fourth. Organization and compilation of this information created an important reference that was used to prioritize the objectives when completing research, brainstorming, or choosing design alternatives. The ranking displayed in the PCC reflects informed opinions about the proper approach to solve a complex problem. Unfortunately, there were a few mentionable discrepancies in the scoring; the objectives **safe** and **inexpensive** both received the lowest possible score (0/9) and the highest possible score (9/9) from different clients. Regarding safety, the high score could indicate that safety of the user ranks above all, and the low score could be given with the assumption that a device that stretches tissue in a laboratory setting has no potential to harm the user. With expense, one could assume that cost does not compare to the importance of the functionality of the device, whereas another could perceive cost as a significant limiting condition of the design process.

There was also a notable disparity in the ranking of **varied testing regimes**, with scores ranging from (1/9) to (8/9). Most participants considered this an important objective, potentially because customizability would give the device more functionality and value. The low score (1/9) could indicate that this feature, while it expands possibilities in testing and data collection, is not as essential to the device's function.

4.3 Functions and Specifications

The design team came up with functions to generate design alternatives that effectively met the most important design considerations for the device. Then the team met and chose the most feasible options. First, the device needed to **perform uniform, multiaxial loading** of tissue-engineered skin grafts during culture. Tension plays a critical role in the growth and development of skin. Multiaxial testing has shown better effects on the mechanical properties of the skin when compared to uniaxial testing (Daya & Nair, 2008).

The device also needed to **vary the stresses and strain rates** so that the user could control how much stress was applied to the skin sample, as well as the duration of the applied load. This system allowed for reproducibility of force patterns delivered by the device while enabling customizability based on user preference.

The tissue sample needed proper nutrition with constant **access to medium at the air-liquid interface**. A tissue sample would die if no medium were provided, or if removed from the medium for too long. It was critical that the sample was in medium to provide the nutrients it needed to survive and grow.

The device needed to **secure the sample** and **prevent slippage** in order to perform reproducible testing and adequately apply loading. The method of securing the skin sample also needed to cause minimal damage and not destroy the structural integrity of the tissue.

Using the functions established above, the team developed a list of specifications for the device. Specifications are statements that define the device's required properties and attributes. The chosen specifications were based off of the literature review and Dr. Chin's experiment; while the yield strength of skin is much higher than the values chosen from

literature, the device should not even come close to stretching the sample to its endurance limits during testing. The intent was to avoid any unnecessary damage to the sample or its constituents, which could occur with an applied load much lower than the yield stress. From analysis of *in vivo* skin stretching experiments in the literature, it was decided that the maximum stress and strain that the device should apply were **0.04 MPa** and **0.1**, respectively (Pedersen & Jemec, 2006). These values did not harm the tissue and still applied enough force to cause beneficial reactions from the skin. While there was no lower limit for the stress or strain, the device was able to load the sample at small enough intervals that a variety of loading cycles could be achieved.

The device needed to perform testing cycles for a specifiable **duration ranging from 2 seconds to 2 hours, with customizable waveforms and rest periods**, chosen to allow a large range of adjustability. This device should be variable enough to meet all of the user's needs for testing. Allowing for cycles to be as brief as 2 seconds per cycle demanded that the device was precise and controllable enough to provide reliable data and accurate loading. The upper cutoff of two hours was chosen to prevent damage from sustained tension (Sanders, Goldstein, & Leotta, 1995). Both bounds were intended to improve upon the versatility of Dr. Chin's device, increasing the range of cycle durations from his experiment. By extending the range of stresses, strains, and cycle durations that the device is capable of, the team hoped to allow for analysis on how different loading conditions affect the outcomes of testing.

During a brainstorming session, the team came together to generate different means of satisfying each function. Figure 4 is an extensive, creative, and not necessarily feasible compilation of means that could suit each function. The design alternatives that will be described later focus on only a few of the countless means proposed for each function; however, creating a large list was a way to avoid limiting the design space, and an individual's creative (even if not completely realistic) ideas can inspire more ideas, some of which might be possible.

The first mean to discuss was sample fixation. One method of sample attachment could be through the use of hooks. A system involving hooks could be quick and easy to set up,

though the hooks would damage the sample. Another possibility was glue, which would hold the sample very evenly and securely, but it could have been complicated to remove the skin from the device. A third option was clamps, which are a good way to lock a sample into place so that a force can be applied across the sample. Also, clamps provide a secure grip without piercing the skin, avoiding unnecessary damage to the surface of the sample.

After there was a means for sample fixation, ideas were brainstormed for the next function. In order to perform multiaxial testing, potential methods included expanding a moving platform, changing pressure with a vacuum, or expanding a membrane. With a moving platform, the sample could be fixed to separate plates that expand and would induce tension from point locations. With a vacuum or an expanded membrane beneath or above the sample, a uniform stress could be applied across the sample with an induced pressure. While a vacuum alone may be difficult in a wet environment, a membrane could elicit the same pressurized response without disrupting access to the medium.

There were many possibilities to vary stresses and strain rates however an efficient and easy method would be most beneficial. To vary the stresses and strain rates, system control options were looked at. Less expensive, simpler options were knobs or added weights. A pump or linear actuator could be used to increase the precision from that offered by mechanical systems alone. More precision could be gained from a computer programmable control system, which can allow for accurate and specific stress and strain control.

In order for the tissue sample to survive throughout testing, it needed to have access to medium. One option for providing medium was to mist or spray it across the sample continuously, or at set intervals. Another method was to sit the sample atop a sponge saturated with medium, or upon a screen that keeps the sample in contact with the air while maintaining access to the medium.

Prevent slippage/ secure sample	Perform multiaxial testing	Vary stresses and strain rates	Allow access to media
Hooks	Vacuum pressure (pulling/ pushing)	Computer program (e.g. LabView)	Put container in incubator
Fusing (melting/ burning)	Balloon pressure (membrane/ diaphragm)	Heat controlled (e.g. bimetallic strip)	Use existing bioreactor
Friction/ abrasive texture/ grooves	Mechanical (clamping and stretching)	Knobs	Build bioreactor into device
Clamps	Exert force on whole sides	Valve – media/ air inflation	Pump media through sample
Velcro, glue, tape	Exert force on edges	Pump/ compressor	Spray media
Cryogrips	Exert force around edges of a circular sample	Electric/ magnetic flux	Use a sponge
Vacuum	Pressurize media under/ over sample	Balloons	Flow media over sample
Centripetal/ centrifugal force	Pressurize air over/ under sample	Increase speed (centripetal/ centrifugal force)	Dialysis-type bag
Weights	Centripetal/ centrifugal force	Remote control	Create synthetic capillaries
Elastics	Fix to moving parts	Negative feedback loop	Drip media
Magnets	Expand secured platform	Cranks	Solid media
Sutures	Weights	Actuators	Mist media
Bindings	Magnets	Add weights	

Figure 4: An extensive functions-means list generated during a brainstorming session

After the means were established, they were integrated into an evaluation matrix, shown in Appendix A.4, which allowed for qualitative and quantitative ranking. The matrix was completed by each team member individually then averaged to obtain a final ranking. The upper portion of the matrix is a list of constraints that the design alternative must absolutely meet in order to be considered. Each alternative was either given a check or an "X" to state whether or not the design met that constraint. If the alternative design did not meet the constraint, it was automatically disregarded. Fortunately, all the designs met all the constraints listed above. The lower portion of the matrix is the objectives list. Each objective was graded from 1-4, 1 being the worst and 4 being the best, with a respective set of quantifiers. The designs were not evaluated against each other but rather how well they met the objectives individually. This method eliminated any biases toward a particular device. A quantitative table was created to establish the effective rankings of the means with respect to how well they suited the functions and weighted objectives, as shown in Figure 5.

Rank	Mean	Percent Ranking (100% = completely fulfills function)	Deviation from top score
Function: Prevent slippage/Secure Sample			
1st	**Clamps**	89.22%	-
2nd	**Glue**	87.54%	-2%
3rd	**Sutures**	77.27%	-12%
Function: Perform controlled, multiaxial stretch			
1st	**Expanding secured platform**	89.22%	-
2nd	**Motor**	87.36%	-2%
3rd	**Pressurized air/media**	76.19%	-13%
Function: Vary stresses and strain rates			
1st	**Negative feedback loop**	98.50%	-
2nd	**Computer program (LabView)**	97.92%	-1%
3rd	**Cranks/Knobs**	81.75%	-17%
Function: Allow access to media			
1st	**Use existing bioreactor**	97.67%	-
2nd	**Build bioreactor into device**	96.30%	-1%
3rd	**Create synthetic capillaries**	86.81%	-11%

Figure 5: The results of the evaluation matrix.
The three highest ranked means are shown, in order, for each function, and ranked out of a maximum 100% value corresponding to the maximum score the mean could have achieved. The deviations on the right show the discrepancies between the top value and the lower ranking values. There was not a significant difference between the top two means for any of the four functions.

4.4 Preliminary Designs

With guidance from both the functions-means chart in Figure 4 and the evaluation matrix results in Figure 5, the team generated a number of design alternatives, four of which are outlined below. Each design satisfied the requirements; the designs were easily adaptable in case they needed to be placed in an incubator or bioreactor with a controlled environment suitable for tissue culture. As such, each design would fit in and be fully compatible with an incubator or bioreactor setting.

Multiple design alternatives were drafted in the initial brainstorming session. Presented below are a few examples. These alternative models show the trial and error progression of the device and the evolution of the design. All of the preliminary designs had a method to secure the skin sample and apply multiaxial stretch. Design Alternative 2, shown in Figure 6, proposed the idea of clamping the skin sample in a well plate and having a funnel underneath

direct the cables, which would run on the outside of the funnel and into the well plate to stretch the skin.

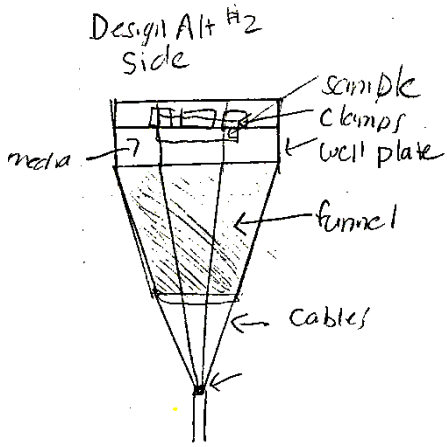

Figure 6: Design alternative 2

The design alternatives ranged from big-picture overall design concepts to small scale details as shown is design alternative 5 (Figure 7). This picture depicts a more in depth solution to secure the sample and ensure that the stress would be evenly applied. Again, the sample is submerged in media and clamped to hold it in place. Additionally, sutures instead of cables are used to stretch the sample in this design.

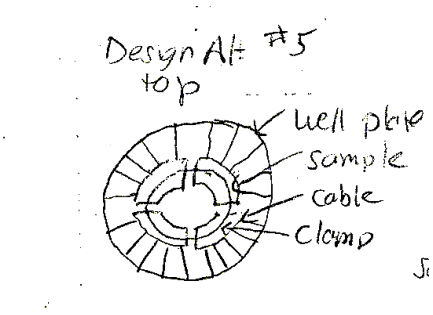

Figure 7: Design alternative 5

Design alternative 10, shown in Figure 8, is more complex and incorporated motors, belts, and gears. The motor would be connected to a gear, which would turn. The turning gear would cause the shaft to move up and down, causing cyclical loading of the skin.

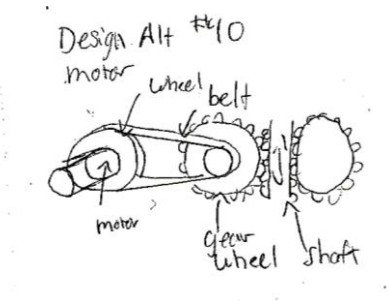

Figure 8: Design alternative 10

Design 21, shown in Figure 9, displays a c-clamp structure with adjustable screws to secure the sample. The screws could be adjusted to properly clamp skin samples of different thicknesses. The screws had attachments to increase the surface area under the clamps and allow for better fixation of the sample.

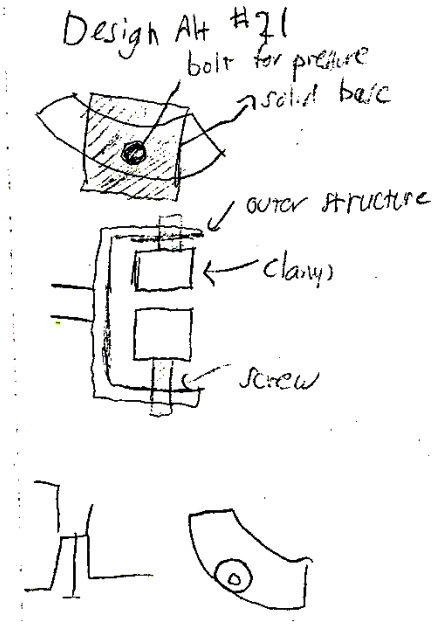

Figure 9: Design alternative 21

4.4 A The Column Design

In this design shown in Figure 10, the skin sample would be secured at the air-liquid interface on all sides. Sitting in media beneath the sample, a series of columns could be linearly actuated and controlled by a computerized system. The columns could have been uniformly actuated or controlled independently, allowing for not only controllable stretch of the sample

but also the application of micro-stresses/-strains. The established pros and cons of this design are listed in Figure 11.

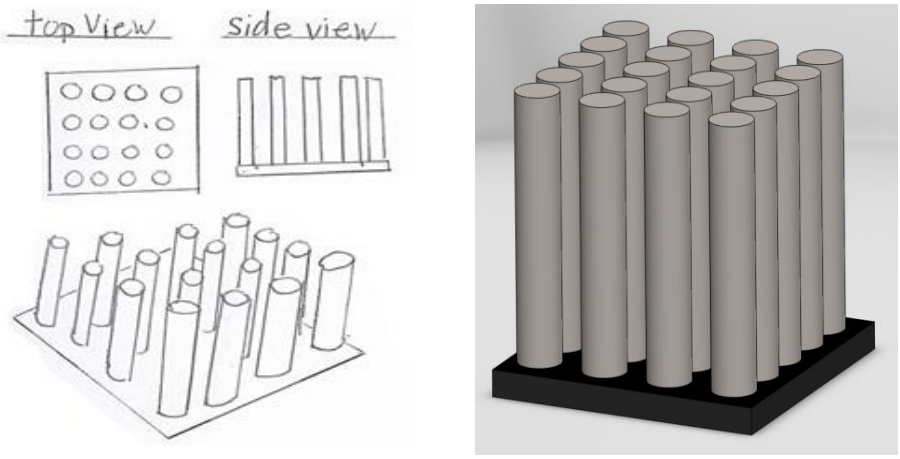

Figure 10: (Left) Column Design initial drawing, (right) computer-aided drawing

Column Design	Pros	Cons
	• Allows for great control of the sample • Multiple data points can be taken from a single sample with varied conditions	• Requires sophisticated (and expensive) technology, equipment • Fabrication of such small parts may be too advanced and expensive for the team's skill level and budget

Figure 11: Pros and Cons of Column Design

4.4 B The Custom Fit Design

Figure 12 features a skin sample held at the air-liquid interface by clamps on all four sides. The clamps would be secured to arms that could expand or contract in the direction perpendicular to the edge of the sample. Beyond expanding and contracting, the arms would be able to move along tracks that would run parallel to the edge of the sample. In this manner, the sample could be stretched to have variable lengths and widths, or potentially be stretched at a skewed angle. Pros and Cons of the Custom Fit design are outlined in Figure 13.

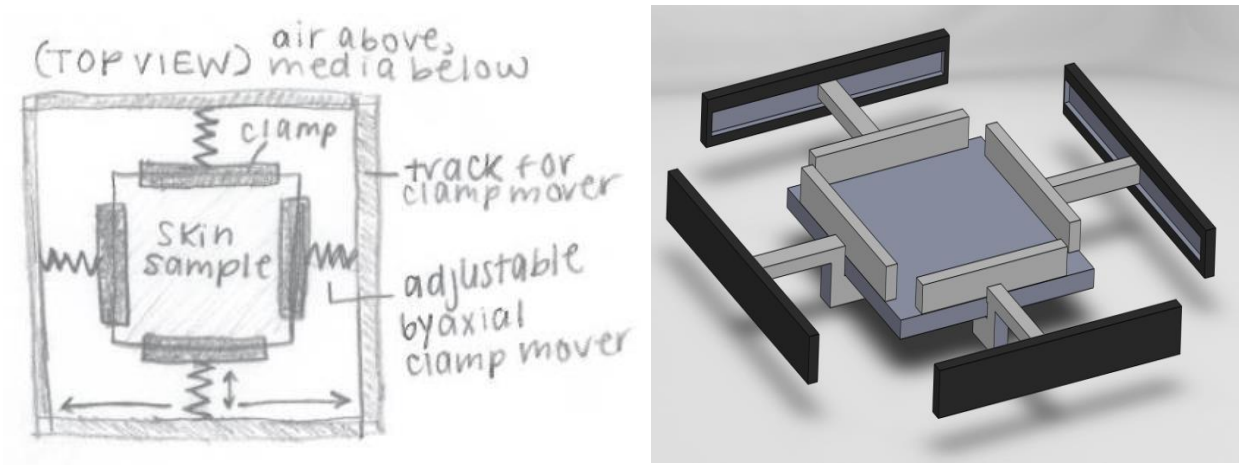

Figure 12: (Left) Custom Fit Design initial drawing, (right) computer-aided drawing

Custom Fit Design	Pros	Cons
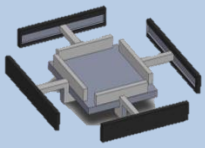	• Allows for significant variability in the desired size and shape of the sample • Enables a wide range of stretching cycles • Device could supply user with grafts of shapes and sizes tailored to his specific need	• Requires four motors that can move biaxially, independent of each other • Creates a challenge with sterility

Figure 13: Pros and Cons of Custom Fit Design

4.4 C The Expanding Ring Design

In the Expanding Ring Design shown in Figure 14, has a skin secured on a cylindrical base that is filled with media. The sample would be clamped to sections of an expanding ring, with a smaller diameter than the base, which would be attached to multiple cords. The cords would run around and down the base of the cylinder, meeting at the bottom. A motor would actuate the system, pulling the cords around the lip to expand the ring and the sample. The advantages and disadvantages of this design are shown in Figure 15.

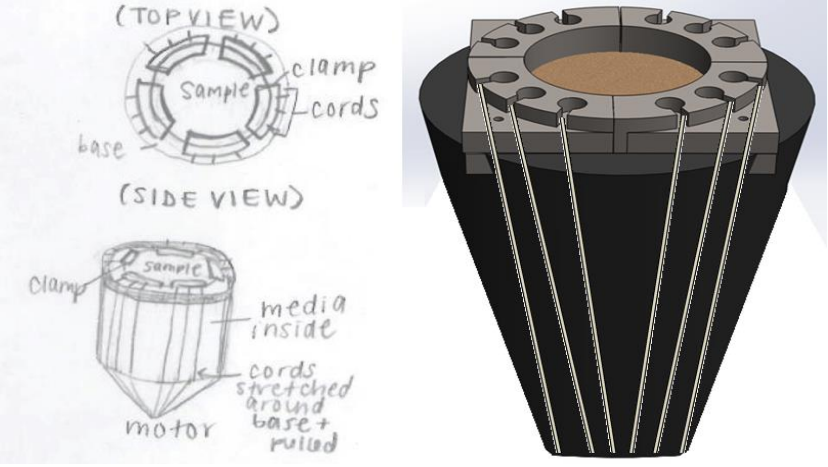

Figure 14: (Left) Expanding Ring initial drawing, (right) computer-aided drawing

Expanding Ring Design	Pros	Cons
	• Only one motor to actuate in one direction • Less expensive • Easier to program and control • Easier to calculate applied loading than other less uniform methods of fixation	• Challenge to maintain sterility • Can only apply a uniform stretch, not as versatile as other designs

Figure 15: Pros and Cons of Expanding Ring Design

4.4 D The Piston Design

The Piston Design shown in Figure 16 would use a piston and a cylinder filled with medium to stretch a sample. As the piston was fired, the pressurized media inside the cylinder would exert a uniform force on the sample, assuming that the sample is fixed uniformly with either a clamp or glue. Pros and cons are shown in Figure 17.

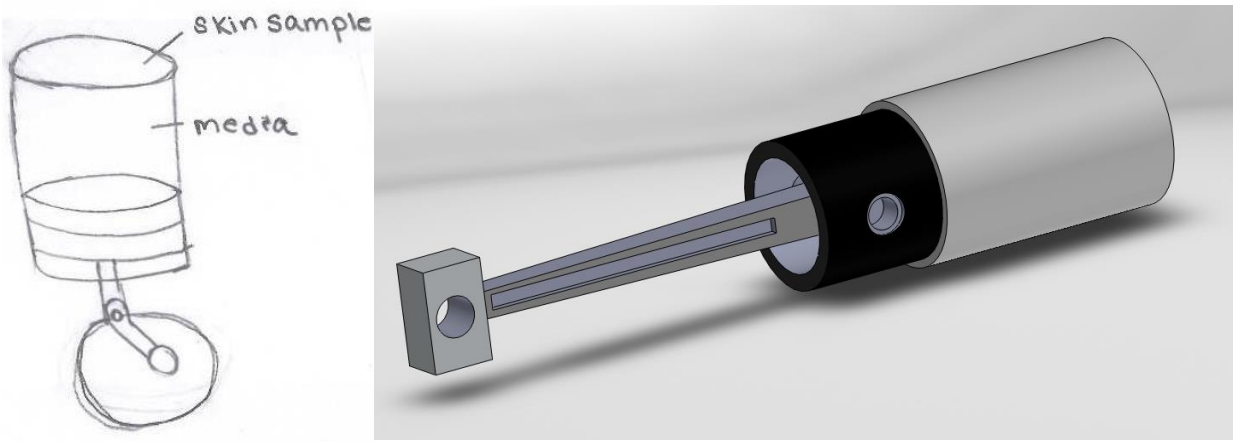

Figure 16: (Left) Initial sketch of The Piston Design, (right) computer-aided drawing

Piston Design	Pros	Cons
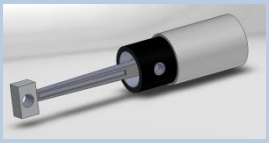	• Least expensive – uses simple, traditional technology • Highly reproducible because motion is applied by one mechanical movement • Few parts means easy setup	• Pressure would be exerted uniformly so this device is less versatile than others • Using media to pressurize the sample introduces uncertainties • Small size of device would be difficult to produce and load accurately and reproducibly

Figure 17: Pros and Cons of Piston Design

4.4 E Summary

While these four designs featured were merely a few of the proposed ideas, they give a good representation of the flexibility of the design space. More importantly each design identifies a unique solution that achieves the same overall goal. As shown in Figure 18, there were pros and cons associated with the different designs, although each still satisfied the minimal requirements and did not conflict with any project constraints. Full sketch models of all alternative designs can be seen in Appendix A.5. Without constructing each design, only educated assumptions could be made to the viability of each design; with research into materials required for manufacturing and testing and their respective costs, it seemed feasible that each could be constructed within the available time and budget. However, models such as the column design were clearly associated with higher costs and more sophisticated

technology. With the team's abilities and the project's scope in mind, the pros and cons of each possibility were assessed in order to establish the most feasible and functional options.

Design	Pros	Cons
Column Design 	• Allows for great control of the sample • Multiple data points can be taken from a single sample with varied conditions	• Requires sophisticated (and expensive) technology, equipment • Fabrication of such small parts may be too advanced and expensive for the team's skill level and budget
Custom Fit Design 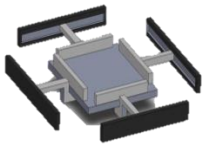	• Allows for significant variability in the desired size and shape of the sample • Enables a wide range of stretching cycles • Device could supply user with grafts of shapes and sizes tailored to his specific need	• Requires four motors that can move biaxially, independent of each other • Creates a challenge with sterility
Expanding Ring Design 	• Only one motor to actuate in one direction • Less expensive • Easier to program and control • Easier to calculate applied loading than other less uniform methods of fixation	• Challenge to maintain sterility • Can only apply a uniform stretch, not as versatile as other designs
Piston Design 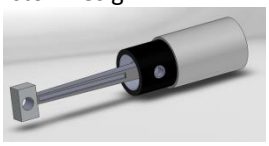	• Least expensive – uses simple, traditional technology • Highly reproducible because motion is applied by one mechanical movement • Few parts means easy setup	• Pressure would be exerted uniformly so this device is less versatile than others • Using media to pressurize the sample introduces uncertainties • Small size of device would be difficult to produce and load accurately and reproducibly

Figure 18: Summary of pros and cons

4.5 Final Design

Choosing a final design involved both qualitative and quantitative analysis. The evaluation matrix was used to rank the designs quantitatively, as shown in Figure 19. After the team combined its scores, the final rankings for the designs were established. The Ring design came in first, followed by the Custom-Fit design, the Column design, and then the Piston design. While a numerical ranking was used to quantitatively and objectively determine the best choice, the results showed a very slim margin between first, second, and third. As the three highest ranking designs had scores that were not significantly different, the team could

not choose a top choice. Upon meeting with the client, it was agreed that the Expanding Ring held the most promise as a design option.

Total Scores			
1st	ring	93.16%	0.00%
2nd	custom fit	93.04%	-0.12%
3rd	column	92.62%	-0.54%
4th	piston	84.79%	-8.38%

Prevent slippage/ secure sample			
custom fit	ring	column	piston
89.22%	89.22%	87.54%	89.22%
1st	1st	4th	1st

Vary stresses and strain rates			
custom fit	ring	column	piston
97.92%	97.92%	97.92%	77.45%
1st	1st	1st	4th

Perform controlled, multiaxial stretch			
custom fit	ring	column	piston
87.36%	89.22%	87.36%	76.19%
2nd	1st	2nd	1st

Allow access to media			
custom fit	ring	column	piston
97.67%	97.67%	97.67%	96.30%
1st	1st	1st	3rd

Figure 19: Results of design ranking.
The quantitative evaluation of our preliminary designs, with the total rankings at the top. The rankings are grouped by function, and they are ranked first out of a maximum score of 100%, and then beneath they are ranked against each other.

After the team combined its scores, the final rankings for the designs were established. The Ring design came in first, followed by the Custom-Fit design, the Column design, and then the Piston design. While there is a numerical ranking, the method of ranking them and the very slim margin between first, second, and third suggest all three options are good. Upon meeting with our client, it was agreed that the Expanding Ring held the most promise as a design option.

4.5 A Design Refinement

The final design was assessed by taking each individual component and determining the best way to implement it. The functions means list was used to substitute alternatives into each design consideration. Design considerations are a physical building component of the entire device or a means of performing a function that is integral to the overall performance of the device. The most promising options were ordered from best to worst. These options were then drawn as they would appear in the design or function normally in the device. In several instances, one component, such as a clamp, was considered in several different forms. One form was an upper and lower plate attached by a screw. Another form was similar to a c-clamp

where the sample is fixed between a plate and a surface that is tightened onto the screw. Similarly, the shape of the sample was considered, assessing the benefits of using a circular sample over a square or a rectangle. This procedure highlighted each possible choice for the final design. The choices could then be evaluated to determine which combination of design considerations yielded the best possible product.

4.5 B The Device

The device can be seen in its entirety in Figure 20, with each component outlined in Figure 21.

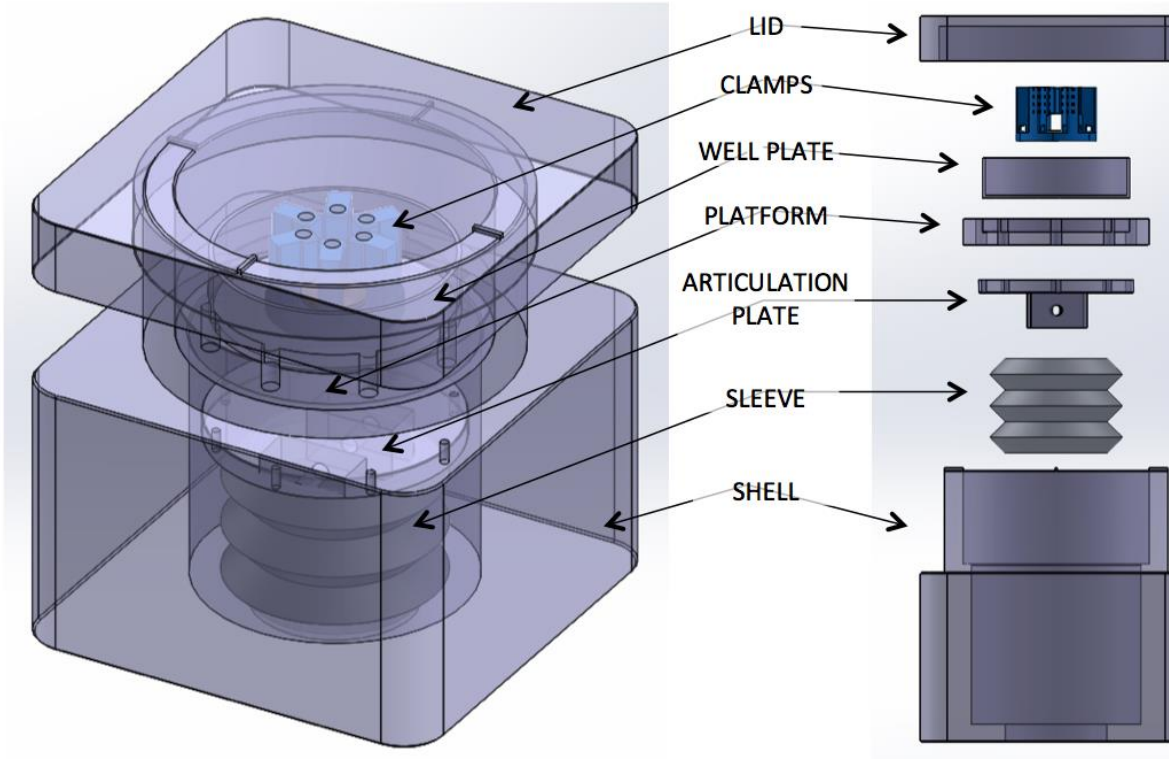

Figure 20: The final device.

Component	Picture	Description
LID (Polycarbonate)	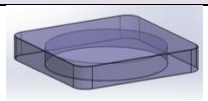	The lid must enable gas exchange while restricting the passage of contaminants from the incubator, working identically to the tortuous path mechanism of a well plate lid.
SHELL (Polycarbonate)	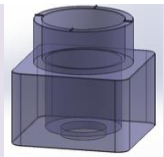	The shell will house the entire device, with exception of the motor, and will be covered by the lid to preserve sterility.
WELL PLATE (Polycarbonate)	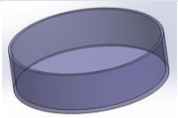	The standard polystyrene 60 mm^2 well plate will hold the sample and the medium.
CLAMPS (Medical Grade 316L Stainless Steel)		The clamps (6) will grip the sample with a screw that enters at the top and grips the sample on the base. There will be a hole that is level with the sample that will connect to a cord that will enable stretching of the sample.
AVERTERS (Posts: Polycarbonate Pins: Stainless Steel)	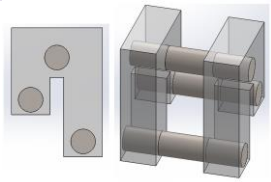	The averters (6) sit on the edge of the well plate and redirect the motion of the cords so that the clamps' path of motion remains level with the sample but the cords are able to pass around the side of the well plate.
PLATFORM (Polycarbonate)	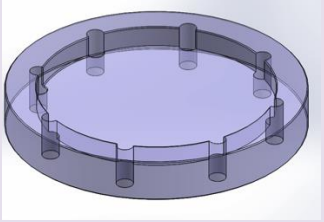	The platform will be the support structure for the well plate, and will have holes through which cords can pass to stretch the sample. The platform will sit atop a lip running across the inner circumference of the shell and held in place.
ARTICULATION PLATE (Polycarbonate)	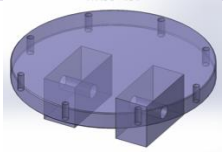	The articulation plate will be in the lower portion of the shell and has holes through it to articulate with each cord, and will be actuated by a motor that connects to the bottom by a screw.
SLEEVE	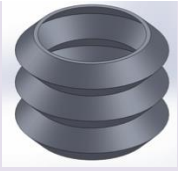	The sleeve will be secured in an air-tight manner to the articulation plate and the shell and will be expandable without exerting a supporting or resisting force on the system. As the motor raises and lowers the articulation plate, the sleeve will maintain that barrier necessary for sterility without restricting motion.

Figure 21: The constituents of the final device

An additional component of the device, used only for assembly, is the cap shown in Figure 22. The cap serves to hold all clamps in place while the sample is being fixed and the cords are attached. This maintains the sample at the center of the well plate and allows for accurate and reproducible fixation and assembly across different users.

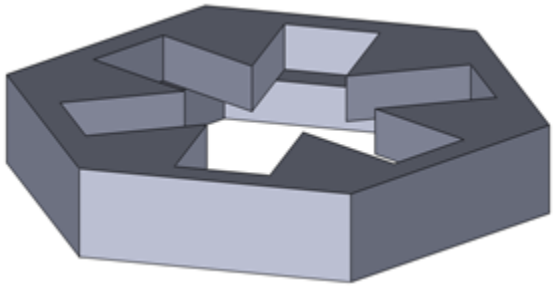

Figure 22: The cap, a custom part used for fixing the sample.

Beyond the custom components of the device, a motor was acquired to actuate the system. The nylon sutures, attached to the clamps in the 60 mm well plate, were fixed into place with crimping beads on the articulation plate. The movement of the articulation plate was guided by the movement of a rack and pinion setup. This movement translated to the application of stress across the sample. The motion of the actuator is executed by the VEX stepper motor that is attached to the rack and pinion; this system is shown in Figure 25. The VEX stepper motor is a 2 ft. /lb. motor with a minimum step of 0.0196 mm. The system has an encoder that recorded the distance the linear actuator traveled in respect to the turning of a 60 and 12 tooth gear system. When the program is run, the rack will initially travel all the way up until it activates the limit switch. When the slide depresses the limit switch, it is in the HOMED position and sets the encoder position to 0. Immediately after being homed, the slide travels down a maximum distance of 3 mm and then after a two second delay returns back to the 0 position. The motor was programmed with C++ and transferred via a USB to an Arduino Uno controller. The travel distance, speed, and delay times can all be manipulated according to the user's specifications. See Appendix E: Arduino Uno code.

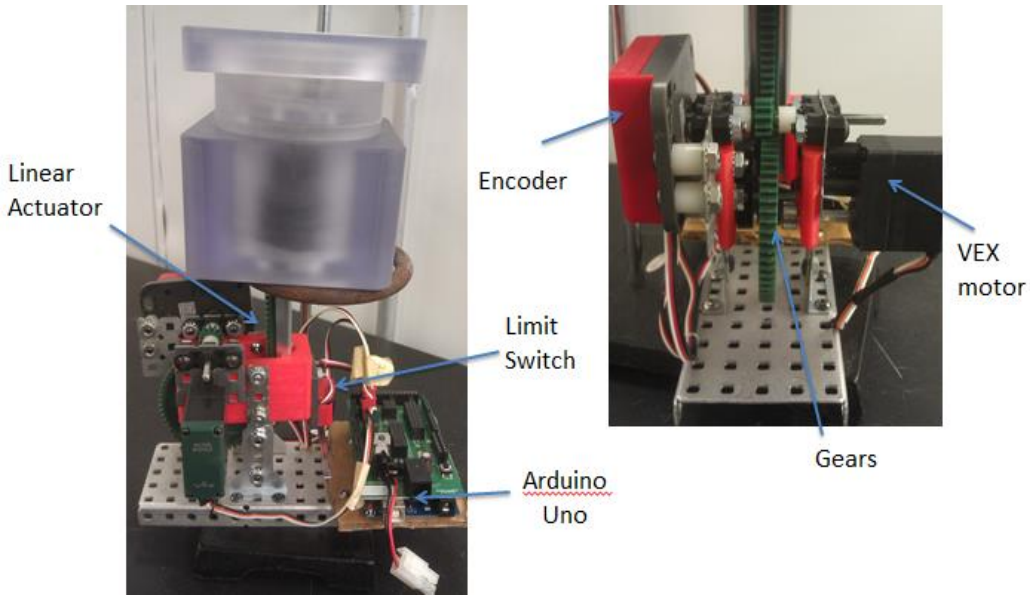

Figure 23: The rack and pinion setup with motor.

4.5 C Dimensional Analysis

Before a comprehensive CAD model could be created, the dimensions of the device needed to be established. In order to establish bounds, the necessary dimensions were accounted for by first measuring from the inside outward. Starting with the skin sample size, dimensions for a well plate were chosen, some room was allowed for the internal components of the device, and a wall thickness for the shell was added. This gave a minimum value for the spatial footprint of the device. Next, the dimensions were assessed from the outside in; the outer dimensions of the available stock material served as the maximum outer bound of the shell. Room was incorporated for the width of the shell, and a maximum inner space was established. With these bounds for the size of the device, dimensions were chosen that kept the spatial footprint in the incubator to a minimum, used the least material to reduce cost and waste, and allowed for the greatest possible sample expansion within the size limits.

The device tested a circular skin sample with a 15mm diameter. The clamps, as seen in Figure 24, extended 7.5mm off the sample in all directions creating an outer diameter of 30mm.

Figure 24: Clamps

According to design specifications, a max distension of 3mm of the sample along the radius needed to be allowed for during testing. The maximum outer diameter of the sample in addition to the clamps during testing was calculated as 50mm. A 60mm well plate was chosen to house the sample and clamps because it was large enough to contain them with some additional room for attachment purposes. The 60mm well plate set the base mark for the minimum area needed to properly test samples according to the specifications of the device.

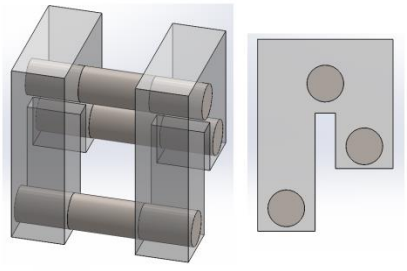

Figure 25: Averters

The nylon cords loop over the top of the clamps and are secured behind the screw. The nylon cords move from the back of the clamps through the averters. The main purpose of the averters is to reduce friction on the cords. The averters create an arch over the well plate that is also useful in keeping the clamps from being pulled out of the well plate. The averters shown in Figure 29 were 0.625 in. wide and made up of two polycarbonate posts and three 316L stainless steel dowel pins.

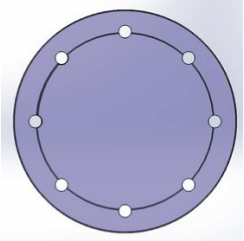

Figure 26: Platform

The well plate sat on the platform component of the ring design, seen in Figure 26. The holes on the ring design were drilled along the circumference of an interior circle with a 56mm diameter. The location of the holes allowed passage of cords from the clamps in a well plate to an articulation plate below without contact with any other surface of the device, avoiding losses due to friction. The inner diameter of the ledge was finalized at 63.6mm based off of the required wall thicknesses associated with machining the parts, approximately 3 mm.

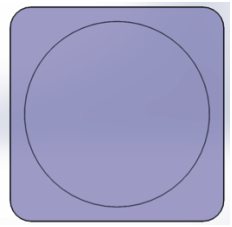

Figure 27: Lid

The original analysis yielded dimensions for a device that would be machined out of a 6in by 6in (~150mm x 150mm) block of polycarbonate. In order to reduce the spatial footprint, the chosen material was downsized to a 4in by 4in cross section (~100mm x 100mm). The lid, seen in Figure 27, was machined with a 7mm wall thickness due to limitations of the machining process. This set the inner diameter of the lid at 87.6mm. A 2 mm gap was left between the inner diameter of the lid and the outer diameter of the shell, seen in Figure 28.

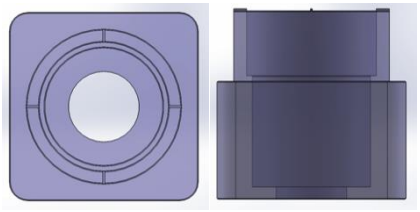

Figure 28: Shell top: side view; bottom: top view

The outer diameter of the shell was set at 83.6 mm with the initial dimensions of the stock material being 4 in. by 4 in. (~100x100mm^2). With a 7mm wall thickness, the inner

diameter of the shell was set at 69.6mm. The top of the shell was castellated to space the lid 1mm off the rim to allow for regulated gas exchange. The ledge designed to hold the platform was set at an inner diameter of 63.6 as stated earlier. This inner diameter allowed the platform to rest securely and left a 2.5mm between the edges of the lip and the outer diameter of the holes in the platform (see Figure 26: Platform).

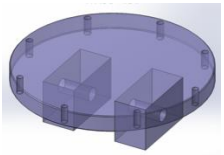

Figure 29: Articulation Plate

The articulation plate seen in Figure 29 was designed to be smaller than the inner diameter of the lip inside of the shell. The diameter was set at 58mm. Not only did this allow for the articulation plate to be placed inside of the shell, but it also allowed free movement of the plate in the vertical z axis of the device during tests. At the bottom of the plate, two columns extended downward to create a site at which the plate can connect to the linear actuator. The blocks were spaced 13mm apart with a hole bored and centered at 6.5mm below the lower surface of the articulation plate and the 10.5mm from the vertical edge of the block. The linear slide interfaced with the articulation plate between the two blocks to avoid any creation of a moment during testing. A screw fixed the linear slide to the articulation plate. On the bottom surface of the shell a hole was machined that grants the linear slide access to the inside of the shell and the lower surface of the articulation plate. The linear slide measured 23mm at its longest dimension for the cross sectional area. The hole was then bored with a diameter of 38mm to accommodate the slide comfortably. Calculations can be seen in Appendix A.8.

4.5 D CAD Drawings

Once the calculations were finalized and checked for accuracy, the model could proceed to a CAD model. The CAD model was created on SolidWorks. All dimensions were input according to the values specified in the dimension analysis. Fillets and chamfers were added to the design to remove all sharp edges making it more user friendly as well as asthetically pleasing. Each of the components of the design were inserted into an assembly and mated to ensure the dimensions were accurate.

4.5 E Machining

The CAD model for the clamps was saved under the proper .stl format and sent to the rapid prototyping quote request. The CAD models were uploaded into the computer-aided machining (CAM) software ESPRIT. The CAM software sets each cutting pass the computer numerical control (CNC) machine makes. The block of raw material must be faced first to ensure a smooth cutting surface. The software includes features to turn down the outer diameter of parts. This procedure was used for the shell, platform, and articulation plate. Creation of pockets was used for the shell, lid, and articulation plate. Bore holes were created in both the articulation plate and the platform. Chamfers and filletts were added to all parts. The island pass removes material around a raised feature. Islands were used to castellate the rim of the shell. The depth of cut of the shell created a unique problem for machining. Normal tool sets contain a maximum cut length around 2.25in. Very few milling tools can reach a depth of 4in from the top surface. Lathes can reach 4in but will cause deformation around the rim of the part the deeper it goes. To overcome this problem, a bore bar was used to remove material from the center of the stock material. This tool has a variable cutting diameter and can be custom fit to reach greater depths than the other tools.

Chapter 5: Design Verification

5.1 Preliminary Data

The device needed to be capable of fulfilling the required objectives before it could be used to evaluate the effects of mechanical loading on skin grafts. In order to establish the functionality of our device, preliminary data was collected.

5.1 A Pullout Testing

Pullout testing was conducted for the first generation of clamps. Since rapid prototyped parts cannot be tapped due to their hollow structure and loosely printed internal layers the clamps were fixed using binder clips. An elastic sample of circular geometry was placed between the clamps. A line was traced along the edge of the grips to set the zero line for the pullout testing. A weight was attached to the sample and the sample was then raised to a height of six inches off the table. The weights tested were 2kg, 1kg, and 0.1kg. The gravitational force for each mass is 19.62N, 9.81N, and .981N respectively. The test yielded complete pullout of the sample for each mass. The current base value for force applied by each clamp on the sample was .941N. Results from testing were unacceptable for proper performance of device, indicating that new clamps had to be designed.

Revisions were made to the design of the clamps in an iterative process; after continued fabrication and pullout testing, it was determined that the design must be changed altogether. Clamps resembling C-clamps were designed and fabricated from 316L stainless steel, and withstood initial pullout testing with much greater performance than the initial designs. Testing was performed on synthetic materials and then on porcine skin samples and the results confirmed their efficacy.

5.1 B Force Calculations

A force value was determined for the particular loading of the skin sample. The sample was approximated as a series of concentric rings of finite cross sectional area with an applied pressure normal to the surface and radial outward from the center of the sample. Using the equation $\sigma=F/A$, where σ=stress, F=applied force, A= cross sectional area yields;

$40\,000 = \frac{F}{2.35 \times 10^{-5}}$ → F= .941N. This value of force is only a tentative value and will be reevaluated once the proper research has been conducted to determine the proper model for the system.

5.1 C Power Output Required for Motor

In order to select a motor a power calculation was conducted. The equation used was $P = \frac{F * d}{t}$ in which P=power, F= force, d=total travel, t= time or 1/frequency. The force value was used from the previous calculation. The value for frequency was obtained from the specifications of the device that the testing cycle must be from 2s to 2 hours. A 2s cycle was the highest frequency so that was the value used in the power calculation. The distance for travel was generated from the limitation of available space. According to calculations, in Appendix A.8, of the maximum distention with respect to the maximum stress, a travel of 5mm was more than sufficient to stretch the sample and was not too long a distance that it extended beyond the boundaries of usable space in the culture plate. The value generated was .02826W. That value must then be multiplied by six to account for the force balance at the articulation plate yielding0.16956 W, or 0.125ftlb/s. The value for the motor available to us from the robotics department was 2ftlbs/s. This motor was capable of performing necessary functions as well as accounting for losses due to friction and efficiency of the rack and pinion device.

5.1 D Rack and Pinion, Motor, and Load Cell

A stepper motor is a brushless, synchronous electrical motor that converts digital vibrations into mechanical rotation (Omega Engineering). Every revolution of the stepper motor is divided into a discrete number of steps and the motor must have a separate pulse for each step. An advantage of the stepper motor is the precise positioning and repeatability of movements, since steppers have 3 to 5% accuracy (Omega Engineering). Dr. Chin used a 6mm stepper motor that was designed for voltages between 3 and 6 volts. The inertial moment of the rotor is a minimum 0.7 $kgm^2 * 10^{-9}$, and the angular acceleration reaches 165 000 rad/s which means that a power rating of between 125~250 mW can be achieved.

A load cell is defined as a transducer that converts an input mechanical force into an electrical output signal. Load cells are commonly referred to as load transducers or load sensors

(FUTEK Advanced Sensor Technology). The S215 Ultra-Low Profile Point Load Cell is intended for limited space applications requiring accurate measurement of full scale forces of 2, 4, and 12 lbf. It can be used with a rigidly mounted platform or to measure tensile or compressive force. It has an extended battery life. Mounting is from the bottom to minimize the total height of the assembly. Dr. Chin used this type of load cell in his device. Another load cell researched was the Model 31 by Honeywell. This was also a miniature load cell with a rugged diaphragm and male attachment threads. DermiGen used an older style heavy duty 2-mV/V output cell. A limitation with the load cells is the extremely high cost.

The rack and pinion was evaluated for a motor with a power output of 2ftlbs/s and a maximum angle of 180°. The maximum travel of the rack and pinion was determined using a 12 tooth gear. The vex 12-tooth gear has a radius of 7.404mm. For radial motion $\theta = s/r$, where θ = angle, s = arc length, and r=radius. For a rack and pinion set up, the linear slide will travel the arc length of the gear as the gear travels θ. For a maximum angle of 180° and a radius of 7.404mm, the maximum travel will be 23.26mm. Since this is greater than the 10mm specification, it is an acceptable set because the angle can be limited to set the maximum travel at 10mm. Also for this motor, a minimum step distance was evaluated. The controller can program 254 points. The minimum rotation angel θ^* is equal to θ, the maximum angle, divided by the total number of programmable points. For the motor obtained from the robotics department, the minimum step angle is 0.0123° and applying the travel formula above, the minimum displacement is 0.0916mm.

5.2 Design Feasibility

Initial experiments were performed to evaluate design feasibility on a basic, conceptual level. A sample of porcine skin was used for the experiment, as seen in Figure 30. Pig skin was chosen to test the proof of concept for the final design because pig skin is similar to human skin in terms of hair follicles, sweat glands, and subcutaneous fat. Clips were attached to each side of a square sample. The sample was stressed through cyclical loading first in the y-direction, next in the x-direction, and finally in both directions at the same time. The skin appeared to stretch evenly in all directions during the last test. The skin returned to its original position once the stress was removed proving that the forces applied remained within the elastic retention region for skin. The test showed that clips could stay attached to the sample during testing, and it indicated, on a basic level, that equi-biaxial loading can apply a uniform load across the entire sample.

Figure 30: Device proof of concept.
(Left) uniaxial stretch in the y-direction, (middle) in the x-direction, (right) equi-biaxial stretch

As the design process advanced toward a prototype, more sophisticated testing was performed. With respect to theoretical analysis, ANSYS was used to evaluate the stress pattern across the surface of the sample as an effect of the setup and testing conditions. The visual results from the analysis can be seen in Figure 31. Simulated loads on each site for different specified lengths simulated the size of the clamps used to attach the device to the sample. The goal for this modeling was to achieve the smallest size grips that applied a uniform load across the entire sample. This testing also enumerated the stress concentrations created by multiaxial loading in order to confirm that the load was in fact uniform across the entire sample.

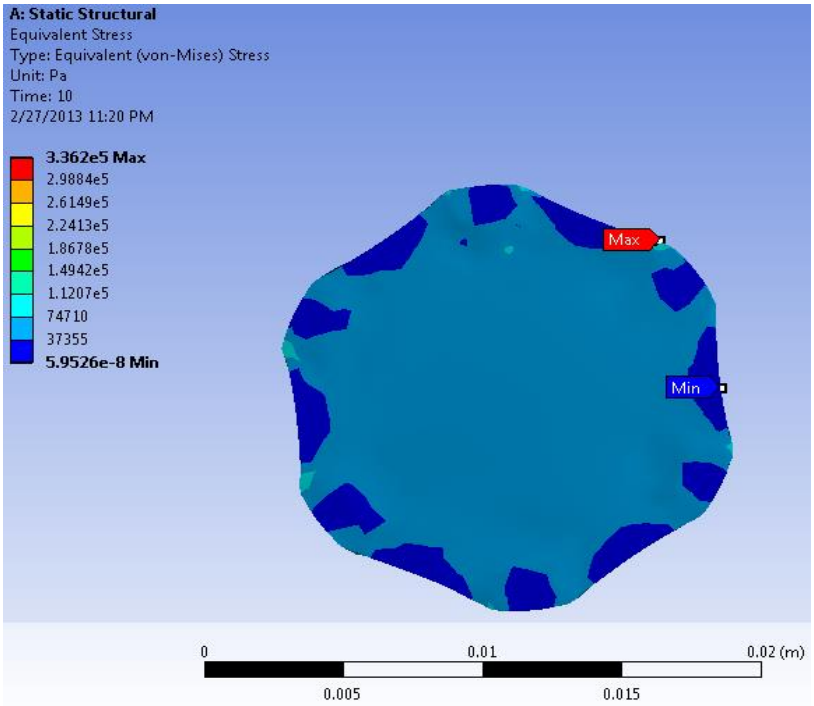

Figure 31: An ANSYS analysis of the device's setup.

Moving on from theoretical and conceptual analysis, testing was done to assess the feasibility of the prototype setup. A circular, 15 mm diameter porcine skin sample was sutured in place. The skin sample that was being pulled was observed visually, and a relatively uniform force was observed, as shown in Figure 32.

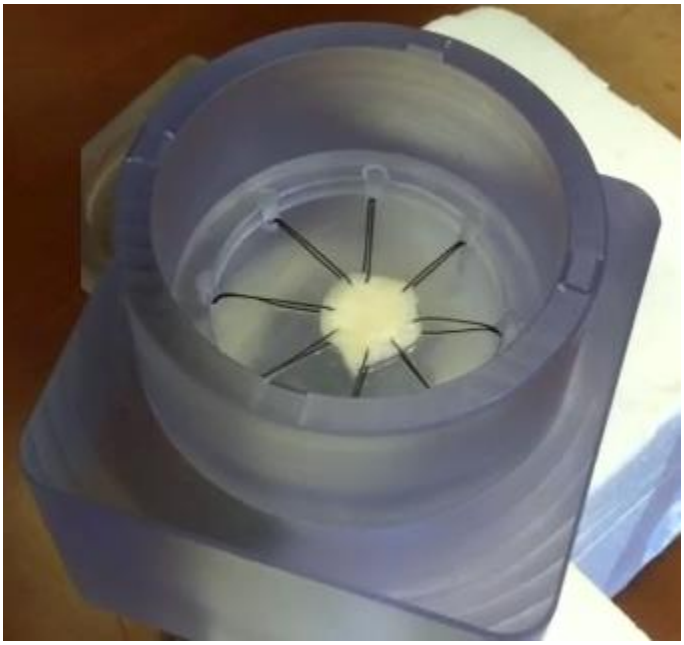

Figure 32: Initial testing of porcine skin in the prototype.

A materials/cost list was completed to determine if the required parts for this device meet the budget of $508. Each part was specified in exact dimensions as well as the method of creation of the part or method of acquiring the part. All costs were added up and compared to the budget. An extensive list of parts and prices can be viewed in Appendix B.2. The total cost amounted to $133 for the device and $140 total.

Chapter 6: Discussion

The main goal of this project was to design and fabricate a novel device that can multiaxially stretch tissue-engineered skin grafts *in vitro* in order to improve the mechanical integrity of the grafts and also accelerate growth. The end product successfully completed all requirements. All objectives, functions, and specifications defined during the initial phase of the project were met. The device was able to secure the sample, prevent slippage, perform multiaxial stretch, vary the stress and strain rates, and apply stretch at the air liquid interface.

The sample was secured and slippage was prevented with the design and fabrication of the clamps. The c-clamp design utilized an adjustable screw to apply adequate gripping force to a discrete location on the sample and allow skin samples with different thicknesses to be tested. Six clamps secured the sample at six equally spaced locations along the perimeter of the sample Initial pullout testing suggested that pullout would not occur at the maximum allowable force of 0.2N. During validation testing when samples were secured in the device and test cycles were applied to different types of samples, there was no slippage observed for porcine or chicken skin samples.

The device was able to perform multiaxial stretch with a rack and pinion actuation system. A 2ft·lb VEX motor powered a series of gears to move a metal linear slide up and down. This slide attaches to the articulation plate where cords run from the articulation plate to the clamps. As the linear slide moved down, it pulled on the cords, and the clamps were pulled radially outward. The uniform cord length pulls on each clamp at the same time inducing a multiaxial stress on the strain on the sample. ANSYS finite element modeling was used to display the deformed shape of the skin sample after a downward displacement of the slide. The results show the uniformity of stress across the sample. The skin sample deformed evenly in all directions, showing a large area of a uniform stress in the middle of the sample. This type of loading can be defined as multiaxial because the deformation occurs along more than one or two axes. The deformation of skin samples during testing was consistent with the finite element model. It was important to apply multiaxial stretch as opposed to uniaxial stretch because skin produced by the body grows in an environment with mechanical forces acting on it in all directions.

The stresses and strain rates were customized with C++ programming. Parameters such as displacement and velocity of the rack and pinion setup correlate with the strain and strain rate of the sample being tested and the strain is directly related to the stress in the sample. The velocity of the motor and the total number of steps the motor takes were able to be adjusted in the code. Increasing the speed of the motor increased the strain rate induced on the sample and increasing the displacement increased the total strain. This is useful for robust analysis of the effects mechanical loading has of skin graft development.

The device was able to apply stretch at the air-liquid interface by keeping the sample secure in a 60 mm^2 well plate filled with DMEM medium. The clamps rest on the bottom surface of the well plate and the sample rests on the lower surface of the c-clamps. This relationship between well plate, clamps, and sample maintains the sample at consistent height above the bottom of the well plate. The well plate can then be filled with the appropriate amount of the medium to culture the sample at the air-liquid interface. To ensure that the sample remains at the air-liquid interface during testing, the averters were developed. The averters are designed to fit securely on any standard 60mm well plate while being easily attachable and removable. They serve to prevent the sample from lifting out of the medium when the cords are put in tension by redirecting the motion of the cords up and around the edge of the well plate. They also work to minimize friction in the motion of the assembly.

6.1 Product Impact

Before using this device or putting it on the market for widespread use, it is important to understand the varying impacts this device could have on the economic, political, societal, and environmental status quo.

6.2 Environmental Impact

With regard to the environment, our novel skin stretching device should have a negligible effect. There would be a small amount of waste generated from the manufacturing of the device. The current machining process requires removal of material from stock pieces of polycarbonate and 316 L stainless steel. Reclamation and recycling of waste material could be

implemented to further decrease waste products. Furthermore, with the exception of a disposable 60mm well plate, every component of the bioreactor is autoclavable. Because it was designed to be easily sterilizable, there would be little to no waste associated with use and maintenance.

The device runs on electricity, so a certain amount of energy is lost during testing cycles; however, the associated energy use is minimal, and the system could potentially be optimized to require less power or test larger samples.

If the state of current skin substitutes were improved due to mechanical loading, the field could focus on engineered tissues. Therefore, there would be less of a need for bovine or porcine tissues. The improved stability of the grafts would decrease the incidence of second applications.

6.3 Economics

This device could potentially impact the economy with regard to hospitals, insurance companies, emergency medical care facilities, and hospital patients. A main problem associated with current skin grafts is their high cost; a square foot of Integra or Dermagraft, two commonly used skin grafts, costs ~$5600 or ~$12000, respectively (Bar-Meir, Mendes, & Winkler, 2006). These costs are relative to the supplied size of the graft alone, and do not include the additional medical expenses associated with surgeries and hospital stays. Some instances require additional applications of skin grafts due to the inability of the initial graft to adhere and integrate properly into the body. Additional graft treatments will increase the total medical expenses. Our device can potentially decrease medical expenses by making grafts more durable and easier to apply in practice. Better mechanical stability, easier implementation of grafts, and less initial donor material will decrease the number of grafts needed for treatment decreasing treatment time, ultimately decreasing medical expenses (Boyce, 1996).

6.4 Societal Influence

Our device has the potential to positively affect society. The accelerated growth and improved mechanical integrity resultant from testing with our device will greatly improve skin

substitutes on the market today (Martin, 2004). Burn victims requiring skin grafts will be able to receive treatment more quickly, skin grafts will be easier to handle during surgery decreasing the difficulty of the surgeon's task, effectively decreasing potential for graft failure, and it will be possible to create more mechanically stable grafts at an increased rate. In addition, valuable research can be conducted to study the effects of mechanical stimuli during culture and better understand the phenomenon of mechanotransduction.

6.5 Political Ramifications

The skin stretching device will not influence global politics very much. People do suffer from non-healing wounds all over the globe and in all countries. Many times the treatments of those wounds are experimental and costly. For example one application of Apligraf costs approximately $1,300 (Bar-Meir, Mendes, & Winkler, 2006). While healthcare systems around the world can receive a positive influence from full scale implementation of this device, no political motive can be ascertained, positive or negative, that would cause a meaningful impact.

6.6 Ethical Concerns

There are few ethical concerns associated with this device. The device was created for future testing and stimulation of tissue-engineered grafts to improve their durability and functionality thus improving the quality life of patients requiring skin grafts. Ethical concerns for this device are the same as those associated with stem cells and artificial cell lines. Since this device tests tissues incorporating fibroblasts, keratinocytes, or other cell lines from mice, use of this device could receive the same criticism. Use of stem cells has been extremely controversial over the past decades. In addition, gene exchange from one species to another, specifically from animals to food products, has been a topic of debate. It is possible that, even if genetic materials were procured using ethical and regulated protocols, some would still contend with their use.

6.7 Health and Safety Issue

This device was designed with the intent to improve the current state of engineered skin grafts; with that in mind, it is clear that health and safety are of the utmost importance with

regard to design intent. With regard to the standard of skin grafts, the device is designed to improve the mechanical stability of tissue-engineered skin grafts. Enhanced grafts with properties that are close to native skin will minimize the risk of tears or mechanical failure during or after application. This structural integrity, while reaching that of autografts or allografts, exceeds that of current skin substitutes. On a larger scale, this device enables a more rapid approach to the fabrication of engineered tissues; an increase in the efficiency of production can lead to a decrease in associated expense, resulting to an increase in availability and a decrease in cost associated with skin grafts.

Beyond the health and safety of the patient that will receive the graft, safety of the user of the device was a high priority throughout this design process. Within the ranked objectives prioritizing the end-goal wants of this project, safety of the user was a main criterion, around which many decisions were based. All components of the device are designed to have smooth edges with either chamfers or fillets in machining. Additionally, no sharp objects such as suture needles, pins, or hooks were chosen as the fixation methods for our device. With regard to electrical hazards, the device can function properly in standard operating conditions of an incubator, therefore no wire leads are exposed or pose any sort of risk. The samples used during testing are tissue-engineered skin substitutes hydrated in a medium and should be handled with caution and the proper personal protective equipment required for biohazard material. The lid of the device is designed to eliminate the risk of substances splashing and coming into contact with any sensitive parts of the body. Finally, every component of the bioreactor portion of the device is sterilizable by autoclave, excluding the well plate, which is disposable. The actuator portion can be treated with 70% ethanol. In all, the device is designed to pose a negligible risk to the user while largely benefitting the health of the skin graft recipient.

6.8 Manufacturability

This device is easily manufacturable and reproducible. The time required for machining all components was less than 15 hours. All parts can be machined with readily available tools such as a CNC machine or lathe. There are other methods such as injection molding that could

make the machining process easier. However, such a large scale option would only be necessary if it went into full scale production. The materials required are polycarbonate and 316L stainless steel. If the polycarbonate were injection molded it would require much less time and attention to reproduce all the parts. The clamps can be machined; however they require much more skill to machine properly. 316L stainless steel has a 40% machinability rating and as such needs to be carefully observed during the machining process. Knowledge of programming would also be required to create a working code that can run the motor. Also parts such as a motor, encoder, limit switch, and sleeve would need to be purchased separately and modified to fit the design.

6.9 Sustainability

The device does not use any renewable energy or help to create any renewable energy. It does not require an undue amount of energy for operation either. The device is designed to run with only one motor and because of this does not require a lot of energy. The products used to create this device are polycarbonate and 316L stainless steel. Producing these devices on a larger scale would increase byproducts from the creation of these materials. With the proper precautions to avoid harmful byproducts being placed into the ecosystem, this device should have negligible impacts on the environment.

Chapter 7: Validation

7.1 Sterility and Gas Exchange

In order to ensure that the device could be used in an *in vitro* setting, while in contact with biological items such as mammalian cells and medium, sterility validation was essential. During the device's testing regime, there will be a tissue sample along with medium in a culture dish inside sitting on the stage plate. The dish will have no lid since the sample has to be stretched. For this reason, it is necessary that the bioreactor portion of the device remains sterile so that the tissue is not compromised throughout testing. The lid and the shell of the bioreactor should maintain sterility while allowing gas exchange, similar to the functionality of a standard culture dish. Additionally, the sleeve should form an airtight barrier with both the bottom of the shell and the bottom of the articulation plate in order to allow motion while preventing contamination. The chamber that must be kept sterile is illustrated in Figure 33, in which sterile areas are denoted by blue and green dots.

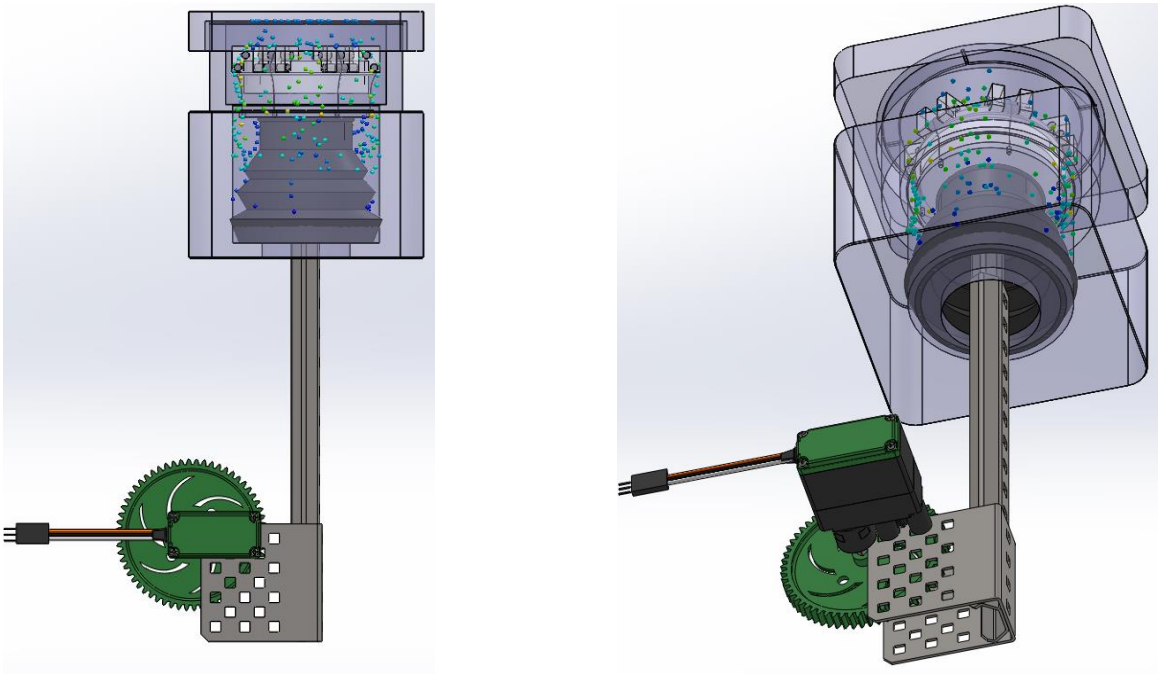

Figure 33: An illustration of the internal sterile chamber of the bioreactor.

The device itself contains a polycarbonate lid, which was machined to have adequate gas exchange so that the culture plate itself would not necessitate a lid. To validate that the inside of the device would remain sterile during testing, the following procedure was implemented and executed.

7.1 A Procedure

The bioreactor portion of the device (i.e. shell, lid, platform, articulation plate) and forceps were autoclaved. DMEM with 2% FBS was aseptically added to two separate 60mm cell culture dishes. The experimental plate was placed, with forceps, on the platform inside the device without a lid, while the control plate was covered by a culture lid. The polycarbonate lid was then placed on the device. The control plate and the device were placed in the incubator. Both plates were imaged at 24, 48, and 72 hours, and changes in color, along with any microorganism growth, were recorded.

There were clear signs to look for when checking for contamination inside the well plates. One key sign in a contaminated dish was the change in medium color from a vibrant red to a yellow-orange tint. Cell culture medium contains phenyl red which is a pH indicator; when culture remains sterile and the medium is not contaminated, the pH remains near 7.0 and the color of the medium is red. If the medium were contaminated the pH would decreases and the color would change. Another clear sign of contamination would be the visual detection of bacteria; for frame of reference, a bacterium at 20x magnification is shown in Figure 34.

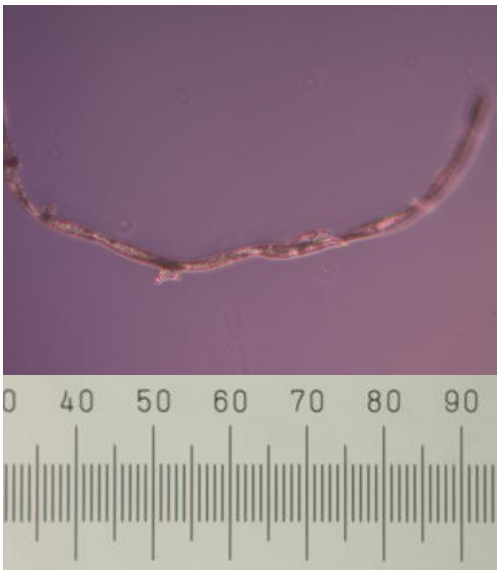

Figure 34: An example of bacterial contamination at 20x magnification. Compared to a 1mm scale with 100 divisions (0.01 mm).

Once experimentation confirmed that the device maintained sterility, gas exchange would be tested to ensure that sufficient exchange was occurring. This was tested by placing dry ice in water inside the device and replacing the lid. As the dry ice sublimated, carbon dioxide should be seen diffusing out of the device, demonstrating proper gas exchange.

7.1 B Results

The team proved that the device is both sterile and allows adequate gas exchange through the described validation procedures. The results of the sterility testing are shown below in Figure 35, in which the color in both plates remained a vibrant red indicating no change in pH.

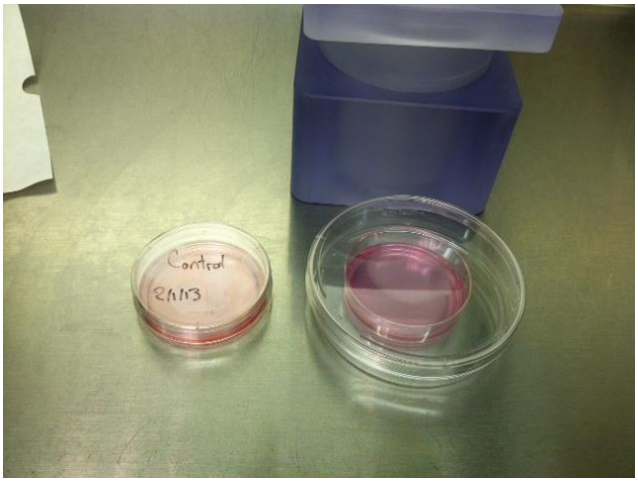

Figure 35: No change in medium color of plates

To further validate the sterility, microscope images were captured of both plates at 20x magnification. The images show no bacteria in the plates at a microscopic level. This is shown in Figure 36 as compared to a 1 mm scale.

Figure 36: No bacterium contamination in 20x magnification

With validation of gas exchange, CO_2 passage from the bioreactor to the outside environment was visually observed during the dry ice procedure.

Chapter 8: Conclusions and Recommendations

8.1 Conclusions

After preliminary research and evaluation, the iterative design process, and fabrication a final device was created that successfully applied multiaxial stretch to skin samples during culture. The device was able to be sterilized and maintain a sterile culture environment. Testing parameters of speed and displacement were able to be changed to fit the user's needs. This device can fit in an incubator and a biosafety cabinet. Also the device was completed within the budget and time frame. Future modifications and testing will be needed to fully evaluate the devices usefulness.

8.2 Recommended Analytical Data

It is recommended that testing on real skin samples is conducted to discover indications of epidermal proliferation test samples. Once the device was created, testing on real samples can begin. The time required for one test set limits the number of test groups possible. The skin can be cultured under cyclic stress using the device alongside an unstretched control. Force displacement values can be collected from the test sets. All data collected can then be analyzed using MATLAB to obtain stress and strain values. Measurements can then be taken from the grip distance as well as marker dots placed on the sample itself to see if the stresses and strains were localized or globalized over the sample.

After the culture of the sample is complete, the histology of the sample can be analyzed. The histological results look for three things: growth factors, damage to the tissue, and cell proliferation. Growth factors can be evaluated from a comparison of growth factors in an unstretched sample alongside a cyclically stretched sampled. Upregulation of growth factors will be a good indicator that the cyclical testing is working. Growth factors should show an upregulation of 120% at the end of testing, a value decided upon by the team. Damage to the tissue can be determined through tallies of cell necrosis after the testing regime is completed. This value will show a comparison of cells proliferated to cell death. Ideally the number of cells created will be greater than the number of cells destroyed by the testing, which will also hopefully show a minimization of tissue damage. Finally, cell proliferation can be tallied up to

determine the rate of production the device can yield. The rate of cells created per time of testing should be 20% better than the original device for *in vivo* testing.

8.3 Characterization of Cells in Scaffold

In order for cells to be characterized in the scaffold, cell proliferation can be observed using immunohistochemical staining that will be performed using the primary antibody against Ki-67, MIB-1 (Orhan, 2006; Faratzis, 2009). The procedure of histological analysis works by sectioning the tissue sample in 3 um section using paraffin. They will then be deparaffinized in xylene and rehydrated using graded ethanol when they are ready to be stained. Ki-67 is a proliferation associated nuclear antigen expressed in all cycling cells except resting cells in the G0 phase. When the sections are stained using the clone MIB-1, cells that are in the G1, S, G2 and M phases of the cell cycle will be detected. The Ki-67 gene is present on the chromosome 10 (10q25).The half-life of Ki-67 protein has been estimated about 60-90 minutes (Faratzis, et al., 2009). Ki-67 is a protein phosphorylated by serine and threonine with a crucial part in cell division. This has been observed from the arrest of cell proliferation when Ki-67 is blocked either by microinjection of blocking antibodies or by inhibition of dephosphorylation (Nabi, Nagi, & Sami, 2008). The last step is counterstaining the sections with hematoxylin for 30 seconds, then dehydrating and mounting them. The count of Ki-67-positively stained nuclei will be performed in areas of greatest density of stained cells within each section. About 1,000 cells will be counted at a magnification of ×400. Ki-67 labeling index (LI) is defined as the number of Ki-67-positive cell nuclei per 100 cells (Orhan, Kale, Cağlar, Göğüş, & Karaağaoğlu, 2006)

8.4 Future Modifications

It is recommended that a load cell be added to the device. The current setup can be easily modified to accommodate a load cell between the articulation plate and the linear slide. A load cell can be used to quantify the forces applied to the sample during testing. This active feedback is extremely important because of the time dependent characteristics of skin such as hysteresis. Over time the same displacement will induce a smaller stress in the sample as the skin sample becomes more compliant. If this were to occur during testing, it would be prudent for the device to incorporate a load cell.

Additionally, once a load cell is installed the programming on the Arduino Uno can be modified to accept input from the load cell. The code can include a feedback loop that will adjust the displacement of the rack and pinion setup in real time. As soon as the force applied deviates from the original test parameters the feedback loop can increase or decrease the displacement accordingly so that the force applied matches the intended value.

References

American Burn Association. (2011). *National Burn Repository Report.*

Balasubramani, M., & Ravi Kumar, T. (2001). Skin substitutes: A review. *Burns, 27*(5), 534-544.

Bannasch, H., Fohn, M., Unterberg, T., Bach, A., Weyand, B., & Stark, G. (2003). Skin tissue engineering. *Clinics in Plastic Surgery, 30*(4), 573-573.

Bar-Meir, E., Mendes, D., & Winkler, E. (2006). Skin substitutes. *Israel Medical Association Journal, 8*(3), 188-191.

Bischoff, J. E., Arruda, E. M., & Grosh, K. (2000). Finite element modeling of human skin using an isotropic, nonlinear elastic constitutive model. *Journal of Biomechanics, 33*(6), 645-652.

Blackstone, B., & Powell, H. (2012). Morphogenesis and biomechanics of engineered skin cultured under uniaxial strain. *Advances in Wound Care, 1*(2), 69-74.

Blotzik, E., & Scherer, M. (2008). Skin replacement therapies for diabetic foot ulcers: systematic review and meta-analysis. *Diabetes Care, 31*(4), 693-694.

Bolland, F., Fisher, J., Ingham, E., Kearney, J., & Korossis, S. (2005). Bioreactors in Tissue Engineering. *Topics in Tissue Engineering*, 1-23.

Bouzari, N., Kim, N., & Kirsner, R. S. (2009). Defense of the skin with LL-37. *The Journal of Investigative Dermatology, 129*(4), 814.

Boyce, S. (1996). Cultured skin substitutes: a review. *Tissue Engineering*, 255-256.

Chin, M. S. (2010). In vivo acceleration of skin growth using a servo-controlled stretching device. *Tissue Engineering, 16*.

Dantzer, E., & Braye, F. M. (2001). Reconstructive surgery using an artificial dermis (integra): results with 39 grafts. *British Journal of Plastic Surgery, 54*(8), 659-664.

Daya, M., & Nair, V. (2008). Traction-assisted dermatogenesis by serial intermittent skin tape application. *Plastic and Reconstructive Surgery, 122*(4), 1047-1054.

DeCarbo, W. T. (2009). Bilayered bioengineered skin substitute to augment wound healing. *Foot & Ankle Specialist, 2*(6), 303-305.

DeFilippo, R., & Atala, A. (2002). Stretch and growth: the molecular and physiologic influences of tissue expansion. *Plastic and Reconstructive Surgery, 109*(7), 2450-2460.

Denkler, K. (2008). Vacuum breast expansion: A look back at the history of this technique. *Plastic and Reconstructive Surgery, 122*(3), 989-990.

DermiGen. (2012). *A Tension Bioreactor System*. Retrieved 2012, from Tissue Growth Technologies: http://www.tissuegrowth.com/prod_skin.cfm

Erba, P., & Meile, L. (2011). A morphometrical study of mechanotransductively induced dermal neovascularization. *Plastic Reconstruction Surgery*.

Faratzis, G., Tsiambas, E., Rapidis, A. D., Machaira, A., Xiromeritis, K., & Patsouris, E. (2009). VEGF and ki 67 expression in squamous cell carcinoma of the tongue: An immunohistochemical and computerized image analysis study. *Oral Oncology, 45*(7), 584-588.

Federico, S., Grillo, A., Giaquinta, G., & Herzog, W. (2008). Convex fung-type potentials for biological tissues. *Meccanica, 43*(3), 279-288.

Fox, S. I. (2011). *Human Physiology* (12th ed.). New York City: McGraw-Hill.

Fung, Y. C. (1993). *Biomechanics: Mechanical Properties of Living Tissues.* New York City: Springer-Verlag.

FUTEK Advanced Sensor Technology. (n.d.). *Load Cells*. Retrieved 2012, from FUTEK: http://www.futek.com/product.aspx?t=load

Gale, E. A. (2002). The rise of childhood type 1 diabetes in the 20th century. *Diabetes, 51*(12), 3353-3361.

Gebelein, C. (1986). Polycarbonates in medical applications. *Encyclopedia of Materials Science and Engineering Vol.5*, 3621-3623.

Ghattaura, A. S., & Potokar, T. S. (2009). Calcified integra membrane: One possible cause of skin graft failure in the second stage of integra use. *European Journal of Plastic Surgery, 32*(1), 47-50.

Griffith, L. G. (2002). Emerging Design Principles in Biomaterials and Scaffolds for Tissue Engineering. *Annals of the New York Academy of Sciences, 961(1)*, 83-95.

Gutierrez, P. (2006). Cultured epithelial autografts. *Australian Nursing, 13*(11).

Hsieh, S., & Lin, W. (1999). Modulation of keratinocyte proliferation by skin innervation. *Journal of Investigative Dermatology, 113*(4), 579-586.

Kishi, K., & Shimizu, R. (2012). Skin graft. *Plastic Surgery International*.

Leventon, W. (2002). Synthetic Skin. *IEEE Spectrum, 39*(12), 28-33.

Manning, D. D. (1973). Maintenance of skin xenografts of widely divergent phylogenetic origin on congenitally athymic (nude) mice. *Journal of Experimental Medicine, 138*(2), 488-494.

Martin, I. W. (2004). The Role of Bioreactors in Tissue Engineering. *Trends in Biotechnology, 22(2)*, 80-86.

Mathieu, D., Linke, J. C., & Wattel, F. (2006). *Handbook on Hyperbaric Medicine.* Netherlands: Springer.

Menke, N. B., Ward, K. R., Witten, T. M., Bonchev, D. G., & Diegelmann, R. F. (2007). Impaired wound healing. *Clinics in dermatology*, 19-25.

Metcalfe, A. D., & Ferguson, M. W. (2007, June 22). Tissue engineering of replacement skin: The crossroads of biomaterials, wound healing, embryonic development, stem cells and regeneration. *Journal of the Royal Society, Interface, 4*(14), 413-437.

Nabi, U., Nagi, A. H., & Sami, W. (2008). Ki-67 proliferating index and histological grade, type and stage of colorectal carcinoma. *Journal of Ayub Medical College, 20*(4), 44.

National Instruments. (2003). Labview: Measurements Manual.

National Instruments. (2011). Teach Tough Concepts: Closed-Loop Control with Labview. 1-6.

Ní Annaidh, A., Bruyère, K., Destrade, M., Gilchrist, M. D., & Otténio, M. (2012). Characterization of the anisotropic mechanical properties of excised human skin. *Journal of the Mechanical Behavior of Biomedical Materials, 5*(1), 139-148.

O'Dell, M. (1998). Skin and Wound Infections: An Overview. *American Family Physician*, 2424-2432.

Omega Engineering. (n.d.). *Introduction to Stepper Motors and Drives*. Retrieved 2012, from OMEGA Engineering Technical Reference: http://www.omega.com/prodinfo/stepper_motors.html

Orhan, D., Kale, G., Cağlar, M., Göğüş, S., & Karaağaoğlu, E. (2006). Histone mRNA in situ hybridization and Ki 67 immunohistochemistry in pediatric adrenocortical tumors. *Virchows Archiv : an international journal of pathology, 448*(5), 591-596.

Padbury, J. F. (2008). Skin—the first line of defense. *The Journal of Pediatrics, 152*(6), A2.

Pataky, T. C., Latash, M. L., & Zatsiorsky, V. M. (2005). Viscoelastic response of the finger pad to incremental tangential displacements. *Journal of Biomechanics, 38*(7), 1441.

Pedersen, L., & Jemec, G. B. (2006). Mechanical properties and barrier function of healthy human skin. *Acta Dermato-Venereologica, 86*(4), 308-308.

Philips, J. R., & Johnson, K. O. (1981). Tactile spatial resolution. III. A continuum mechanics model of skin predicting mechanoreceptor responses to bars, edges, and gratings. *Journal of Neurophysiology, 46*(6), 1204-1205.

Place, E., George, J., Williams, C., & Stephens, M. (2009). Synthetic polymer scaffolds for tissue engineering. *Chemical Society Reviews, 38*(4), 1139-1151.

Powell, C., Smiley, B., Mills, J., & Vandenburgh, H. (2002). Mechanical stimulation improves tissue engineered human skeletal muscle. *American Journal of Physiology, 283*(5), C1557-1565.

Powell, J. (2006). Skin physiology. *Surgery (Oxford), 24*(1), 1-4.

Powell, J. (2006). Skin physiology. *Surgery (Oxford), 24*(1), 1-4.

Reichelt, J. (2007). Mechanotransduction of keratinocytes in culture and in the epidermis. *European Journal of Cell Biology, 86*(11), 807-816.

Ruff, C., Holt, B., & Trinkaus, E. (2006). Who's afraid of the big bad wolff? "Wolff is law" and bone functional adaptation. *American Journal of Physical Anthropology, 129*(4), 484-498.

Sanders, J. E., Goldstein, B. S., & Leotta, D. F. (1995). Skin response to mechanical stress: adaptation rather than breakdown--a review of the literature. *Journal of rehabilitation research and development, 32*(3), 214.

Sanjeev, R., Naresh, M. D., & Arumugam, V. (1994). Effect of strain rate on the fracture behaviour of skin. *Journal of Biosciences, 19*(3), 307-313.

Scanlon, V. C., & Sanders, T. (2011). *Essentials of Anatomy and Physiology* (6th Edition ed.). Philadelphia, Pennsylvania: F.A. Davis Co.

Sen, C. K., Gordillo, G. M., Roy, S., Kirsner, R., Lambert, L., Hunt, T. K., & Longaker, M. T. (2009). Human skinwounds: a major and snowballing threat to public heath and the economy. *Wound Repair and Regeneration, 17*(6), 763-771.

Shevchenko, R. V., James, S. L., & James, E. S. (2010). A review of tissue-engineered skin bioconstructs available for skin reconstruction. *Journal of the Royal Society Interface*, 229-258.

Shores, J. T., Gabriel, A., & Gupta, S. (2007). Skin substitutes and alternatives: a review. *Advances in Skin & Wound Care: The Journal for Prevention and Healing, 20*(9), 493-508.

UK Medicines Information. (2001). *New Drugs in Clinical Development.* National Prescribing. Retrieved from http://www.ukmi.nhs.uk/NewMaterial/Secure/apligraf.pdf

University of Michigan. (2012). *Skin Banking*. Retrieved 2012, from University of Michigan Trauma Burn Center: Retrieved from http://www.traumaburn.org/who/skinbank/banking.shtml

University of Michigan. (n.d.). *Skin Banking*. Retrieved 2012, from University of Michigan Trauma Burn Center: Retrieved from http://www.traumaburn.org/who/skinbank/banking.shtml

Weiss, J. A., Maker, B. N., & Govindjee, S. (1996). Full Text Online Finite element implementation of incompressible, transversely isotropic hyperelasticity. *Computer Methods in Applied Mechanics and Engineering, 135*(1), 107-128.

Wysocki, A. B., & Dorsett-Martin, W. A. (2008). Enhance your knowledge of skin grafts. *Nurse*, 30-38.

Yano, S., Komine, M., Fujimoto, M., Okochi, H., & Tamaki, K. (2004). Mechanical stretching in vitro regulates signal transduction pathways and cellular proliferation in human epidermal keratinocytes. *The Journal of investigative dermatology, 122*(3), 783-790.

Zöllner, A. M., Buganza Tepole, A., & Kuhl, E. (2012). On the biomechanics and mechanobiology of growing skin. *Journal of Theoretical Biology, 297*, 166-175.

Zöllner, A. M., Buganza Tepole, A., Gosain, A. K., & Kuhl, E. (2012). Growing skin: Tissue expansion in pediatric forehead reconstruction. *Biomechanics and Modeling in Mechanobiology, 11*(6), 855-867.

Appendices

Appendix A: The Design Process

Appendix A.1 Gantt chart

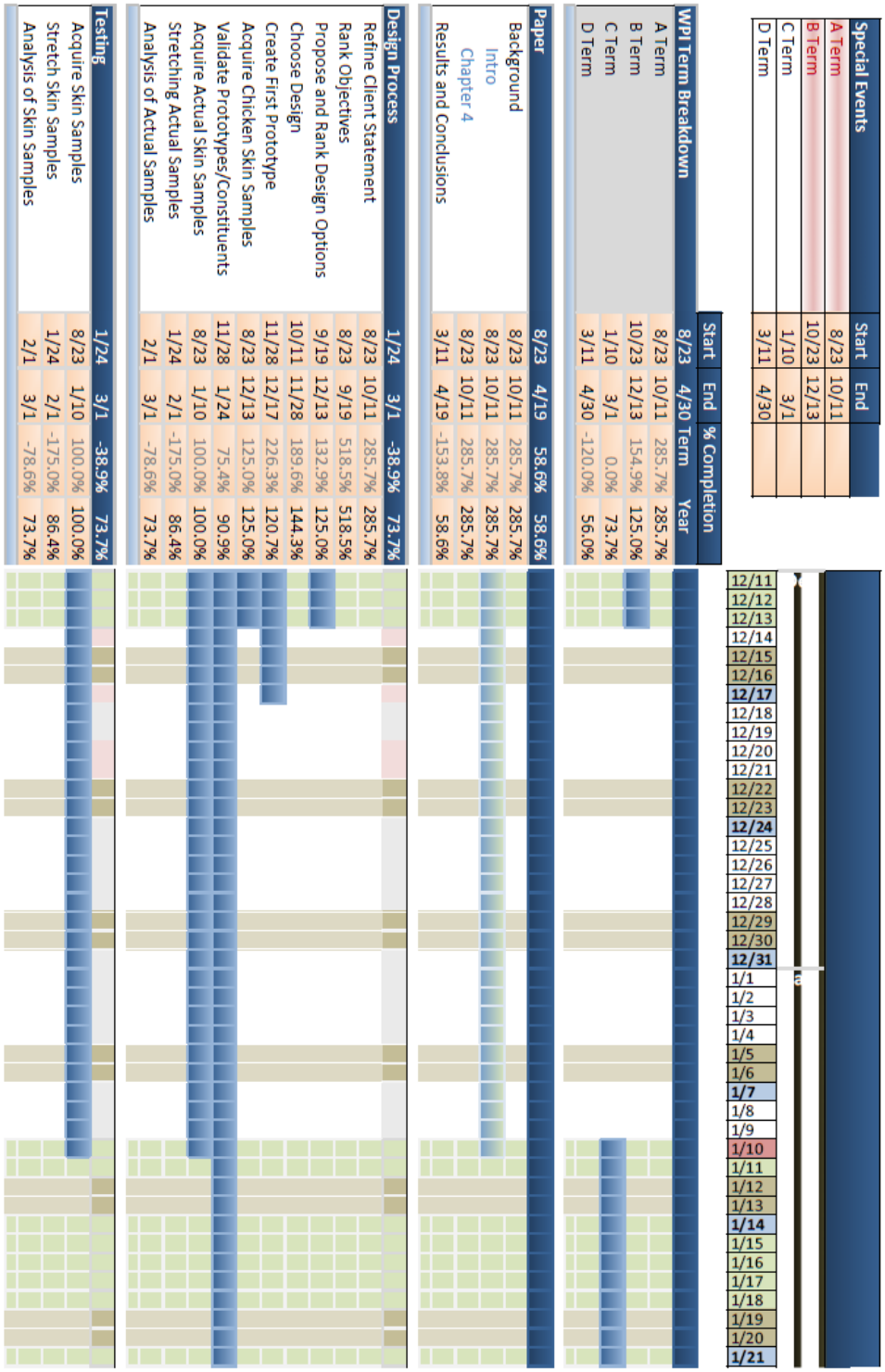

Appendix A.2 Pairwise Comparison Chart

Dr. Lalikos

Client 1 Rank		Minimally damages tissue	Safe for User	Easy to use	Precise	Accurate	Can apply varied testing regimes	Durable	Visually appealing	Efficient	Inexpensive	Total
1st	Minimally damages tissue	X	1	1	0	1	1	1	1	1	1	8
4th	Safe for User	0	X	1	0	0	1	1	1	1	1	6
6th	Easy to use	0	0	X	0	0	1	0	1	1	1	4
1st	Precise	1	1	1	X	0	1	1	1	1	1	8
3rd	Accurate	0	1	1	1	X	1	0	1	1	1	7
9th	Can apply varied testing regimes	0	0	0	0	0	X	0	0	0	1	1
4th	Durable	0	0	1	0	1	1	X	1	1	1	6
8th	Visually appealing	0	0	0	0	0	1	0	X	0	1	2
7th	Efficient	0	0	0	0	0	1	0	1	X	1	3
10th	Inexpensive	0	0	0	0	0	0	0	0	0	X	0

Dr. Ignotz

Client 2 Rank		Minimally damages tissue	Safe for User	Easy to use	Precise	Accurate	Can apply varied testing regimes	Durable	Visually appealing	Efficient	Inexpensive	Total
10th	Minimally damages tissue	X	1	0	0	0.5	1	0	0	0	0	2.5
6th	Safe for User	0	X	1	0	0.5	0	1	0	1	0	3.5
6th	Easy to use	1	0	X	0.5	0.5	1	0	0	0.5	0	3.5
2nd	Precise	1	1	0.5	X	0.5	1	0	1	0.5	0	5.5
5th	Accurate	0.5	0.5	0.5	0.5	X	1	0	1	0.5	0	4.5
8th	Can apply varied testing regimes	0	1	0	0	0	X	1	1	0	0	3
4th	Durable	1	0	1	1	1	0	X	1	0	0	5
8th	Visually appealing	1	1	1	0	0	0	0	X	0	0	3
2nd	Efficient	1	0	0.5	0.5	0.5	1	1	1	X	0	5.5
1st	Inexpensive	1	1	1	1	1	1	1	1	1	X	9

Dr. Chin

Client 3

Rank		Minimally damages tissue	Safe for User	Easy to use	Precise	Accurate	Can apply varied testing regimes	Durable	Visually appealing	Efficient	Inexpensive	Total
1st	Minimally damages tissue	X	1	1	1	1	1	1	1	1	1	9
10th	Safe for User	0	X	0	0	0	0	0	0	0	0	0
9th	Easy to use	0	1	X	0	0	0	0	0	0	0	1
2nd	Precise	0	1	1	X	1	1	1	1	1	1	8
4th	Accurate	0	1	1	0	X	0	1	1	1	1	6
3rd	Can apply varied testing regimes	0	1	1	0	1	X	1	1	1	1	7
8th	Durable	0	1	1	0	0	0	X	0	0	0	2
7th	Visually appealing	0	1	1	0	0	0	1	X	0	0	3
5th	Efficient	0	1	1	0	0	0	1	1	X	1	5
6th	Inexpensive	0	1	1	0	0	0	1	1	0	X	4

Dr. Dunn

Client 4

Rank		Minimally damages tissue	Safe for User	Easy to use	Precise	Accurate	Can apply varied testing regimes	Durable	Visually appealing	Efficient	Inexpensive	Total
4th	Minimally damages tissue	X	0	0.5	1	1	0	1	1	1	0	5.5
1st	Safe for User	1	X	1	1	1	1	1	1	1	1	9
7th	Easy to use	0.5	0	X	0	0	0	0.5	1	0.5	1	3.5
5th	Precise	0	0	1	X	0.5	0	0.5	1	1	1	5
3rd	Accurate	0	0	1	0.5	X	0.5	1	1	1	1	6
2nd	Can apply varied testing regimes	1	0	1	1	0.5	X	1	1	1	1	7.5
6th	Durable	0	0	0.5	0.5	0	0	X	1	1	1	4
8th	Visually appealing	0	0	0	0	0	0	0	X	1	1	2
9th	Efficient	0	0	0.5	0	0	0	0	0	X	1	1.5
10th	Inexpensive	1	0	0	0	0	0	0	0	0	X	1

Professor Pins

Client 5

Rank		Minimally damages tissue	Safe for User	Easy to use	Precise	Accurate	Can apply varied testing regimes	Durable	Visually appealing	Efficient	Inexpensive	Total
4th	Minimally damages tissue	X	1	1	0	0	0	1	1	1	1	6
5th	Safe for User	0	X	1	0	0	0	1	1	1	1	5
6th	Easy to use	0	0	X	0	0	0	1	1	1	1	4
1st	Precise	1	1	1	X	1	1	1	1	1	1	9
3rd	Accurate	1	1	1	0	X	0	1	1	1	1	7
2nd	Can apply varied testing regimes	1	1	1	0	1	X	1	1	1	1	8
9th	Durable	0	0	0	0	0	0	X	1	0	0	1
10th	Visually appealing	0	0	0	0	0	0	0	X	0	0	0
8th	Efficient	0	0	0	0	0	0	1	1	X	0	2
7th	Inexpensive	0	0	0	0	0	0	1	1	1	X	3

MQP Team

Designer

Rank		Minimally damages tissue	Safe for User	Easy to use	Precise	Accurate	Can apply varied testing regimes	Durable	Visually appealing	Efficient	Inexpensive	Total
4th	Minimally damages tissue	X	0	1	0	1	0	1	1	1	1	6
1st	Safe for User	1	X	1	1	1	1	1	1	1	1	9
9th	Easy to use	0	0	X	0	0	0	0	1	0	0	1
3rd	Precise	1	0	1	X	1	0	1	1	1	1	7
5th	Accurate	0	0	1	0	X	0	1	1	1	1	5
2nd	Can apply varied testing regimes	1	0	1	1	1	X	1	1	1	1	8
8th	Durable	0	0	1	0	0	0	X	1	0	0	2
10th	Visually appealing	0	0	0	0	0	0	0	X	0	0	0
7th	Efficient	0	0	1	0	0	0	1	1	X	0	3
6th	Inexpensive	0	0	1	0	0	0	1	1	1	X	4

Average

Rank		Minimally damages tissue	Safe for User	Easy to use	Precise	Accurate	Can apply varied testing regimes	Durable	Visually appealing	Efficient	Inexpensive	Total
2nd	Minimally damages tissue	X	0.67	0.75	0.33	0.75	0.50	0.83	0.83	0.83	0.67	**6.167**
5th	Safe for User	0.33	X	0.83	0.33	0.42	0.50	0.83	0.67	0.83	0.67	**5.417**
9th	Easy to use	0.25	0.17	X	0.08	0.08	0.33	0.25	0.67	0.50	0.50	**2.833**
1st	Precise	0.67	0.67	0.92	X	0.67	0.67	0.75	1.00	0.92	0.83	**7.083**
3rd	Accurate	0.25	0.58	0.92	0.33	X	0.42	0.67	1.00	0.92	0.83	**5.917**
4th	Can apply varied testing regimes	0.50	0.50	0.67	0.33	0.58	X	0.83	0.83	0.67	0.83	**5.75**
7th	Durable	0.17	0.17	0.75	0.25	0.33	0.17	X	0.83	0.33	0.33	**3.333**
10th	Visually appealing	0.17	0.33	0.33	0.00	0.00	0.17	0.17	X	0.17	0.33	**1.667**
7th	Efficient	0.17	0.17	0.50	0.08	0.08	0.33	0.67	0.83	X	0.50	**3.333**
6th	Inexpensive	0.33	0.33	0.50	0.17	0.17	0.17	0.67	0.67	0.50	X	**3.5**

PCC Results

Rank			
1st	Precise	7.083	0
2nd	Minimally damages tissue	6.167	-0.917
3rd	Accurate	5.917	-1.167
4th	Can apply varied testing regimes	5.75	-1.333
5th	Safe for User	5.417	-1.667
6th	Inexpensive	3.5	-3.583
7th	Efficient	3.333	-3.75
7th	Durable	3.333	-3.75
9th	Easy to use	2.833	-4.25
10th	Visually appealing	1.667	-5.417

Appendix A.3 Metrics

	O: Easy to Use		
	time to set up test	**sterilization**	**training**
	minutes	-	-
4	x ≤ 5	standard autoclave/ easy sterilization	requires no training
3	5 < x < 10	larger autoclave/ tougher sterilization procedure	requires verbal/ written instructions
2	10 < x < 30	requires method other than autoclave	requires minimal training
1	30 < x	requires custom method of sterilization	requires elaborate training (certification)
	O: Minimally Damages Tissue		O: Safe with Minimal Training
	Damage to sample	**ability for media to access sample**	**safety**
	% of sample damaged	% of sample damaged	-
4	0 ≤ x < 10	media-sample contact	completely safe for user
3	10 < x < 20	permeable medium-sample contact	causes negligible damage
2	20 < x < 30	diluted media solution (air + media, media + water)	causes easily treatable damage
1	30 < x	partial sample contact with media	requires medical attention
	O: Can Apply Varied Testing Regimes		O: Durable
	increments of stress applied	**waveform variability**	**normal function**
	Pa	(% of range of 2 s to 2 hours)	for x years
4	cont. ≤ x < 500	x = 100%	10 ≤ x
3	500 < x < 1000	90 < x < 100	8 < x < 10
2	1000 < x < 1500	70 < x < 90	4 < x < 8
1	1500 < x	x < 70	x ≤ 4
	O: Accurate		O: Precise
	fixation (slippage)	**Controllability of applied stresses**	**precision**
	amount of slippage	-	% variability
4	none to 0.5 mm	negative feedback loop	0% ≤ x < 10%
3	0.5 to 1 mm	achieved stress value shown	10% < x < 20%
2	1 mm to 1.5 mm	input force value shown	20% < x < 30%
1	1.5 mm+	no force/stress value shown	30% ≤ x
	O: Visually Appealing	O: Inexpensive	O: Efficient
	(subjective, team ranking)	**cost**	**amt of data from each test**
	how does it look	% budget	data per test
4	quality/high-tech	0 ≤ x < 25%	4 < x
3	standard equipment	25% < x < 50%	x = 3,4
2	first prototype	50% < x < 75%	x = 2
1	rough draft	75% ≤ x	x = 1

Appendix A.4 Evaluation Matrix

Function		Objectives (1 – 100)		O: Minimally Damages Tissue		O: Safe with Minimal	O: Easy to Use			O: Precise	O: Accurate		O: Can Apply Varied Testing Realmes			O: Durable	O: Visually Appealing	O: Inexpensive	O: Efficient	
				Damage to sample	ability for media to access sample	safety	training	time to set up	sterilization	precision	Controllability of applied (slippage)	fixation (slippage)	increments of stress	waveform variability	waveforms	normal function	(subjective. how does it look	cost	ant of data from	Total Scores (Weighted based on Objectives)
		(scores)		% of sample damaged	% of sample damaged	-	-	-	-	% variability	-	amount of slippage	Pa	(2 vs 100 hours)		for x years		% budget	data per test	
		4 = best		0 ≤ x < 10	media-sample contact	completely safe for user	requires no training	≤ 5 minutes	standard autoclave/ easy sterilization	0% ≤ x < 10%	negative feedback loop achieved	none to 0.5 mm	cont. ≤ x < 500	≈ 100%		10 ≤ x	quality/high-tech	0 ≤ x < 25%	4 < x	
		3 = good		10 < x < 20	media-permeable	causes negligible	requires verbal/ written instructions	5 < x < 10	larger autoclave/ tougher sterilization	10% < x < 20%	stress value	0.5 to 1 mm	500 < x < 1000	90 < x < 100		8 < x < 10	standard medical	25% < x < 50%	x = 3.4	
		2 = ok		20 < x < 30	medium-sample contact (air + media, media +	causes easily treatable	requires minimal training	10 < x < 30	requires method other than	20% < x < 30%	input force value shown	1 mm to 1.5 mm	1000 < x < 1500	70 < x < 90		4 < x < 8	first prototype	50% < x < 75%	x = 2	
		1 = poor		30 < x	diluted media solution; partial sample contact with media	requires medical	requires elaborate training	30 < x	requires custom method of	30% ≤ x	no force/stress value shown	1.5 mm+	1500 < x	x < 70		x ≤ 4	rough draft	75% ≤ x	x = 1	
		relative weight		13.70%		12.04%		6.30%		15.74%		13.18%		12.78%		7.41%	3.70%	7.78%	7.41%	
		Mean					training	time	sterilization		controllability	fixation	increments	waveforms						
Prevent slippage/ secure sample	how well can we secure the sample and prevent slippage?	Hooks		2.5	4	2.75	3.5	3.75	3.75	2.5	3.25	3	3.13	4	4	3.5	2	3.5	1	72.49
		Sutures		3.25	4	2.75	1.75	2	3	3	4	3.5	3.75	4	4	4	2.5	3	1	77.27
		Clamps		3.75	4	4	4	4	4	3.75	3.75	3.5	3.63	4	4	4	3.25	3.25	1	89.22
		Vacuum		3.5	4	3.75	2	3	1.5	2.75	3.25	2.5	2.88	4	4	4	4	2	1	75.20
		Cryogrips		2.25	4	3.25	2	2.75	3	3.75	3.75	3.75	3.75	4	4	4	3.5	1.5	1	74.06
		Magnets		3.25	4	4	3	3	2.5	3	3	2.25	2.63	4	4	4	2.75	3	1	73.74
		Glue		3	4	4	3.75	3.75	3.25	4	4	4	4	4	4	4	3.5	3.5	1	87.54
Perform controlled, multiaxial stretch	how can we stretch the sample?	Expanding secured Pressurize airfmedia around sample		3.75	4	4	3.25	3.25	4	4	3.75	3.75	3.75	4	4	3.5	3.5	3.5	1	83.22
		Motor		3	4	4	2.5	2.75	2.75	3	3.25	3.5	3.38	3.25	3.5	3	3.5	2.75	1	76.19
		Pull manually		4	4	4	3	3.5	1.75	3	1	4	3.75	4	4	4	3.25	3.25	1	87.36
		Electric/magnetic force		1.5	4	4	3.50	4	4	4	1	4	2.50	1	1	4	4	4	1	56.52
		Heat controlled (bimetallic strip)		3.5	4	3.5	2.5	2.25	3.25	3	2.5	3.5	2.75	2.75	2.5	3	2.75	2.75	1	69.82
		Heat controlled (Nitinol wire)		2.25	4	3	2	3	3.5	3	1.75	3.75	2.75	1.75	1.5	2	2	2	1	55.55
Vary stresses and strain rates	how can we implement variable loading on the sample?	Cranks/Knobs		4	4	4	4	3.75	3.75	4	2.75	3.75	3.25	3.25	3.5	3	3.75	2.25	1	81.75
		Electric/magnetic flux		3.5	4	3.5	2.5	2.25	3.25	3	2.5	3.5	2.75	2.75	2.5	3	2.75	2.75	1	69.82
		Negative feedback loop		4	4	4	3.25	3.75	4	4	4	4	3.88	4	4	4	4	4	4	98.50
		Computer program (e.g.		4	4	4	2.25	3.5	4	3	3.75	4	3.88	4	4	4	4	3.5	4	97.32
		Pump/ compressor		3.5	4	3.75	3.25	2.75	1.75	3	2.5	4	3.25	3.25	3	4	3.25	3	1	77.45
		Pull manually		1.5	4	4	3.50	4	4	1	1	4	2.5	1	1	4	1	4	1	56.52
Allow access to media	how can we supply the sample with	Mist media		2.75	2	4	3.75	3.25	4	4	4	4	4	4	4	2.25	3.5	3	4	84.63
		Use a sponge		3.25	2.75	4	3.75	3.5	2.75	3	4	4	4	4	4	2.5	2.5	3.25	4	84.85
		Dialysis-type bag		3.25	1.75	4	3.5	3	3	3	2.75	4	4	4	4	3	2.5	3	4	86.01
		Use existing bioreactor		4	4	4	3	3.25	4	3	4	4	4	4	4	4	3	3.75	4	97.67
		Build bioreactor into		4	4	4	3	3.5	4	4	4	4	4	4	4	4	4	2.5	4	96.30
		Create synthetic		3.75	3.5	4	1.5	2.75	2	2	3.75	4	4	4	4	2.25	3.75	1.5	4	86.81

	Top 3 means for each function		Rank of Means		
		Function	Mean		
1st	Clamps	Prevent slippage/ secure sample	Clamps	89.22	89.22%
2nd	Glue		Glue	87.54	87.54%
3rd	Sutures		Sutures	77.27	77.27%
			Vacuum	75.20	75.20%
			Cryogrips	74.05	74.05%
			Magnets	73.74	73.74%
			Hooks	72.49	72.49%
1st	Expanding secured platform	Perform controlled, multiaxial stretch	Expanding secured platform	89.22	89.22%
2nd	Motor		Motor	87.36	87.36%
3rd	Pressurize air/media		Pressurize air/media around sample	76.19	76.19%
			Electric/magnetic force	68.82	68.82%
			Pull manually	56.52	56.52%
			Heat controlled (bimetallic strip)	55.55	55.55%
1st	Negative feedback loop	Vary stresses and strain rates	Negative feedback loop	98.50	98.50%
2nd	Computer program (LabView)		Computer program (e.g. LabView)	97.92	97.92%
3rd	Cranks/Knobs		Cranks/Knobs	81.75	81.75%
			Pump/ compressor	77.45	77.45%
			Electric/magnetic flux	68.82	68.82%
			Pull manually	56.52	56.52%
1st	Use existing bioreactor	Allow access to media	Use existing bioreactor	97.67	97.67%
2nd	Build bioreactor into device		Build bioreactor into device	96.30	96.30%
3rd	Create synthetic capillaries		Create synthetic capillaries	86.81	86.81%
			Dialysis-type bag	86.01	86.01%
			Use a sponge	84.85	84.85%
			Mist media	84.63	84.63%

Rank	Mean	Percent Ranking (100% = completely fulfills function)	Deviaton from top score
Function: Prevent slippage/Secure Sample			
1st	**Clamps**	89.22%	0%
2nd	**Glue**	87.54%	-2%
3rd	**Sutures**	77.27%	-12%
Function: Perform controlled, multiaxial stretch			
1st	**Expanding secured platform**	89.22%	0%
2nd	**Motor**	87.36%	-2%
3rd	**Pressurize air/media**	76.19%	-13%
Function: Vary stresses and strain rates			
1st	**Negative feedback loop**	98.50%	0%
2nd	**Computer program (LabView)**	97.92%	-1%
3rd	**Cranks/Knobs**	81.75%	-17%
Function: Allow access to media			
1st	**Use existing bioreactor**	97.67%	0%
2nd	**Build bioreactor into device**	96.30%	-1%
3rd	**Create synthetic capillaries**	86.81%	-11%

Appendix A.5 Brainstorming

Design considerations

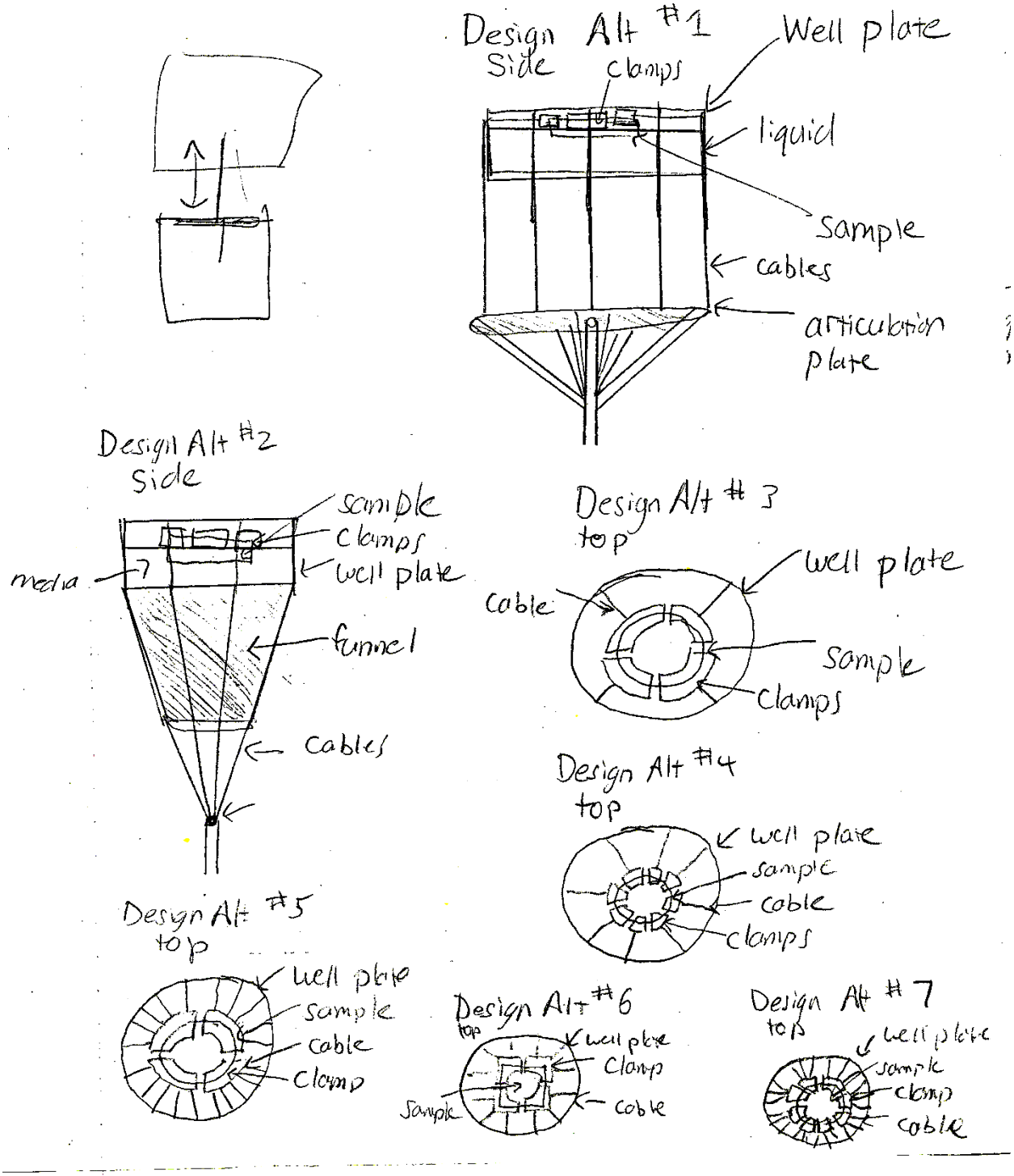

Clamps, Sterilemethod of force transduction

Design Alt #8

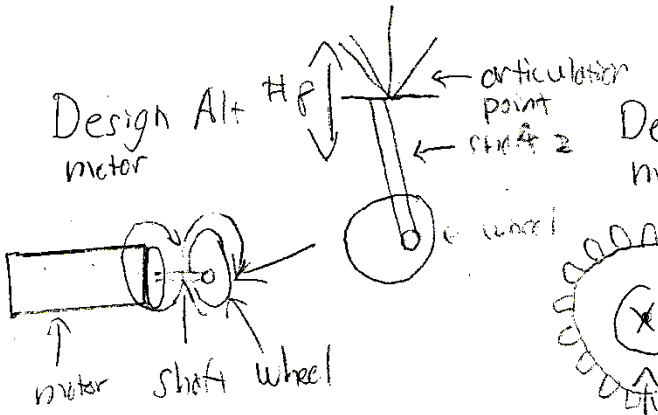

Design alt #9

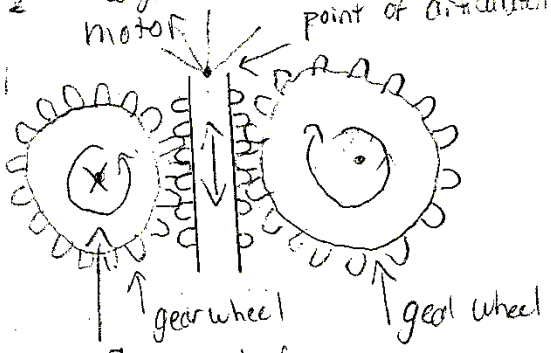

Design Alt #10

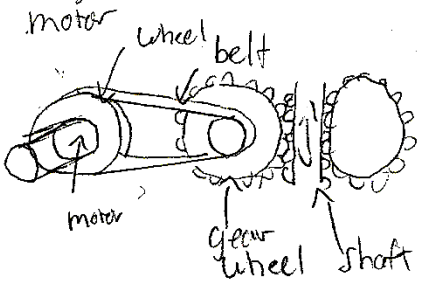

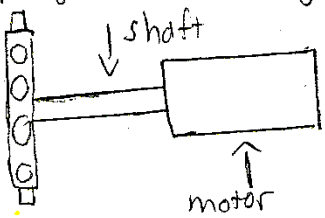

Design Alt #11

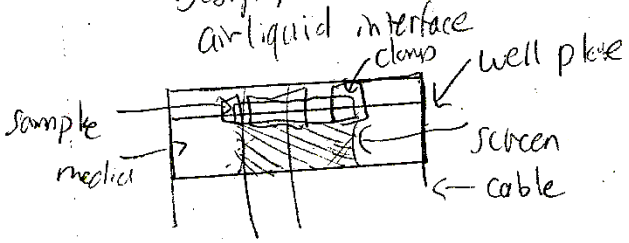

Design Alt #12

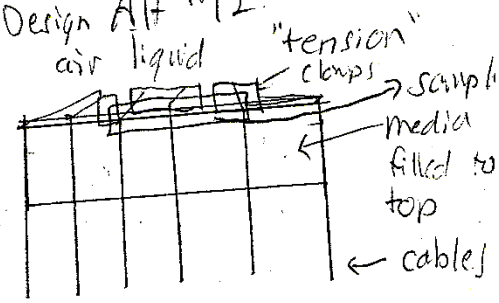

Design Alt #13

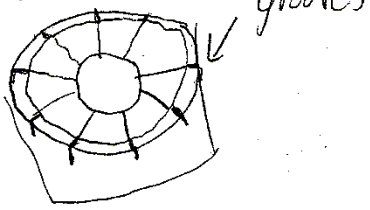

Design Alt #14

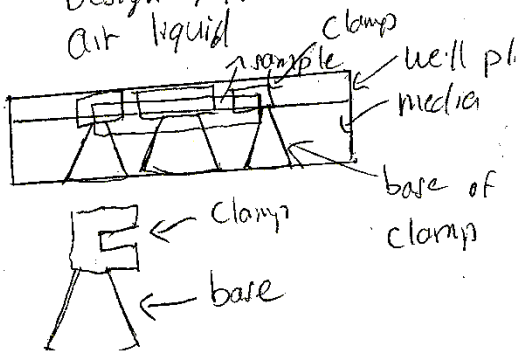

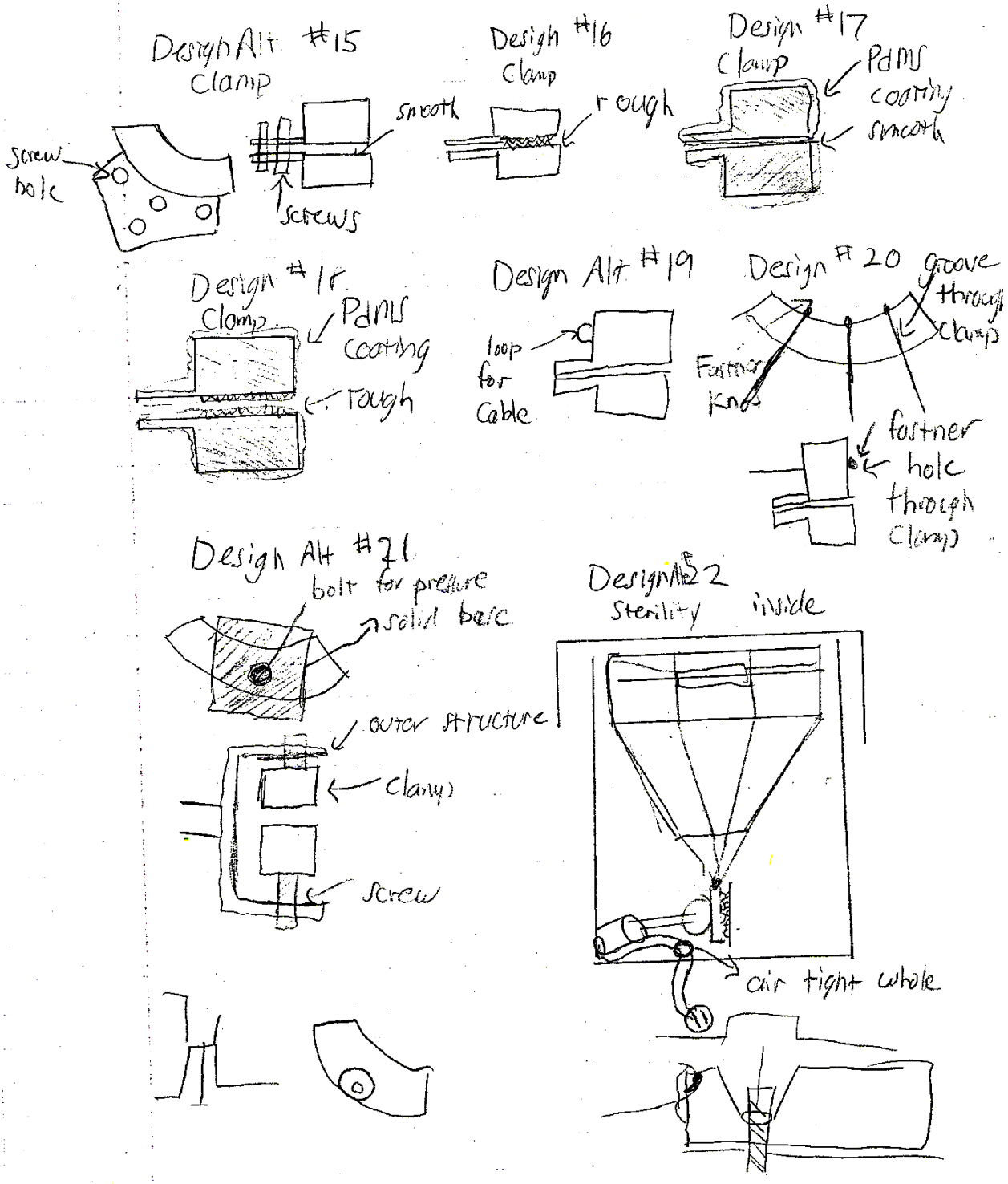
Design Alt #15
Clamp
screw hole
smooth
screws
Design #16
Clamp
rough
Design #17
Clamp
PdMS coating
smooth
Design #18
Clamp
PdMS coating
rough
Design Alt #19
loop for Cable
Design #20
groove through Clamp
fastner hole through Clamp
Design Alt #21
bolt for pressure
solid base
outer structure
clamp
screw
Design #22
Sterility inside
air tight whole

$$\frac{1.7451 \cdot 10^{-9}\,(T_1^4 - 473^4)\,K^4}{.6444 \qquad t.25}$$

$$\frac{1.7451 \cdot 10^{-9}}{25 \cdot .6444}$$

3,140 +

Design Alt #2
sterility outside

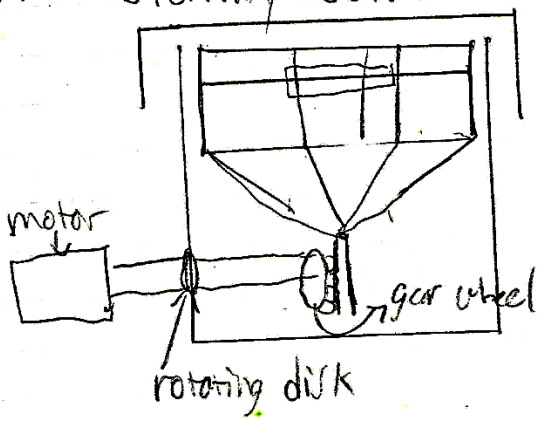

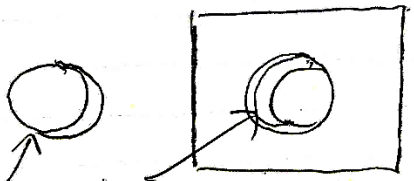

air tight disk hole in wall

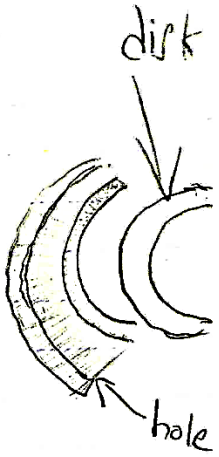

Design Choice

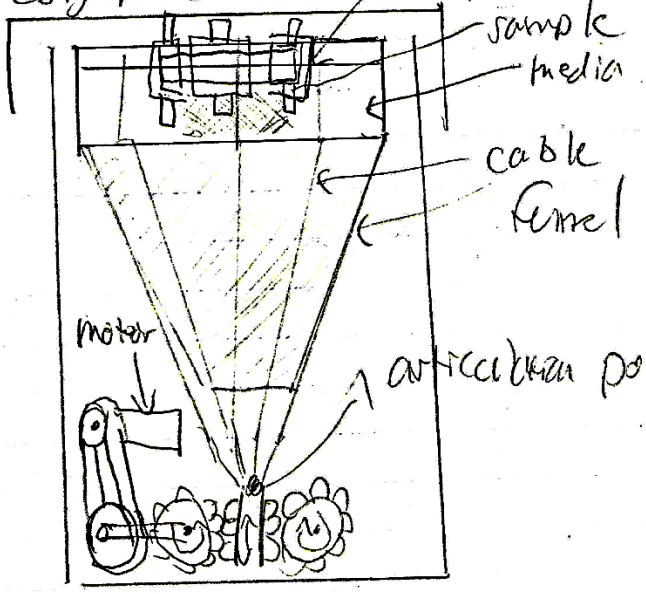

Appendix A.6 Conceptual Designs

Easy sterilization, rotation of base/wall

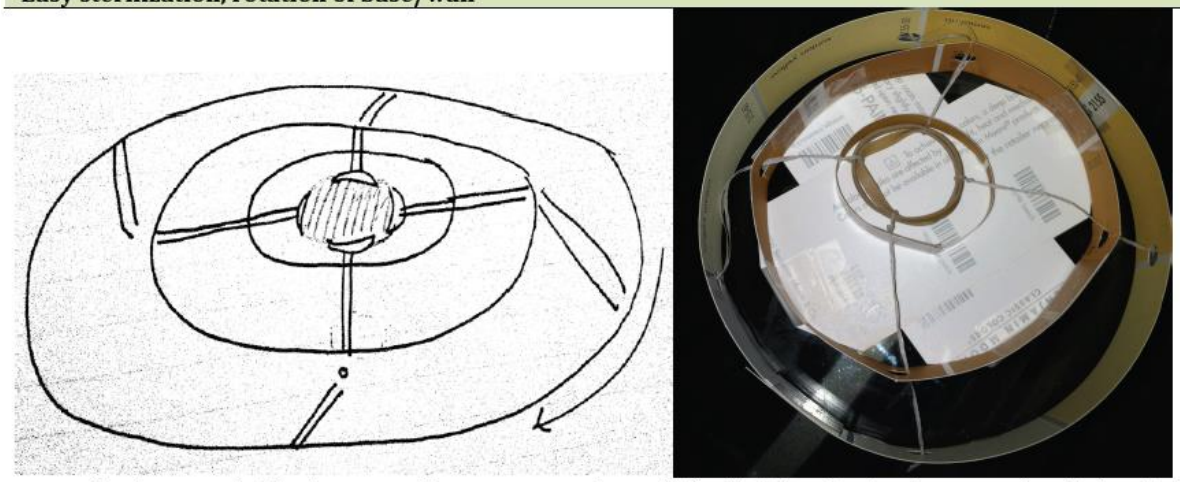

- Cords connected to clamps rest in grooves coming out of well plate. Cords enter second wall of well plate by going through hole (or across pully) of second wall.
- Hole (pully) has minimal friction, is designed to allow easy passage of cord.
- Cords then affix to either third wall of well plate (or base) of total system.
- Third wall (or base) will rotate clockwise or counterclockwise (or both) while well plate and second wall of well plate are held stationary.
- Rotation will pull cords sideways, but second wall will direct cords so that pulling on sample is linear and directly outward from center.
- A variety of methods can be used to enable motor-actuated rotation of base or third wall. Lid can rest on top of system easily and rotation will not disrupt sterilization

Small, enclosed motor (or larger motor, but still inside incubator)

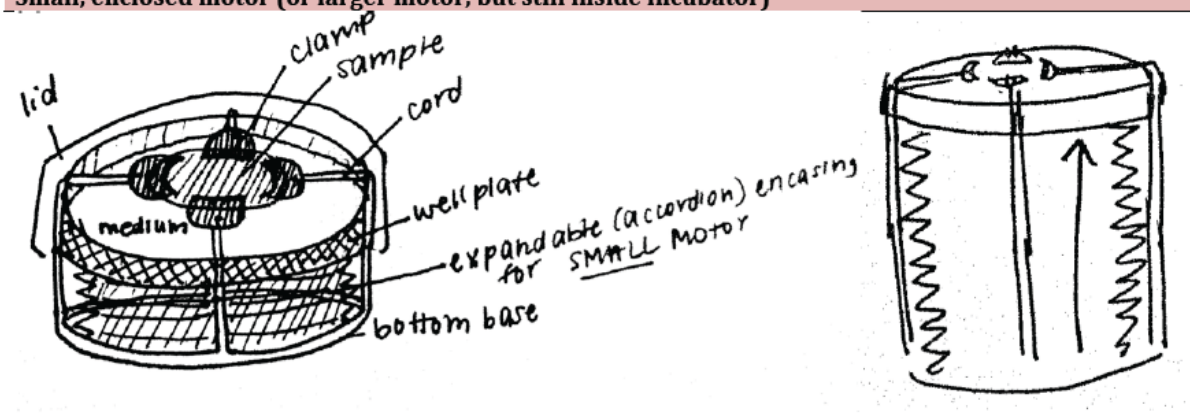

- Sample is secured by clamps and suspended at air-medium interface by fixation setup.
- Cords run across grooves on well plate and down side of well plate, connect to a base that is separate from well plate.
- Motor inside accordion/expandable encasing increases distance between base and bottom of well plate, pulling cords/clamps/sample.

Excessively large motor, shaky motor, hot motor, etc.

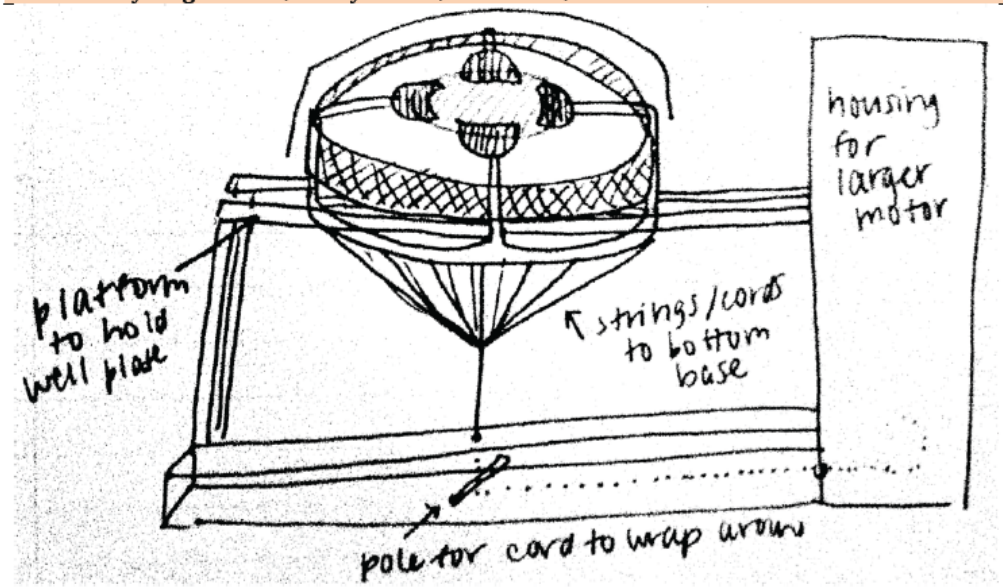

- Well plate is suspended by platform, separate base connected to cables (same as before) has cord(s) that pull base directly downward, wraps around pole inside bottom portion of platform, goes into housing for motor where it is being pulled from.
- Cord is pulled linearly downward, pulls on separate base, base pulls on cords attached to clamps/sample.

Appendix A.7 Alternative Designs

Column Design

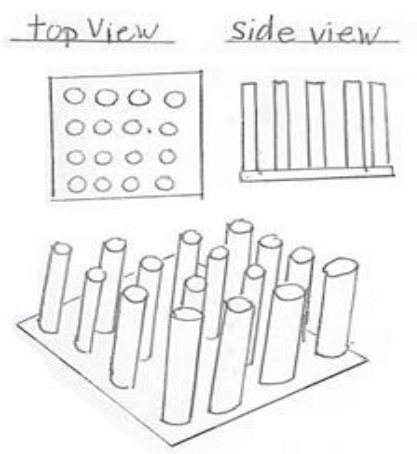

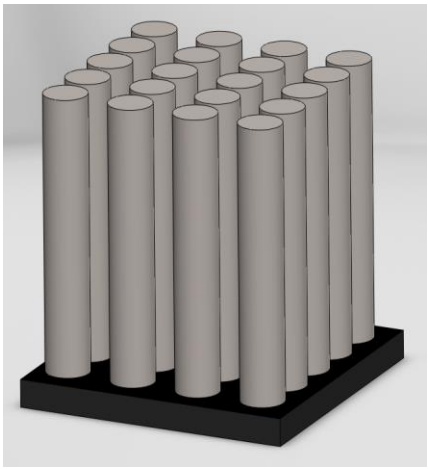

Column Design	Pros	Cons
	*Allows for great control of the sample *Multiple data points can be taken from a single sample with varied conditions	*Requires sophisticated (and expensive) technology, equipment *Fabrication of such small parts may be too advanced and expensive for the team's skill level and budget

Expanding Ring Design

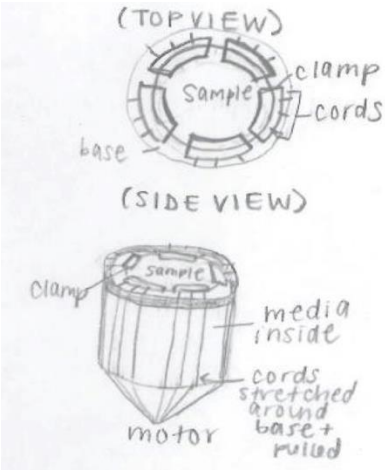

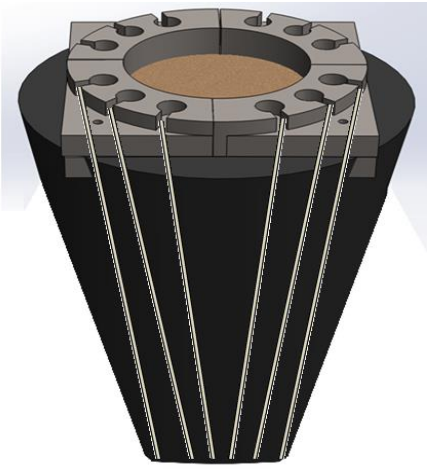

Expanding Ring Design	Pros	Cons
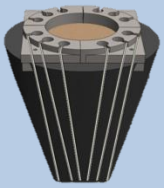	*Only one motor to actuate in one direction *Less expensive *Easier to program and control *Easier to calculate applied loading than other less uniform methods of fixation	*Challenge to maintain sterility *Can only apply a uniform stretch, not as versatile as other designs

Custom Fit Device

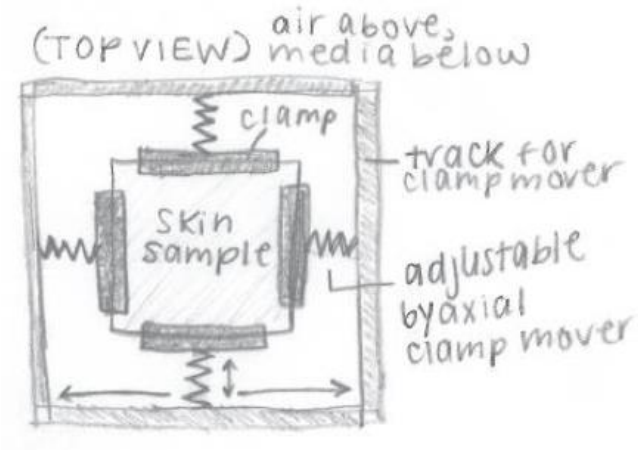

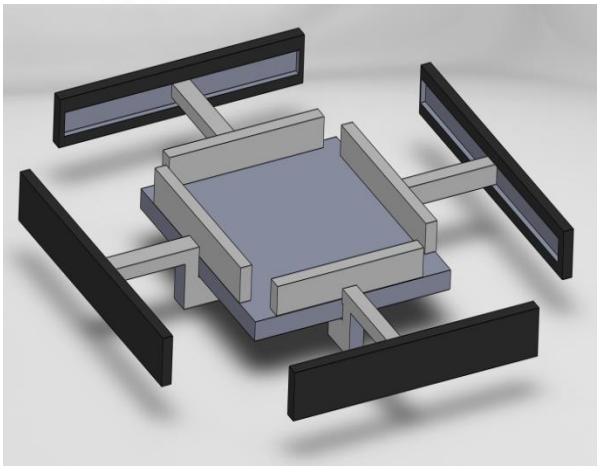

Custom Fit Design	Pros	Cons
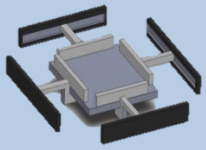	*Allows for significant variability in the desired size and shape of the sample *Enables a wide range of stretching cycles *Device could supply user with grafts of shapes and sizes tailored to his specific need	*Requires four motors that can move biaxially, independent of each other *Creates a challenge with sterility

Piston Device

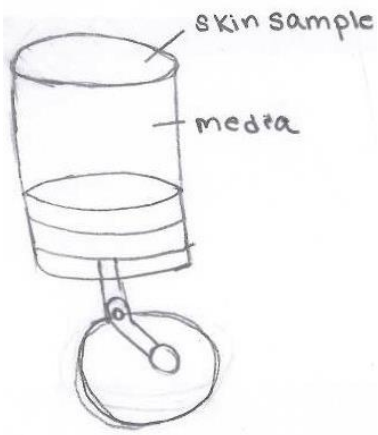

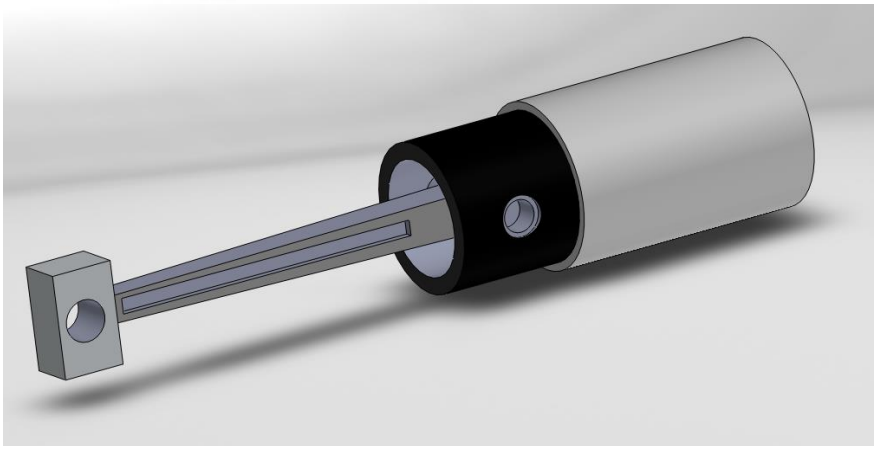

Piston Design	Pros	Cons
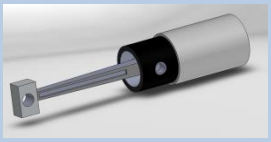	*Least expensive – uses simple, traditional technology *Highly reproducible because motion is applied by one mechanical movement *Few parts means easy setup	*Pressure would be exerted uniformly so this device is less versatile than others *Using media to pressurize the sample introduces uncertainties *Small parts would be difficult to produce and load accurately and reproducibly

Appendix A.8 Calculations

Evaluation of new clamp design

Calculation of moments

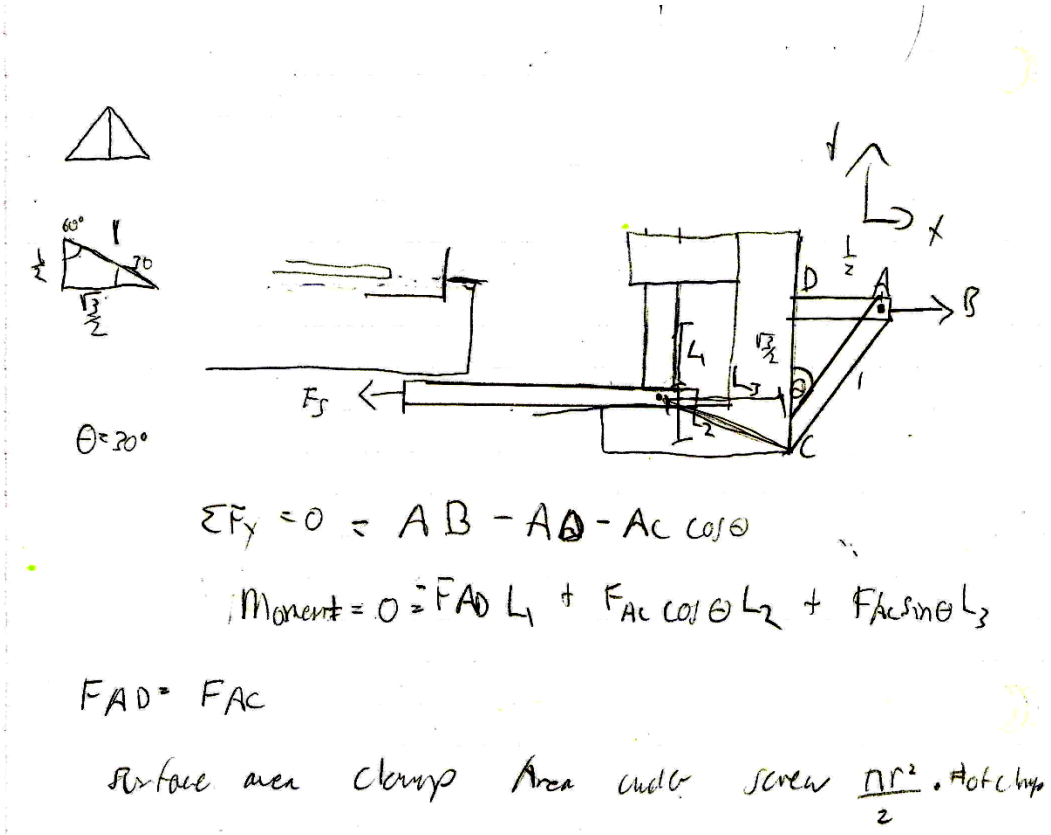

$\Sigma F_y = 0 = AB - AD - AC\cos\theta$

$\text{Moment} = 0 = F_{AD} L_1 + F_{AC}\cos\theta L_2 + F_{AC}\sin\theta L_3$

$F_{AD} = F_{AC}$

Surface area clamp Area end of screw $\frac{\pi r^2}{2}$. Hatchup

Creation of prototype

Diameter calculation for lid and shell

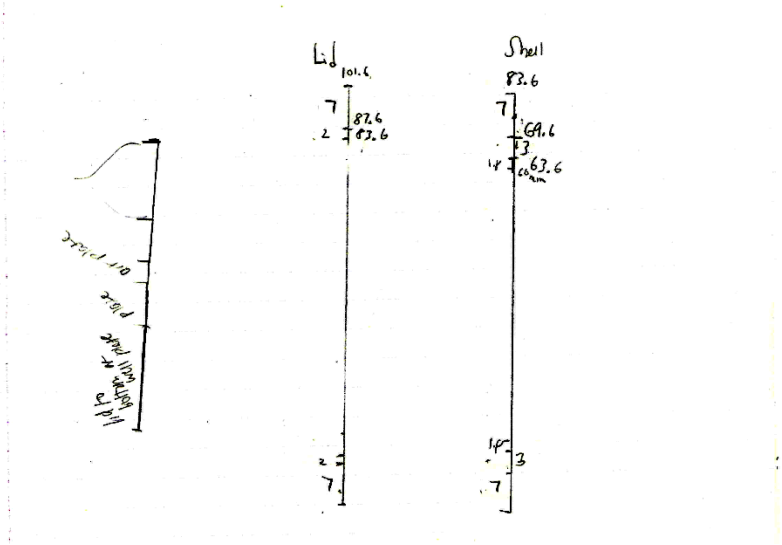

Diameter calculation for platform and articulation plate

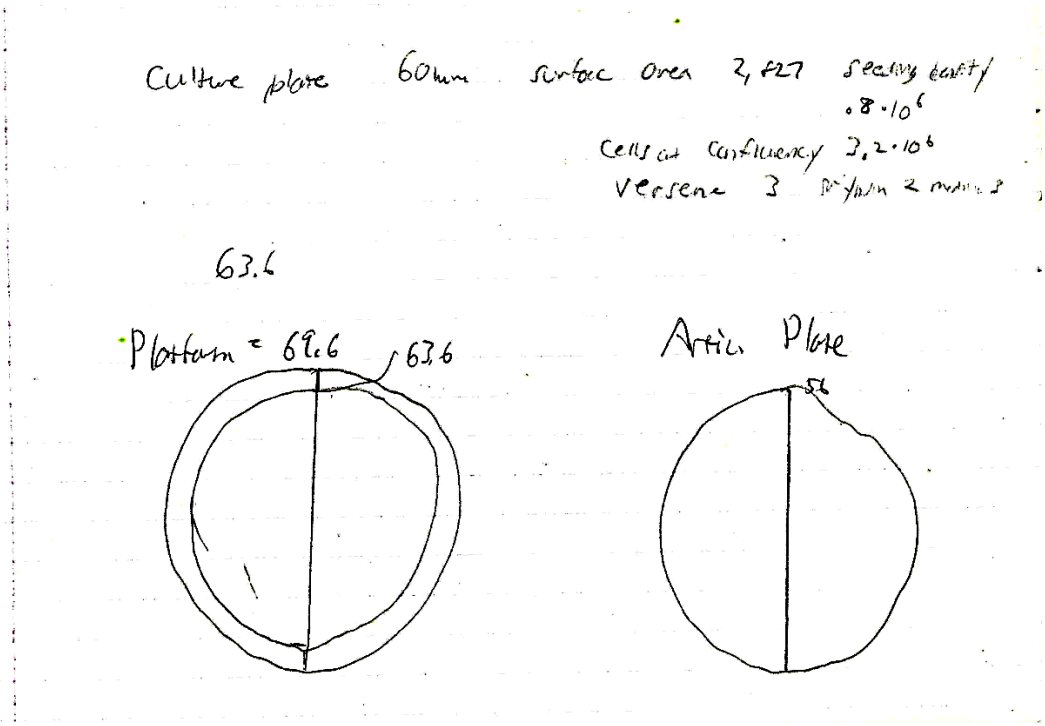

Dimension calculations for components of design

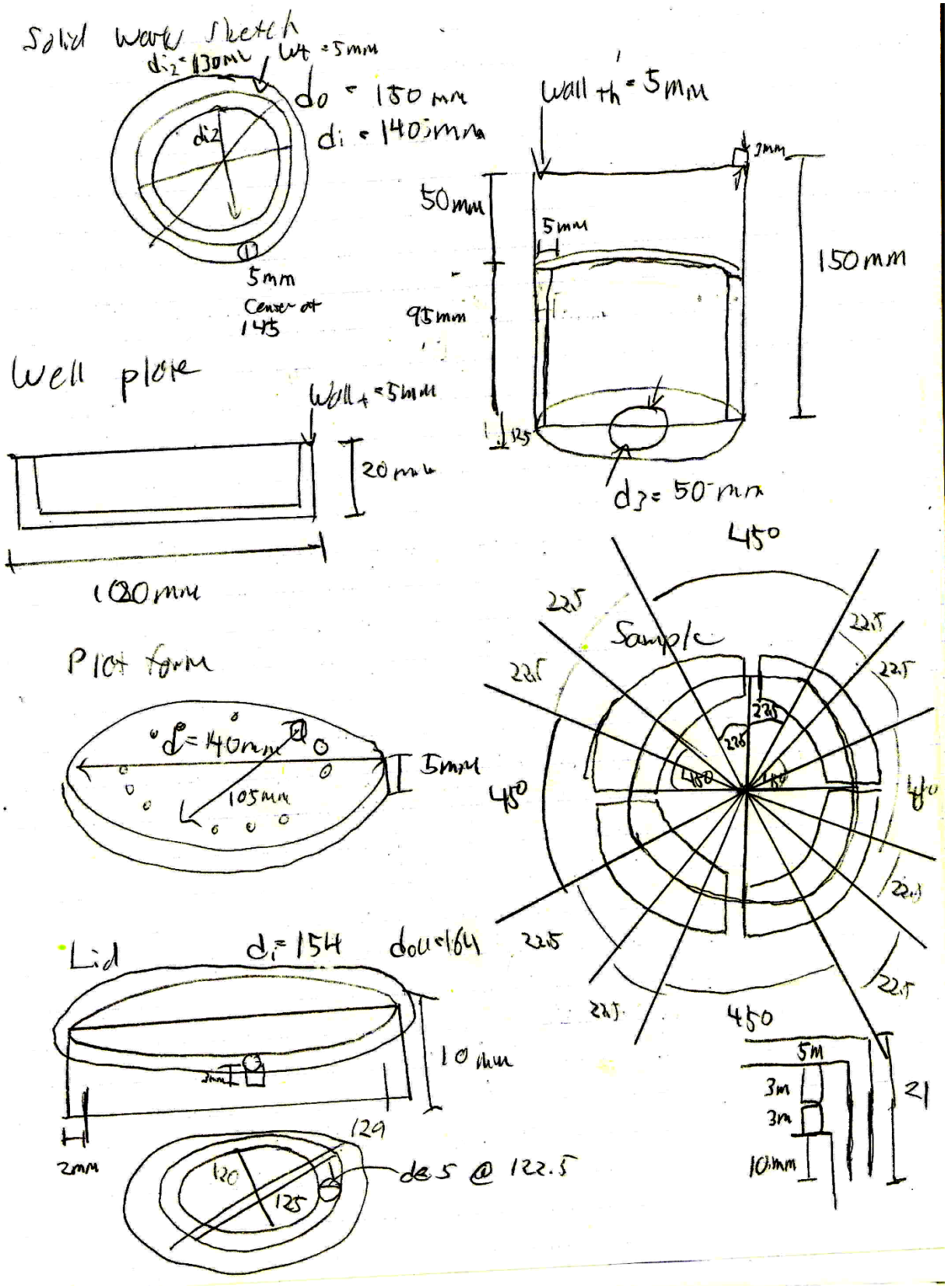

Appendix B: Expanding Ring Design

Appendix B.1 CAD Drawings

Component	Picture	Description
LID (Polycarbonate)	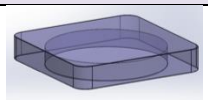	The lid must enable gas exchange while restricting the passage of contaminants from the incubator, working identically to the tortuous path mechanism of a well plate lid.
SHELL (Polycarbonate)	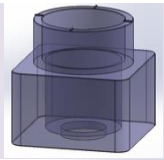	The shell will house the entire device, with exception of the motor, and will be covered by the lid to preserve sterility.
WELL PLATE (Polycarbonate)	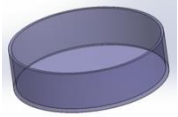	The standard polystyrene 60 mm^2 well plate will hold the sample and the medium.
CLAMPS (Medical Grade 316L Stainless Steel)	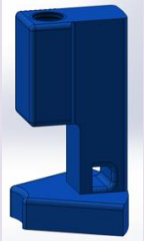	The clamps (6) will grip the sample with a screw that enters at the top and grips the sample on the base. There will be a hole that is level with the sample that will connect to a cord that will enable stretching of the sample.
AVERTERS (Posts: Polycarbonate Pins: Stainless Steel)	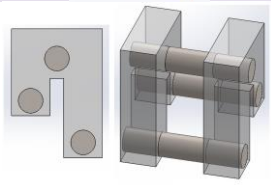	The averters (6) sit on the edge of the well plate and redirect the motion of the cords so that the clamps' path of motion remains level with the sample but the cords are able to pass around the side of the well plate.
PLATFORM (Polycarbonate)	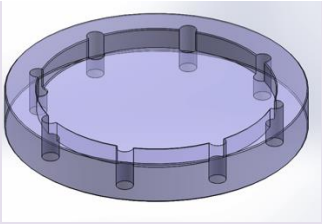	The platform will be the support structure for the well plate, and will have holes through which cords can pass to stretch the sample. The platform will sit atop a lip running across the inner circumference of the shell and held in place.
ARTICULATION PLATE (Polycarbonate)	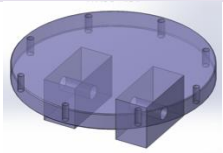	The articulation plate will be in the lower portion of the shell and has holes through it to articulate with each cord, and will be actuated by a motor that connects to the bottom by a screw.
SLEEVE	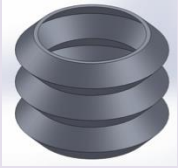	The sleeve will be secured in an air-tight manner to the articulation plate and the shell and will be expandable without exerting a supporting or resisting force on the system. As the motor raises and lowers the articulation plate, the sleeve will maintain that barrier necessary for sterility without restricting motion.

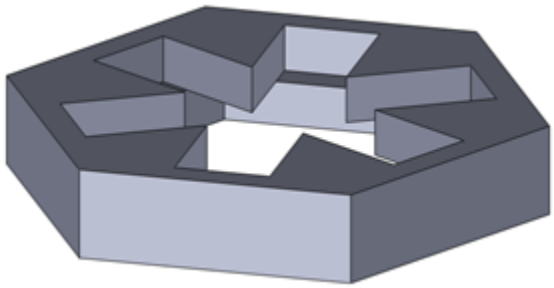

The Cap for fixation

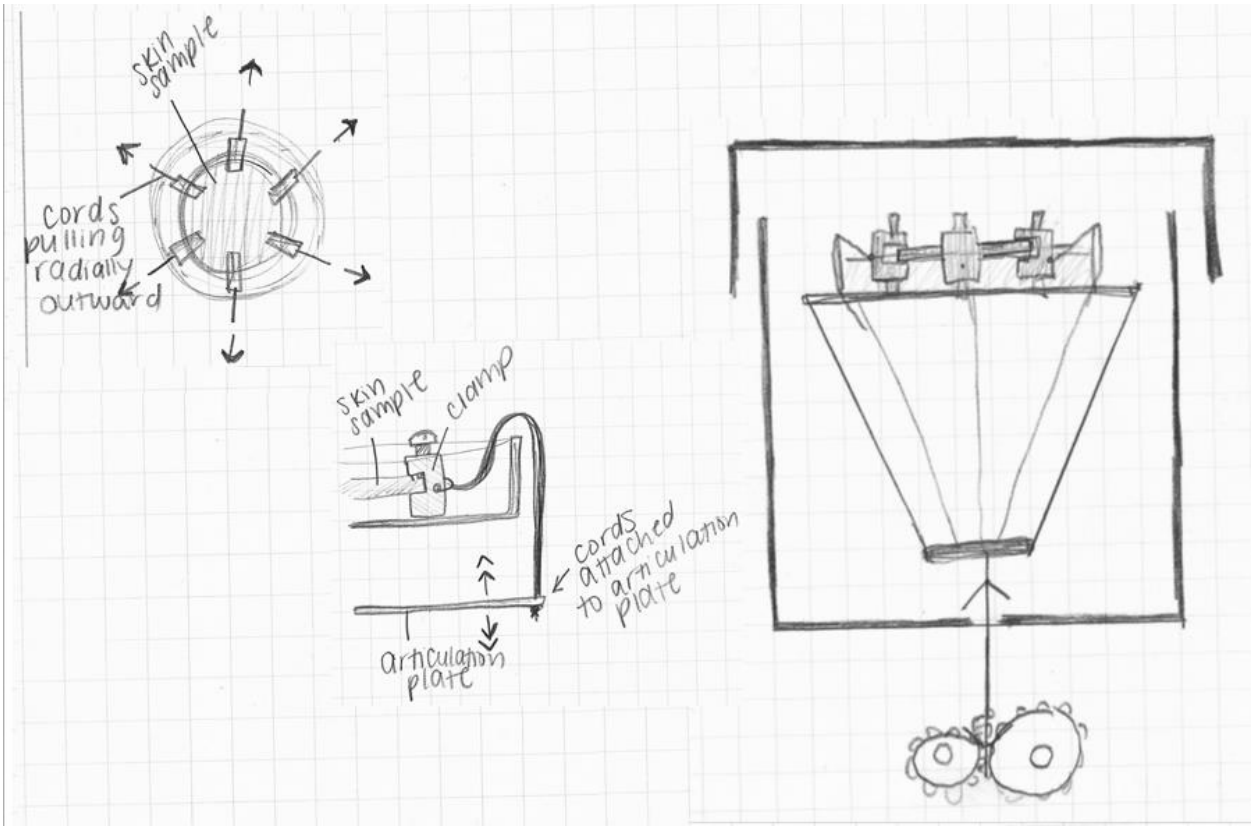

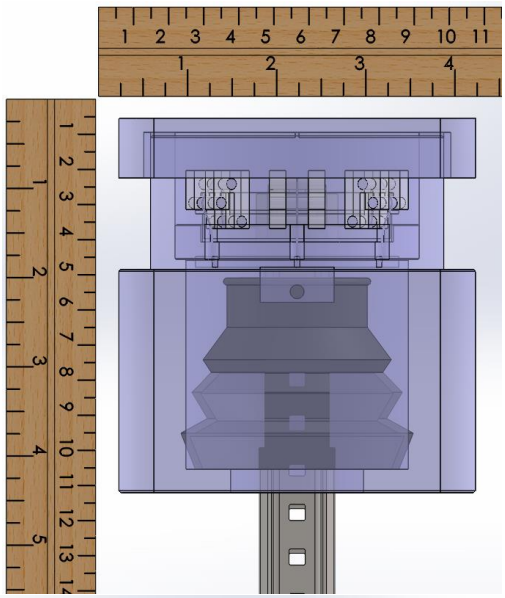

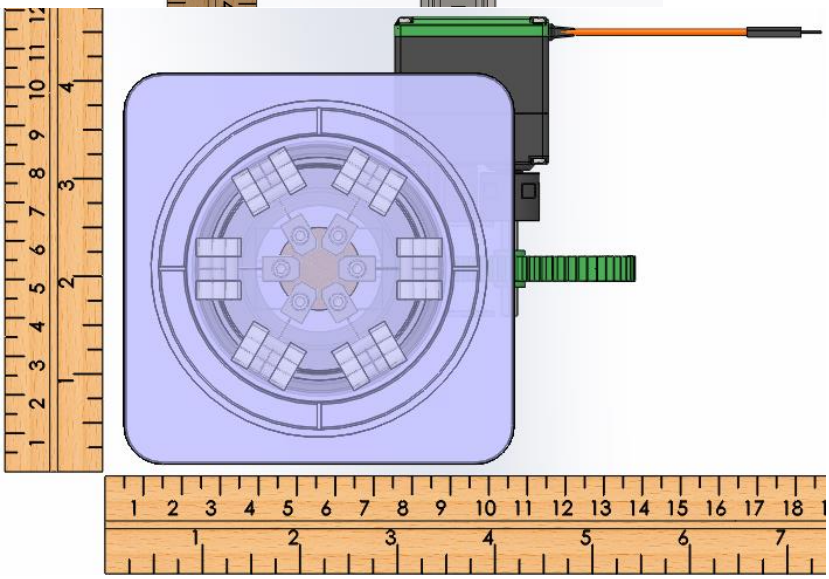

Measurement

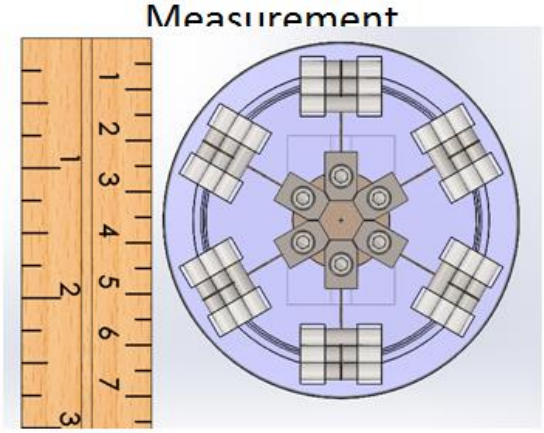

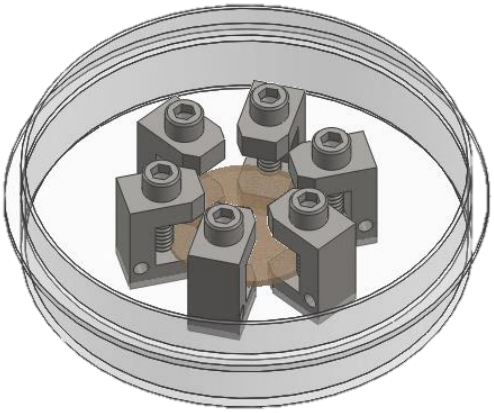
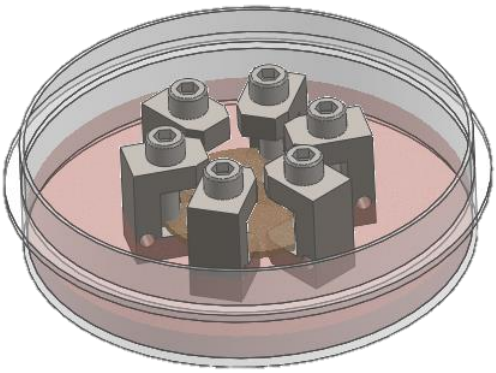
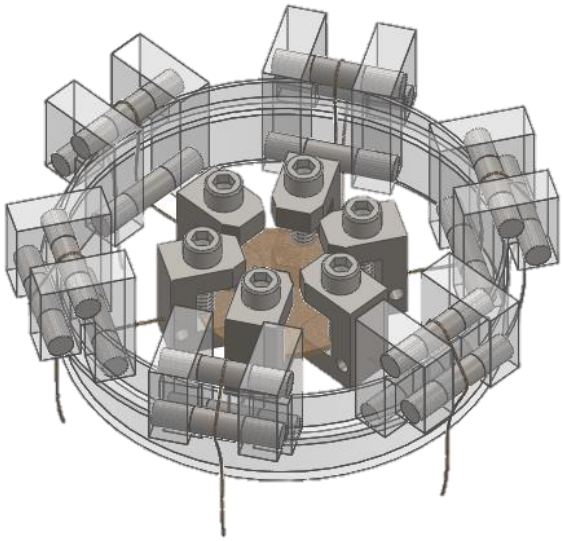
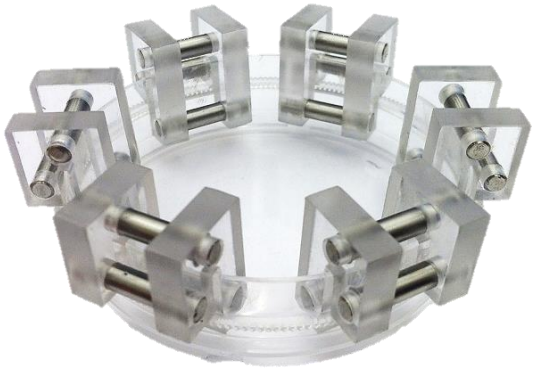
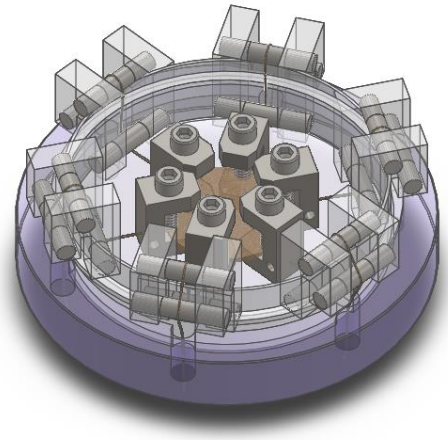
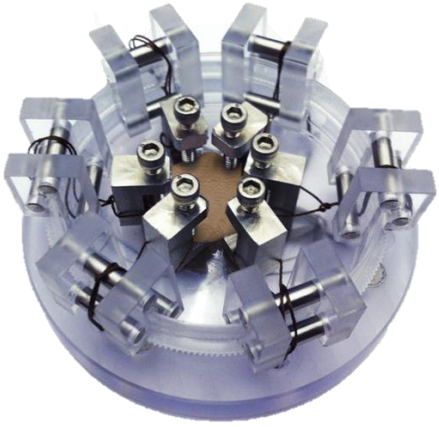

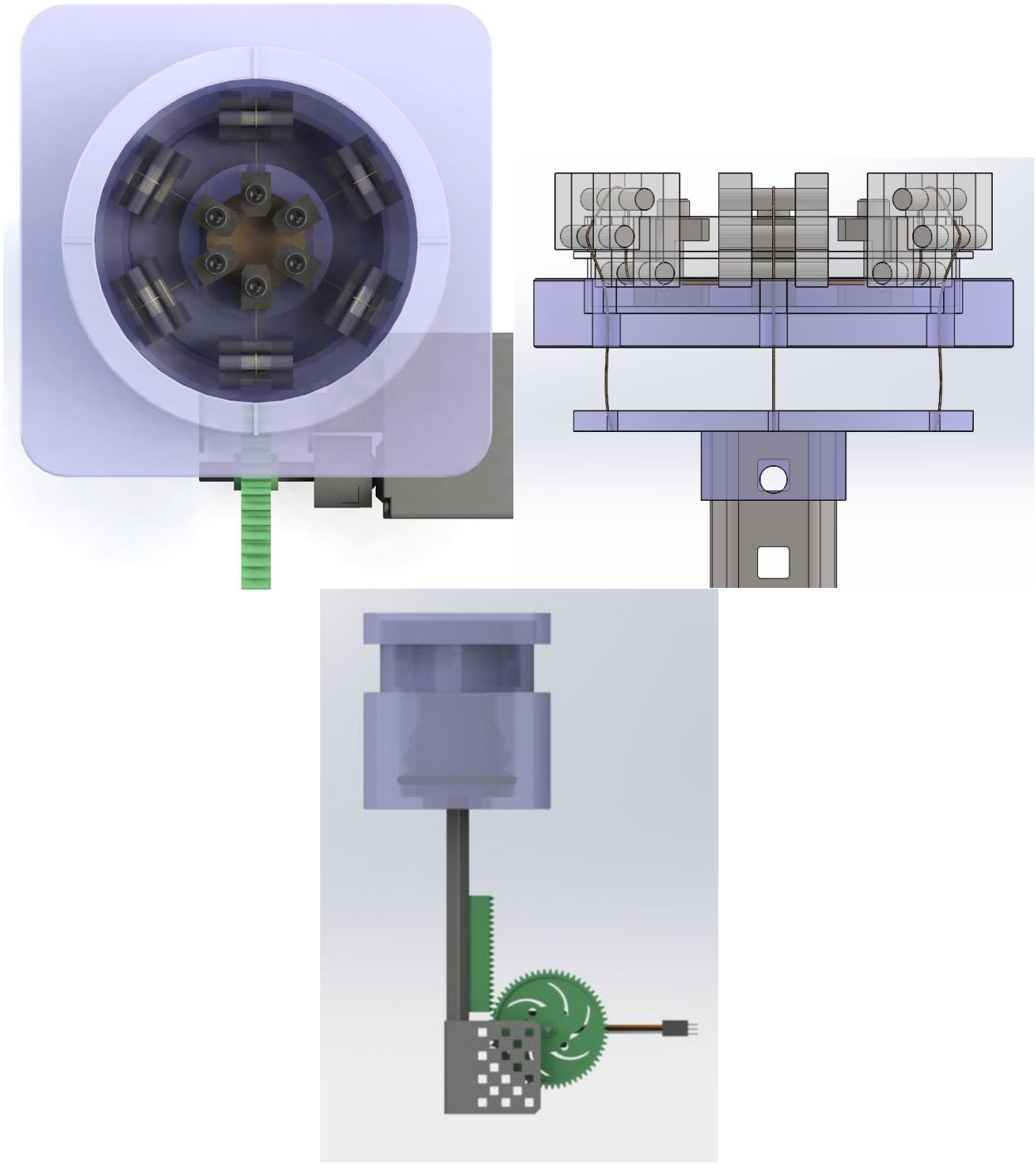

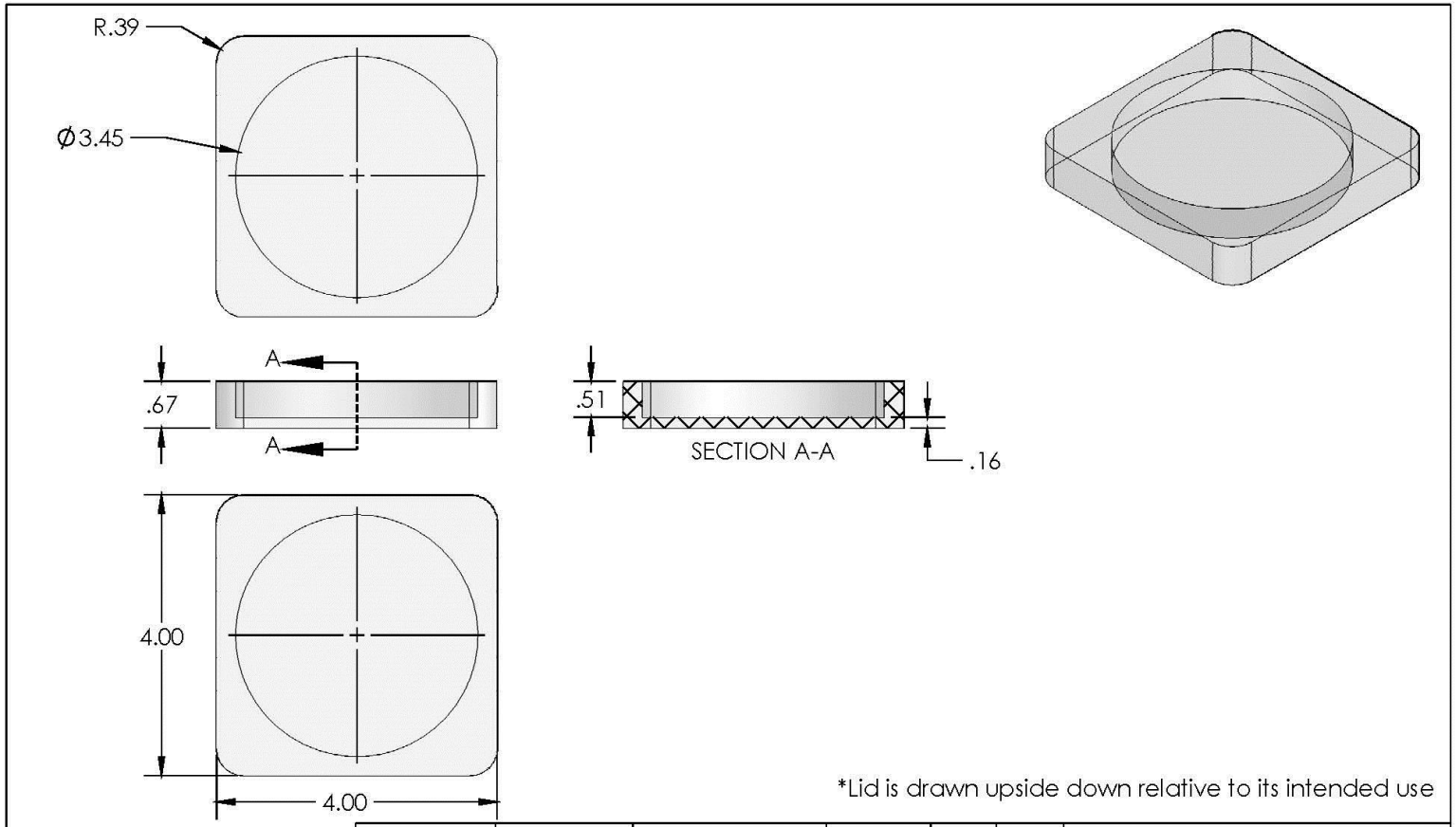

*Lid is drawn upside down relative to its intended use

UNLESS OTHERWISE SPECIFIED:		NAME	DATE	Worcester Polytechnic Institute	
DIMENSIONS ARE IN INCHES TOLERANCES: FRACTIONAL ± ANGULAR: 0 °30' BEND ± TWO PLACE DECIMAL ± THREE PLACE DECIMAL ±	DRAWN	LNP	3/29/2013	TITLE: Lid	
	CHECKED				
	ENG APPR.				
	MFG APPR.				
INTERPRET GEOMETRIC TOLERANCING PER:	Q.A.				
MATERIAL Makrolon Polycarbonate	COMMENTS:			SIZE A / DWG. NO. Lid / REV A	
FINISH				SCALE: 1:2 / WEIGHT: / SHEET 1 OF 1	

NEXT ASSY | USED ON | APPLICATION | DO NOT SCALE DRAWING

PROPRIETARY AND CONFIDENTIAL

THE INFORMATION CONTAINED IN THIS DRAWING IS THE SOLE PROPERTY OF WORCESTER POLYTECHNIC INSTITUTE (WPI). ANY REPRODUCTION IN PART OR AS A WHOLE WITHOUT THE WRITTEN PERMISSION OF WPI IS PROHIBITED.

5 4 3 2 1

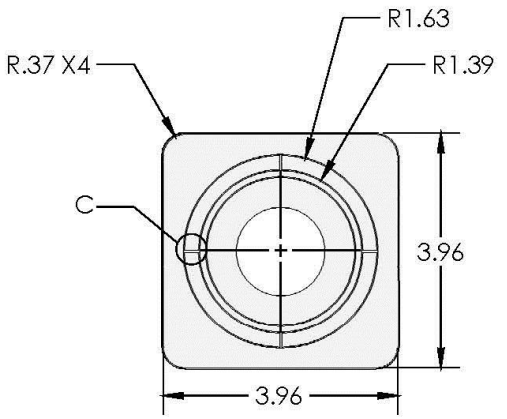

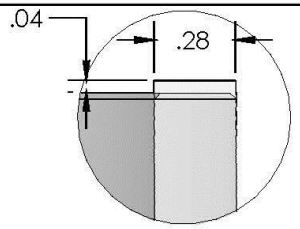

DETAIL B
SCALE 2 : 1

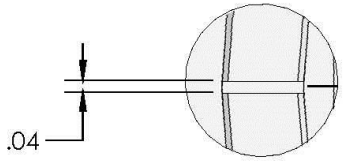

DETAIL C
SCALE 2 : 1

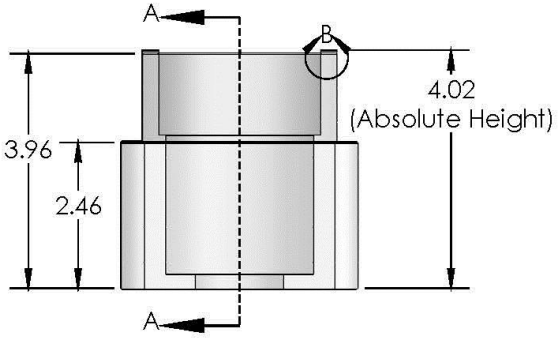

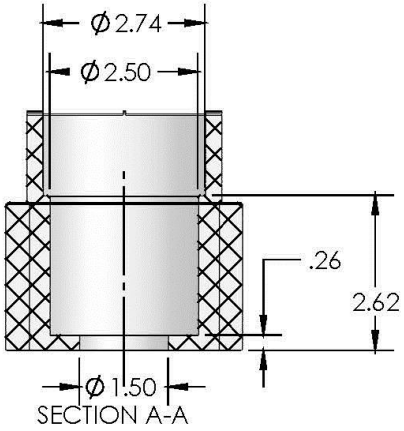

SECTION A-A

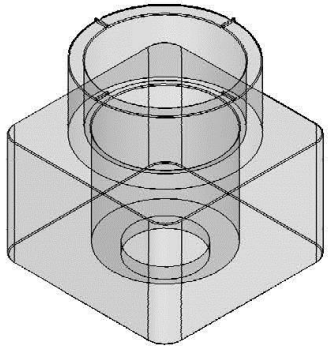

UNLESS OTHERWISE SPECIFIED:		NAME / DATE
DIMENSIONS ARE IN INCHES TOLERANCES: FRACTIONAL ± ANGULAR: 0 °30' BEND ± TWO PLACE DECIMAL ± THREE PLACE DECIMAL ±	DRAWN	LNP 3/29/2013
	CHECKED	
	ENG APPR.	
	MFG APPR.	
INTERPRET GEOMETRIC TOLERANCING PER:	Q.A.	
MATERIAL Makrolon Polycarbonate	COMMENTS:	
FINISH		
NEXT ASSY / USED ON		
APPLICATION / PROPRIETARY AND CONFIDENTIAL		

Worcester Polytechnic Institute

TITLE: Shell

SIZE	DWG. NO.	REV
A	Shell	A
SCALE: 2:5	WEIGHT:	SHEET 1 OF 1

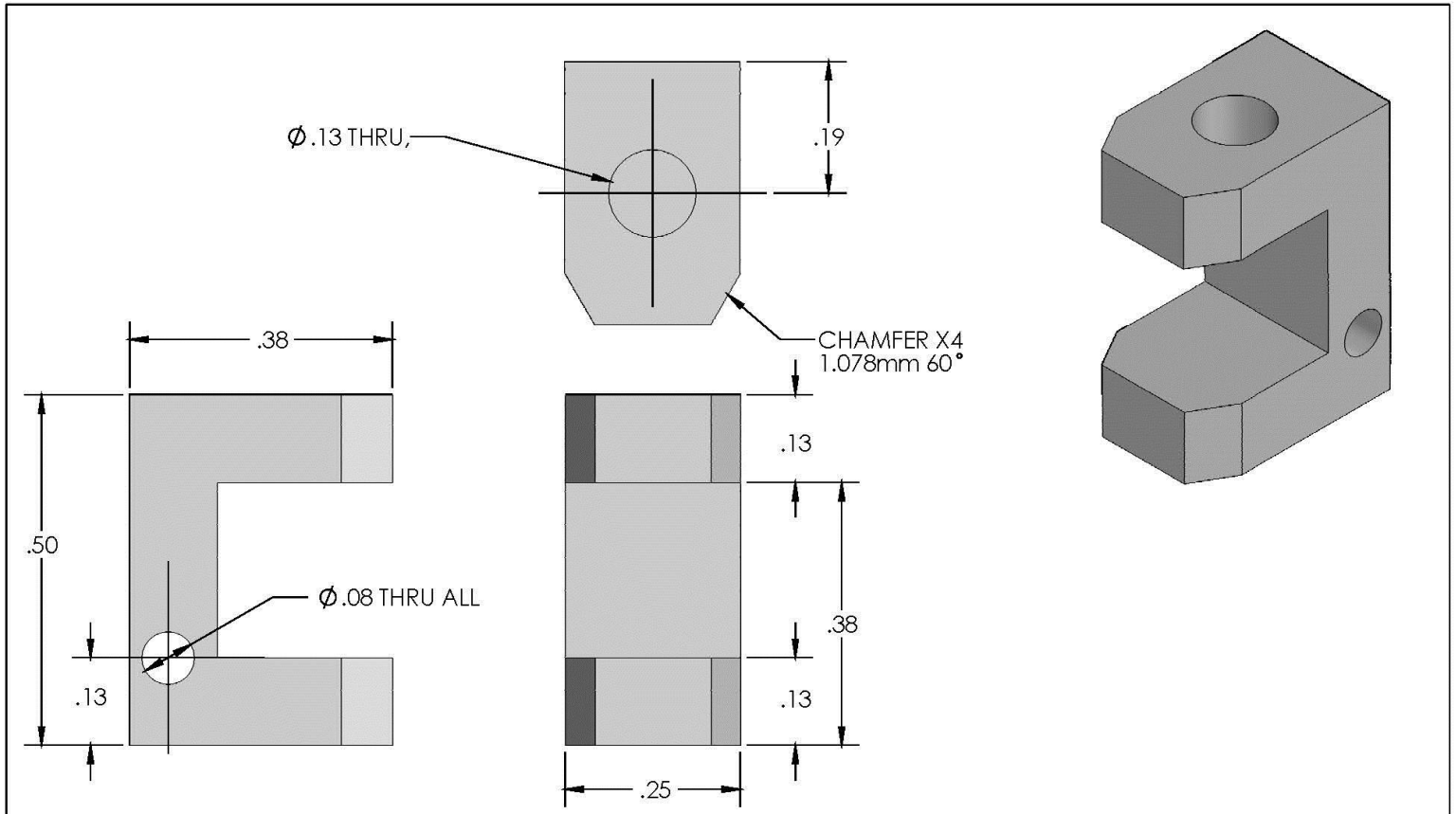

		UNLESS OTHERWISE SPECIFIED:		NAME	DATE
		DIMENSIONS ARE IN INCHES TOLERANCES: FRACTIONAL ± ANGULAR: 0°30' BEND ± TWO PLACE DECIMAL ± THREE PLACE DECIMAL ±	DRAWN	LNP	3/29/2013
			CHECKED		
			ENG APPR.		
			MFG APPR.		
		INTERPRET GEOMETRIC TOLERANCING PER:	Q.A.		
		MATERIAL 316L Stainless Steel	COMMENTS:		
NEXT ASSY	USED ON	FINISH			
APPLICATION		DO NOT SCALE DRAWING			

WPI

Worcester Polytechnic Institute

TITLE:
Clamps

SIZE	DWG. NO.	REV
A	Clamps	A
SCALE: 5:1	WEIGHT:	SHEET 1 OF 1

5 4 3 2 1

ITEM NO.	PART NUMBER	MATERIAL	QTY.
1	Post	Polycarbonate (Makrolon)	2
2	Pin	316L Stainless Steel	3

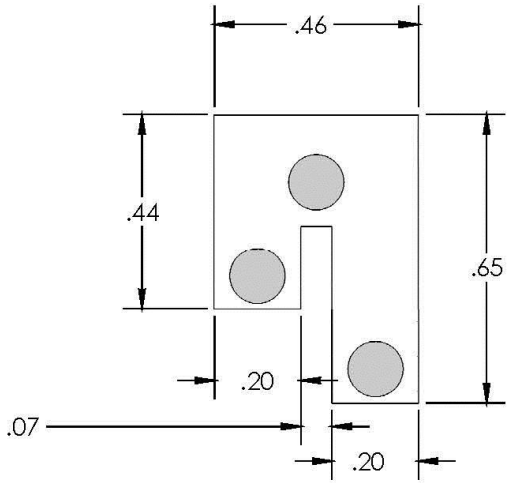

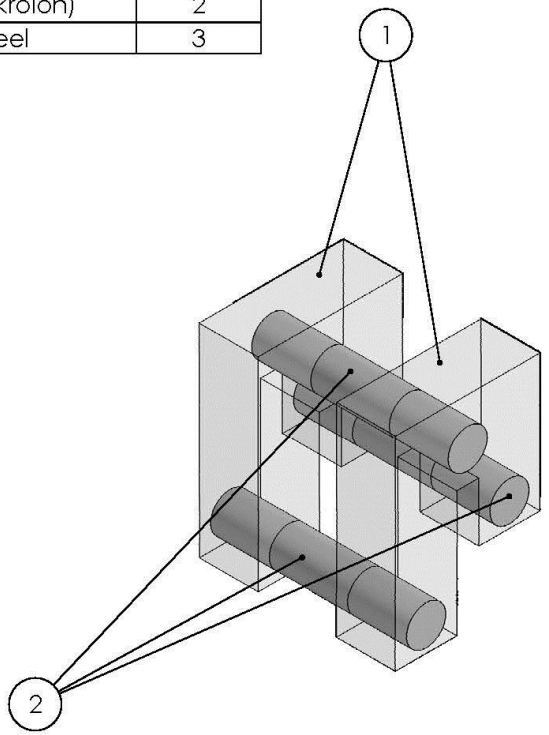

WPI

NEXT ASSY	USED ON	
APPLICATION	DO NOT SCALE DRAWING	

UNLESS OTHERWISE SPECIFIED:
DIMENSIONS ARE IN INCHES
TOLERANCES:
FRACTIONAL ±
ANGULAR: 0° 30' BEND ±
TWO PLACE DECIMAL ±
THREE PLACE DECIMAL ±
INTERPRET GEOMETRIC TOLERANCING PER:
MATERIAL
FINISH

	NAME	DATE
DRAWN	LNP	3/29/2013
CHECKED		
ENG APPR.		
MFG APPR.		
Q.A.		

COMMENTS:

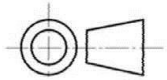

Worcester Polytechnic Institute

TITLE:
Averter Assembly

SIZE	DWG. NO.	REV
A	Averter	A
SCALE: 3:1	WEIGHT:	SHEET 1 OF 3

5 4 3 2 1

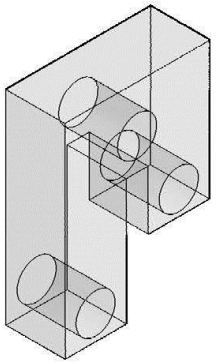

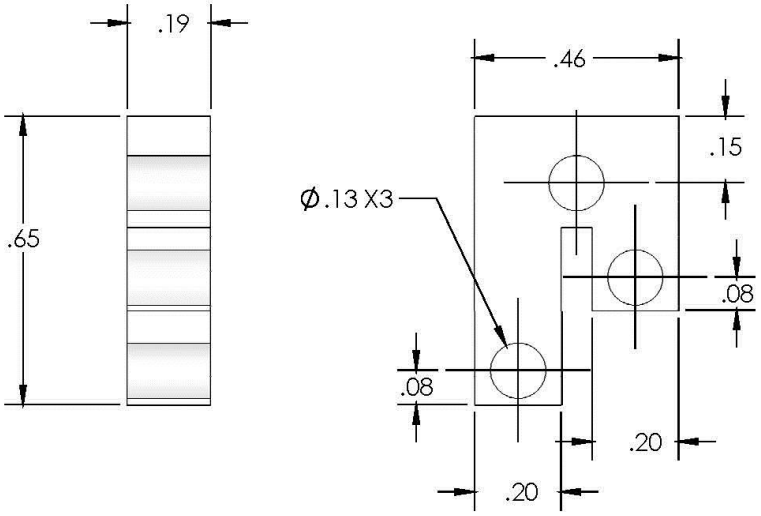

		UNLESS OTHERWISE SPECIFIED:		NAME	DATE
		DIMENSIONS ARE IN INCHES TOLERANCES: FRACTIONAL ± ANGULAR: 0 °30' BEND ± TWO PLACE DECIMAL ± THREE PLACE DECIMAL ±	DRAWN	LNP	3/29/2013
			CHECKED		
			ENG APPR.		
			MFG APPR.		
		INTERPRET GEOMETRIC TOLERANCING PER:	Q.A.		
		MATERIAL Polycarbonate (Makrolon)	COMMENTS:		
NEXT ASSY	USED ON	FINISH			
APPLICATION		PROPRIETARY AND CONFIDENTIAL			

THE INFORMATION CONTAINED IN THIS DRAWING IS THE SOLE PROPERTY OF WORCESTER POLYTECHNIC INSTITUTE (WPI). ANY REPRODUCTION IN PART OR AS A WHOLE WITHOUT THE WRITTEN PERMISSION OF WPI IS PROHIBITED.

Worcester Polytechnic Institute

TITLE: Post

SIZE	DWG. NO.	REV
A	Averter	A
SCALE: 3:1	WEIGHT:	SHEET 2 OF 3

5 4 3 2 1

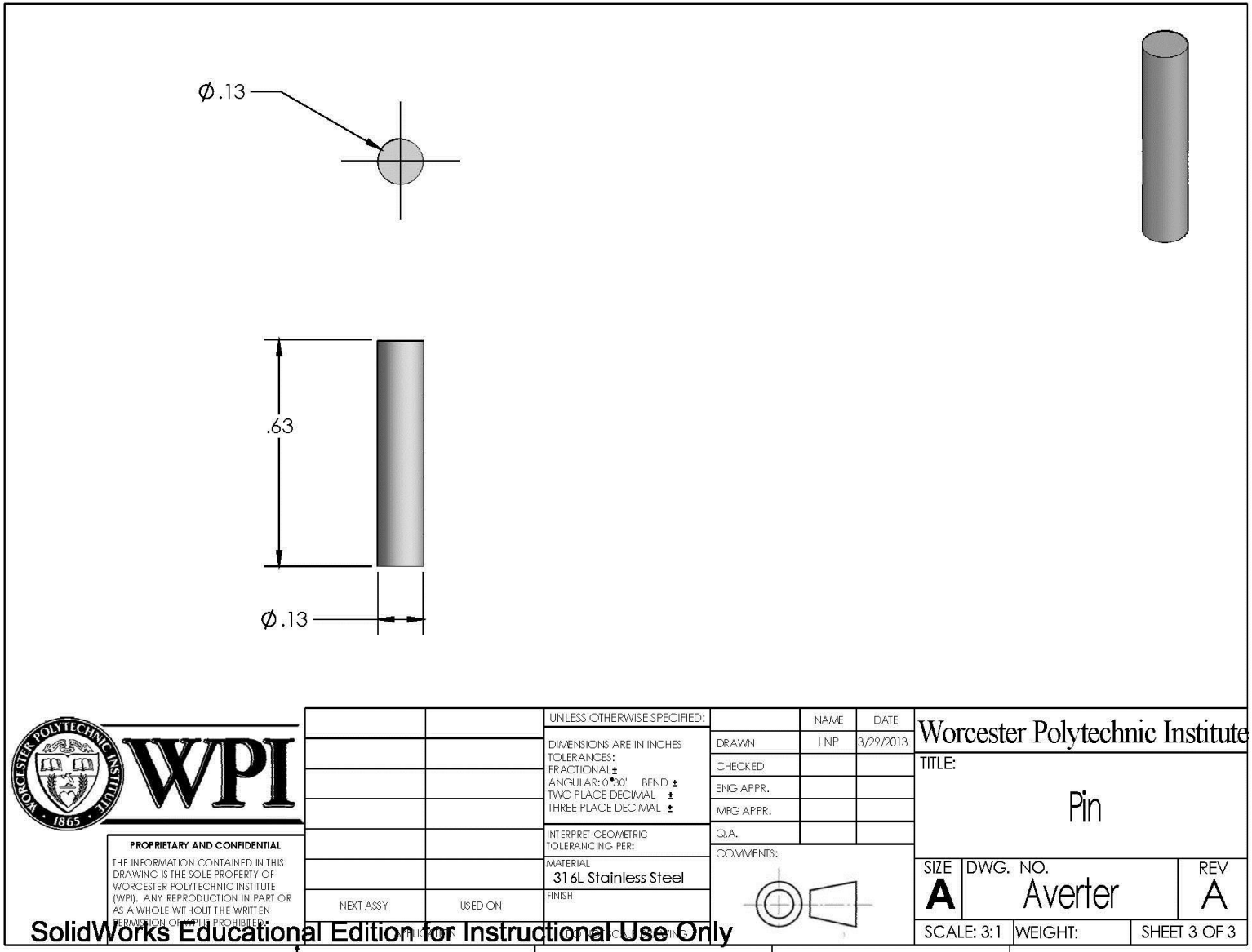

		UNLESS OTHERWISE SPECIFIED:		NAME	DATE
		DIMENSIONS ARE IN INCHES TOLERANCES: FRACTIONAL ± ANGULAR: 0° 30' BEND ± TWO PLACE DECIMAL ± THREE PLACE DECIMAL ±	DRAWN	LNP	3/29/2013
			CHECKED		
			ENG APPR.		
			MFG APPR.		
		INTERPRET GEOMETRIC TOLERANCING PER:	Q.A.		
		MATERIAL 316L Stainless Steel	COMMENTS:		
NEXT ASSY	USED ON	FINISH			
APPLICATION		DO NOT SCALE DRAWING			

WPI

Worcester Polytechnic Institute

TITLE: Pin

SIZE	DWG. NO.	REV
A	Averter	A

SCALE: 3:1 | WEIGHT: | SHEET 3 OF 3

5 4 3 2 1

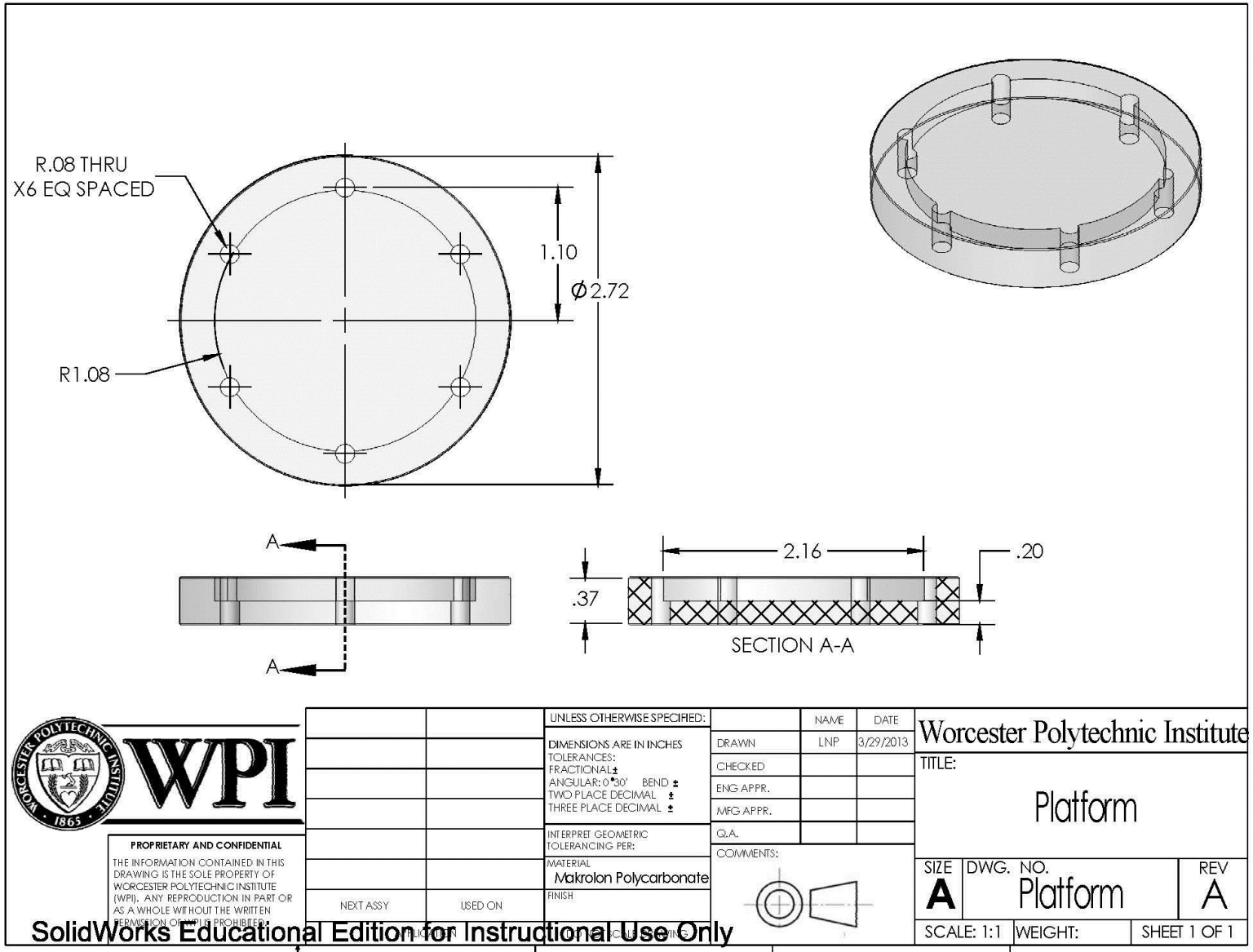
R.08 THRU
X6 EQ SPACED
R1.08
1.10
Ø2.72
A
A
2.16
.20
.37
SECTION A-A
WPI
PROPRIETARY AND CONFIDENTIAL
THE INFORMATION CONTAINED IN THIS DRAWING IS THE SOLE PROPERTY OF WORCESTER POLYTECHNIC INSTITUTE (WPI). ANY REPRODUCTION IN PART OR AS A WHOLE WITHOUT THE WRITTEN PERMISSION OF WPI IS PROHIBITED.
NEXT ASSY
USED ON
APPLICATION
UNLESS OTHERWISE SPECIFIED:
DIMENSIONS ARE IN INCHES
TOLERANCES:
FRACTIONAL ±
ANGULAR: 0 °30' BEND ±
TWO PLACE DECIMAL ±
THREE PLACE DECIMAL ±
INTERPRET GEOMETRIC TOLERANCING PER:
MATERIAL
Makrolon Polycarbonate
FINISH
DO NOT SCALE DRAWING
NAME
DATE
DRAWN
LNP
3/29/2013
CHECKED
ENG APPR.
MFG APPR.
Q.A.
COMMENTS:
Worcester Polytechnic Institute
TITLE:
Platform
SIZE
A
DWG. NO.
Platform
REV
A
SCALE: 1:1
WEIGHT:
SHEET 1 OF 1
SolidWorks Educational Edition for Instructional Use Only
5
4
3
2
1

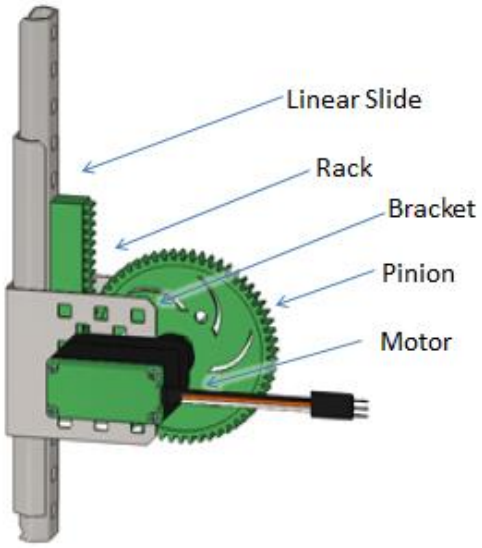
Linear Slide
Rack
Bracket
Pinion
Motor

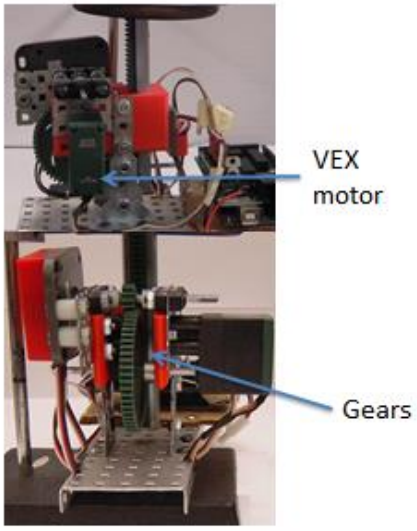
VEX
motor
Gears

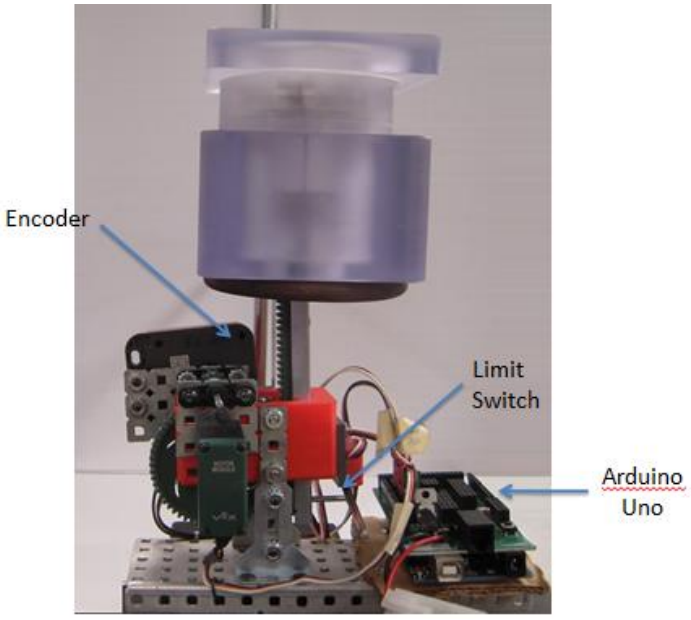
Encoder
Limit
Switch
Arduino
Uno

Appendix B.2 Budget list

Expenses					
Device					
Part		Quantity	**Purchase Cost**	**Unit Cost**	**Cost for Assembly**
Bioreactor		1		$55.14	$73.17
> Lid		1	$5.00	$5.00	$5.00
> Shell		1	$5.00	$5.00	$5.00
> Averter		6			
> >	Post	12	$8.00	$0.67	$8.00
> >	Pin	18	$7.59	$0.42	$7.59
> Clamp		6	$3.16	$0.53	$3.16
> Suture		6	$15.50	$15.50	$15.50
> Well Plate		1	$19.20	$0.96	$0.96
> Platform		1	$5.00	$5.00	$5.00
> Articulation Plate		1	$5.00	$5.00	$5.00
> Screw		6	$4.50	$0.18	$1.08
> Sleeve		1	$16.88	$16.88	$16.88
Actuator		1		$139.14	$140.04
> Linear Slide		1	$14.95	$14.95	$14.95
> VEX Rack		1	$19.99 for kit	$19.99	$19.99
> Universal Joint		1	$2.56	$2.56	$2.56
> VEX 60 tooth gear		1	$12.99 for gear kit	$12.99	$12.99
> VEX stepper motor		1	$20.00	$20.00	$20.00
> Limit Switch		1	$12.99	$12.99	$12.99
> VEX Encoder		1	$19.99	$19.99	$19.99
> Arduino Uno		1	$25.00	$25.00	$25.00
> VEX Bracket		1	$9.99	$5.00	$5.00
> Screw		6	$4.50	$0.18	$1.08
> Drive Shaft		1	$5.49	$5.49	$5.49
Total Device				**$194.27**	**$213.21**
Lab Fee					$100.00
Lab Notebook					$7.00
Total Cost					$320.21
Total Budget					$608
Net Budget Remaining					$287.80

Appendix B.3 Parts list

Device Component:	Part		Quantity	Material	Vendor	Part Number	Description
Bioreactor			1				
>	Lid		1	Makrolon Polycarbonate	Piedmont Plastics	MA-28303246	top of device encloses testing setup, polycarbonate
>	Shell		1	Makrolon Polycarbonate	Piedmont Plastics	MA-28303247	outer enclosure of device, polycarbonate
>	Averter		6				
>	>	Post	12	Makrolon Polycarbonate	Piedmont Plastics	MA-28303248	inserts that attach to rim of well plate, polycarbonate and 316 stainless steel
>	>	Pin	18	316 Stainless Steel	McMaster-Carr	97395A445	
>	Clamp		6	316L Stainless Steel	Online Metals	T-316/316L	fixtion part for testing, 316 L stainless steel
>	Suture		6	Nylon	AD Surgical	N/A	standard medical sutures, nylon
>	Well Plate		1	Polystyrene	Corning Life Sciences	3261	60mm standard culture dish, polystyrene
>	Platform		1	Makrolon Polycarbonate	Piedmont Plastics	MA-28303247	resting location of well plate, polycarbonate
>	Articulation Plate		1	Makrolon Polycarbonate	Piedmont Plastics	MA-28303248	Location of cord insertion, polycarbonate
>	Screw		6	316 Stainless Steel	McMaster-Carr	92185A073	
>	Sleeve		1	Neoprene	The Rubber Store	BT-1090	Encloses bottom to ensure sterility, neoprene
Actuator			1				
>	Linear Slide		1	Steel	VEX	P/N: 276-1096	metal slides that translate rotational motion into linear motion
>	VEX Rack		1	Delrin	VEX	P/N: 276-1957	Articulates with gear
>	Universal Joint		1	Acetal	SDP-SI	A 5M 8-D206	provides free roation of articulation plate
>	VEX 60 tooth gear		1	Delrin	VEX	P/N: 276-2169	articulates with rack
>	VEX stepper motor		1	N/A	VEX	P/N: 276-2162	provides motion for actuator
>	Limit Switch		1	N/A	VEX	P/N: 276-2174	sets home point for motor
>	VEX Encoder		1	N/A	VEX	P/N: 276-2156	counts steps of motor
>	Arduino Uno		1	N/A	Mouser Electronics	782-A000066	micro-controller
>	VEX Bracket		1	Steel	VEX	P/N: 276-1926	houses motor, linear slide, rack, and gear
>	Screw		6	Steel	McMaster-Carr	91251A051	provide attachment
>	Drive Shaft		1	Steel	VEX	276-2011	connects gear to motor

Appendix C: Operating Instructions

Appendix C.1 Programming

This Code will run a vex motor connected to a vex rack gear by a 60 tooth gear. The system has an encoder recording distance traveled connected to the 60 tooth gear by a 12 tooth gear. There is a limit switch located at the top of the slide movement. The slide will first travel all the way up until it activates the limit switch when the slide depresses the limit switch it is in the HOMED position and will set the encoder position to 0. Immediately after being HOMED, the slide will travel down to the distance described in the variable travel height. For the user these parameters are changeable with the capability to vary the wait time between stretching and the maximum displacement of the slide.

```
*/

#include "Arduino.h"

#include <Servo.h>


//encoder variables

#define encoder0PinA 2

#define encoder0PinB 3

volatile int encoder0Pos = 0;


//Limit Switch variables

#define c_LimitPin 4

volatile bool _Home;
```

```
//Servo Motor variables

#define c_ServoPin 9

int servoSpeed = 75; //How fast the motor turns Values 0<90
down 90 = stopped 90<180 up

int servoStop = 90;

double travelHeight = 10; // mm

double travelTicks =0; // (calculated
later)

Servo myservo; // create servo object to control a servo

        // a maximum of eight servo objects can be created


// sequence variables

bool Homed = false;

bool Finished = false;


void setup() {


//encoder Setup

  pinMode(encoder0PinA, INPUT);

  pinMode(encoder0PinB, INPUT);
```

Change how fast the motor turns

Change to set the desired position below the home position that you want to move in mm

Change to set the number of ticks you want gear to move. For this particular motor 1

```
// encoder pin on interrupt 0 (pin 2)
  attachInterrupt(0, doEncoderA, CHANGE);
// encoder pin on interrupt 1 (pin 3)
  attachInterrupt(1, doEncoderB, CHANGE);


//limit switch setup
  pinMode(c_LimitPin, INPUT);     //sets Limit pin as an input
  digitalWrite(c_LimitPin, HIGH);  //Turn on pullup resistors


//Servo motor setup
  myservo.attach(c_ServoPin,1000,2000);  // attaches the servo on pin 9 to the servo
object



//calculate number of ticks to go
travelTicks = (travelHeight/.445); // .445 mm/tick
```

Calculated smallest step value for motor per movement = .445mm

```
//Serial communication rate
  Serial.begin (9600);
}
```

```
//do stuff here

void loop(){


if(Finished == false){

 //Home the encoder so zero is at the highest postion

 if (Homed == false){

   if(digitalRead(c_LimitPin) == HIGH){

     myservo.write(130);

     delay(2);

     Serial.print(" NOT Home");

     Serial.print("\n");

    }

    else{

     myservo.write(servoStop);

     encoder0Pos = 0;

     Homed = true;

    Serial.print(" Home ");

    delay(2000);

    }
```

Sets HOMED (zero) position where screw hits the limit switch

Change wait time (seconds) between stretches. In the code it is described as the “delay”

```
}
else{
  if (encoder0Pos < travelTicks){
    myservo.write(servoSpeed);
  }
  else{
    myservo.write(servoStop);
    Serial.print("\n");
    Serial.print(encoder0Pos);
    Serial.print("ticks\n");
    Serial.print(travelTicks);
    Serial.print("ticks\n");
    delay(2000);
    Homed= false;
```

Appendix C.2 Test Preparation

1. Preparation of Cords

- Nylon cords should be cut double actual cord length because they are doubled up when being attached. In total, there should be 6 sets of cords for all 6 clamps.

2. Sterilization

- Components of the device made out of makrolon polycarbonate (shell, lid, articulation plate, and stage plate), 316 stainless steel (clamps), nylon (cords), and rubber (sleeve) can be sterilized through autoclave.
- The metal linear actuator can be sprayed with ethanol.
- The 60 mm2 culture plate is disposable and can be changed when needed, as long as its packaging remains sterile.

3. Preparation of Cords (Continued)

- Once all components are sterilized, they should be removed from packaging inside a fume hood.
- The cords should have weights hung weights at the ends overnight to be pre-conditioned (90% UTS).
- This step allows cords to pre-creep, which will avoid creep later during testing.
- It also causes cords to assume generally standard dimensions relative to one another.

Appendix C.3 Device Assembly

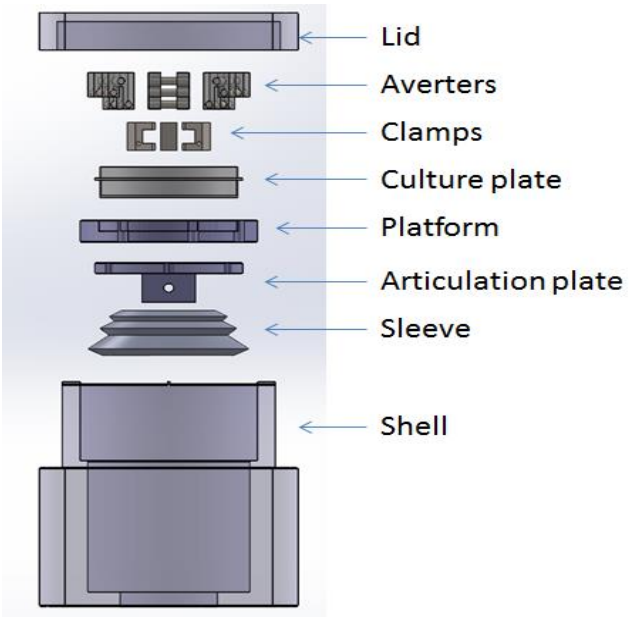

- In the fume hood, place sleeve into the shell
- Attach the 6 averters to the culture place using the holes on the platform as a placement guide as seen in the image below

- Thread the cords in between the neck on the clamps and the screw
- Run cords up and around the averters through the holes in the platform down to the articulation plate as seen in the image below

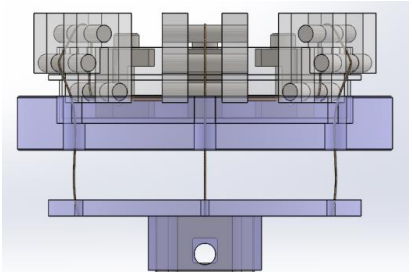

- Once threaded through the articulation plate, mark points on the cords that are consistent on all cords
- Crimp these marked points with silver beads
- Screw metal linear slide to the bottom of the articulation plate as seen in the image below

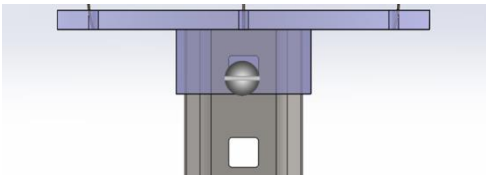

- Place components into the shell, with linear slide attaching to rack and pinion system underneath as seen in the images below

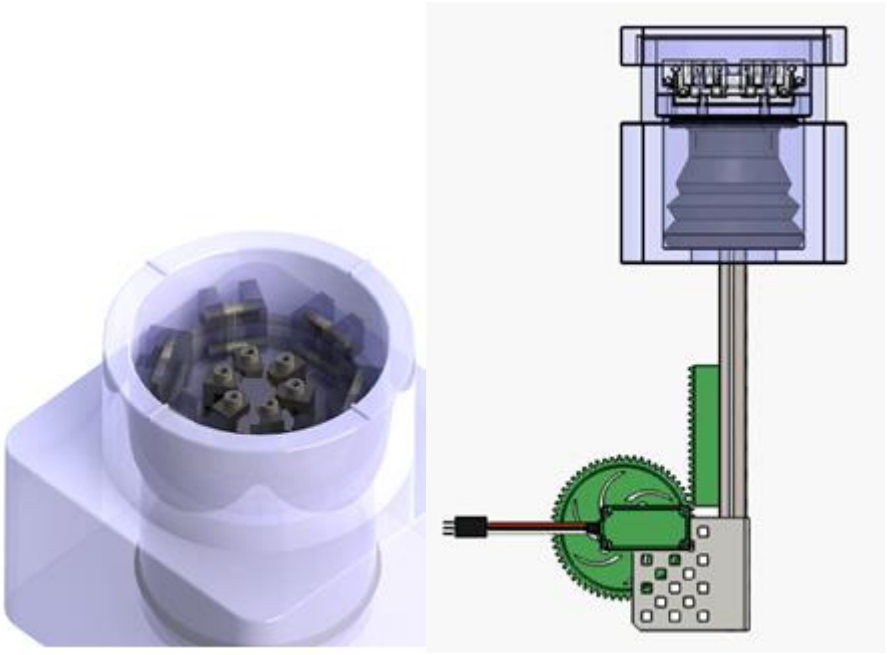

Appendix C.4 Device Operation

Sample preparation

- Acquire desired tissue sample and place in fume hood

- Orient the clamps so the sample is fixed by all 6 clamps, equally spaced, as seen in the image below

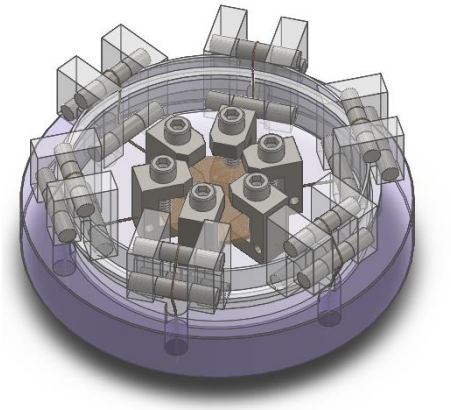

- Use the “cap” to hold the clamps at a fixed location
- Screw each individual clamp to secure the sample
- Remove “cap”
- Hydrate sample with saline solution so it maintains its viscoelastic properties for longer testing cycle durations. More solution may need to be added depending on the duration of testing.
- Sample is ready for testing

Testing protocol

- Fill medium in culture dish once tissue sample is secure at an air-liquid interface
- Place control tissue sample (non-stretched) in culture dish
- Place lid on device and move both device and control into incubator
- Plug in battery into actuator portion of device, if using an outlet an outlet, plug into wall
- Turn switch on
- Check periodically depending on testing duration
- When testing cycle has ended, remove device carefully following the reverse of the fixation protocol
- Section and fix samples for histology
- Stain slides using ki-67 antigen

- Observe cell proliferation in both experiment and control using microscope
- Take ratio of proliferating cells/non-proliferating cells
- Analyze data

Appendix C.5 Comprehensive Code

Code written by Timothy Sharood, adapted relative to experiments:

```
/*
Linear actuator Code
Tim Sharood
3/28/13
This Code will run a vex motor connected to a vex rack gear by a 60 tooth gear.
The system has an encoder recording distance traveled connected to the 6o tooth
gear by a 12 tooth gear. There is a limit switch located at the top of the slide
movement. The slide will first travel all the way up until it activates the limit
switch. when the slide depresses the limit switch it is in the HOMED position and
will set the encoder position to 0. Immediately after being homed the slide will
travel down to the distance described in the variable travelHeight.
*/


#include "Arduino.h"
#include <Servo.h>


//encoder variables
#define encoder0PinA 2
#define encoder0PinB 3
```

```
volatile int encoder0Pos = 0;


//Limit Switch variables
#define c_LimitPin 4
volatile bool _Home;


//Servo Motor variables
#define c_ServoPin 9
int servoSpeed = 75; //How fast the motor turns Values 0<90 down 90 = stopped 90<180 up
int servoStop = 90;
double travelHeight = 10; // mm change to set the desired postion below the home postion that you want to move in mm
double travelTicks =0; // number of ticks to move (calculated later)


Servo myservo;  // create servo object to control a servo
                // a maximum of eight servo objects can be created


// sequence variables
bool Homed = false;
bool Finished = false;
```

```
void setup() {


//encoder Setup
  pinMode(encoder0PinA, INPUT);
  pinMode(encoder0PinB, INPUT);
// encoder pin on interrupt 0 (pin 2)
  attachInterrupt(0, doEncoderA, CHANGE);
// encoder pin on interrupt 1 (pin 3)
  attachInterrupt(1, doEncoderB, CHANGE);


//limit switch setup
  pinMode(c_LimitPin, INPUT);     //sets Limit pin as an input
  digitalWrite(c_LimitPin, HIGH);  //Turn on pullup resistors


//Servo motor setup
  myservo.attach(c_ServoPin,1000,2000);  // attaches the servo on pin 9 to the servo
object



//calculate number of ticks to go
```

```
travelTicks = (travelHeight/.445); // .445 mm/tick


//Serial communication rate
  Serial.begin (9600);
}


//do stuff here
void loop(){


if(Finished == false){
  //Home the encoder so zero is at the highest postion
  if (Homed == false){
    if(digitalRead(c_LimitPin) == HIGH){
      myservo.write(130);
      delay(2);
      Serial.print(" NOT Home");
      Serial.print("\n");
    }
    else{
      myservo.write(servoStop);
```

```
    encoder0Pos = 0;
    Homed = true;
   Serial.print(" Home ");
   delay(2000);
  }
 }
 else{
  if (encoder0Pos < travelTicks){
    myservo.write(servoSpeed);
  }
  else{
    myservo.write(servoStop);
    Serial.print("\n");
    Serial.print(encoder0Pos);
    Serial.print("ticks\n");
    Serial.print(travelTicks);
    Serial.print("ticks\n");
    delay(2000);
    Homed= false;
  }
```

```
   }
  }
  else{
    delay(5000000);
  }
}



void doEncoderA(){
  // look for a low-to-high on channel A
  if (digitalRead(encoder0PinA) == HIGH) {
    // check channel B to see which way encoder is turning
    if (digitalRead(encoder0PinB) == LOW) {
      encoder0Pos = encoder0Pos + 1;         // CW
    }
    else {
      encoder0Pos = encoder0Pos - 1;         // CCW
    }
  }
  else   // must be a high-to-low edge on channel A
```

```
  {
    // check channel B to see which way encoder is turning
    if (digitalRead(encoder0PinB) == HIGH) {
      encoder0Pos = encoder0Pos + 1;         // CW
    }
    else {
      encoder0Pos = encoder0Pos - 1;         // CCW
    }
  }
}

void doEncoderB(){
  // look for a low-to-high on channel B
  if (digitalRead(encoder0PinB) == HIGH) {
   // check channel A to see which way encoder is turning
    if (digitalRead(encoder0PinA) == HIGH) {
      encoder0Pos = encoder0Pos + 1;         // CW
    }
    else {
      encoder0Pos = encoder0Pos - 1;         // CCW
```

```
    }
  }
  // Look for a high-to-low on channel B
  else {
    // check channel B to see which way encoder is turning
    if (digitalRead(encoder0PinA) == LOW) {
      encoder0Pos = encoder0Pos + 1;         // CW
    }
    else {
      encoder0Pos = encoder0Pos - 1;         // CCW
    }
  }
}
```